Nickel Oxide Nanoparticle based Thin Film as an Antibacterial and Self-Cleaning Glass

By

Syeda Wara Zehra

Registration Number: 00000172651

Supervised by

Dr. Hussnain Ahmed Janjua

Industrial Biotechnology

Atta ur Rahman School of Applied Biosciences (ASAB)

National University of Sciences and Technology (NUST)

Islamabad

Nickel Oxide Nanoparticle based Thin Film as an Antibacterial and Self-Cleaning Glass

By

Syeda Wara Zehra

Registration Number: 00000172651

A thesis submitted in partial fulfillment of the requirements for the degree of

MS Industrial Biotechnology

Supervisor

Dr. Hussnain Ahmed Janjua

Atta ur Rahman School of Applied Biosciences (ASAB)

National University of Sciences and Technology (NUST)

Islamabad, Pakistan

2019.

بسم الله الرحمن الرحيم

IN THE NAME OF ALLAH, THE MOST BENEFICENT

AND THE MOST MERCIFUL

Read! And thy Lord is Most Honorable and Most Benevolent,

Who taught (to write) by pen, He taught man that which he knew not

(Surah Al-Alaq 30: 3-5)

Al-Quran

THESIS ACCEPTANCE CERTIFICATE

Certified that the contents and form of thesis entitled "**Nickel Oxide Nanoparticle based Thin Film as an Antibacterial and Self-Cleaning Glass**" submitted by Syeda Wara Zehra, have been found satisfactory for the requirement of the degree.

Supervisor: __________________________________

Dr. Hussnain Ahmed Janjua

ASAB, NUST

Head of Department: ____________________________

Dr Saadia Andaleeb

ASAB, NUST

Principal: ____

Dr Hussnain Ahmed Janjua

ASAB, NUST

Dated: ____

Signature of Supervisor

CERTIFICATE FOR PLAGIARISM

(Turnitin Report)

It is certified that the thesis entitled, **“Nickel Oxide Nanoparticle based Thin Film as an Antibacterial and Self-Cleaning Glass’’** of Syeda Wara Zehra Registration Number: 00000172651 has been checked for Plagiarism. Turnitin report endorsed by Supervisor is attached.

Signature of Student

SYEDA WARA ZEHRA

Registration Number

00000172651

Declaration

I certify that this research work titled "**Nickel Oxide Nanoparticle based Thin Film as an Antibacterial and Self-Cleaning Glass**" is my own work. The work has not been presented elsewhere for assessment. The material that has been used from other sources it has been properly acknowledged / referred.

Signature of Student

SYEDA WARA ZEHRA

2016-NUST-MSIB

ACKNOWLEDGMENTS

I am thankful to Almighty Allah who is the most merciful, beneficent and the most fine, who bestowed upon me the power to use all my senses in the search of benefits for the mankind and the mind and spirit to gather my thoughts into reality through hard work. Peace and blessing of Allah be upon the Holy prophet Mohammad who exhorted his follower to seek the knowledge from cradle to grave.

It has been an honor working under the expert guidance and supervision of Prof. Dr. Hussnain Ahmed Janjua, Principal, Atta ur Rahman School of Applied Biosciences, National University of Sciences and Technology, Islamabad. I would like to utilize this opportunity to express my gratitude to him for his advices and support during the period of my research.

I am thankful to Dr Sadia Andaleeb, Head of the Department, Industrial Biotechnology for her best possible support and thankful to Dr Fazal Adnan (ASAB), Dr Zakir Hussain (SCME) and Dr Bilal Niazi (SCME) for their presence and guidance as GEC members.

I can never forget the efforts of my friends, Maira, Sheeza, Dania, Fatima who helped me throughout my research project, both academically and motivationally.

I am also thankful to Ms. Shehla Mushtaq of SNS, Mr Asad, Mr Arman, Mr Nouman and Dr Nasir Mehmood Ahmad of SCME for their help in my project completion. I am also thankful to the staff of Combined lab Casen, for making characterization procedure easier for me. I am also thankful for SCME lab staff for their help in conducting characterizations.

I am thankful to my husband, parents, siblings and my parents-in-law for their patience, support and guidance and sincere wishes throughout.

Finally, I am especially thankful to my lovely daughter, Mominna for being so understanding despite her tiny age, it has been a journey of productive learning and strength, both academically and emotionally.

-Syeda Wara Zehra

Dedicated to,

Bilal and Momina

Table of Contents

List of Figures

List of Tables

List of Symbols and Abbreviations

°	Degree
2D	Two dimensional
3D	Three dimensional
kV	Kilo volt
KeV	Kilo electron volt
mm	Millimeter
(A)	Absorbance
g	Gram
%	Percent
Rpm	Revolution per minute
(T)	Transmittance
OD	Optical Density
L	Liter
µL	Microliter
nm	Nanometer
µm	Micrometer
mg	Milligram
M	Molar
Ra	Area roughness
CDC	Centre for disease control & prevention
WHO	World Health Organization
HAI	Hospital Acquired infection
VRE	Vancomycin resistant enterococcus
MRSA	Methicillin resistant Staphylococcus aureus
ICU	Intensive care unit
JCPDs	Joint Committee for powder diffraction
Eg	Energy band gap

CA	Contact angle
WCA	Water contact angle
KHz	Kilohertz
cm^{-1}	Per centimeter
FTIR	Fourier transform infrared spectroscopy
DSC	Differential Scanning Calorimetry
TGA	Thermogravimetric Analysis
WCA	Water Contact Angle
SEM	Scanning Electron Microscopy
EDS	Energy Dispersive Spectrum
UV	Ultraviolet
XRD	X-Ray Diffractometer
AFM	Atomic force Microscopy

ABSTRACT

Nickel oxide nanoparticles, synthesized from microalgal specie, *Dictyosphearium* were characterized thoroughly and a nearly transparent thin film of Nickel oxide nanoparticle was synthesized by spin coating for combined applications of self-cleaning and antibacterial. The self-cleaning and antibacterial coatings can be applied on glass surfaces on clinical settings which account for major percentage of indirect-contact transmissions. Nosocomial infections are a leading cause of many post-hospitalization deaths worldwide accounting to a total of 99000 deaths a year as per Centre for Disease Control and Prevention report and the need of the time is to reduce the rate of nosocomial diseases. Various methods are being adopted in this line and Nano coatings are one of them. In present study, for working solution, we used bio-inspired Nickel oxide Nanoparticles, synthesized in lab and made their emulsion in a mixture of Tetrahydrofuran and deionized water. Thin film of nickel oxide was deposited on soda lime glass (SLG) to evaluate the self-cleaning and antibacterial properties. Scanning electron micrographs show nanoparticles size range from 20 to 90nm with good X-Ray Diffraction results confirmed the presence of Nickel oxide in the thin film produced by spin coating. Atomic force microscopy images showed maximum surface coverage and enhanced roughness by nanoparticles deposited as a result of spin coating. Contact angle of the prepared thin film shows maximum hydrophilicity in range closer to the criteria of superhydrophilicity, this is due to enhanced roughness imparted to the surface due to uniform nature of coating. The self-cleaning ability of the thin film coated glass were tested by performing antifogging, self-cleaning using dirt model and rainfall spraying assays. For antibacterial aspect, the coating had been tested through antibacterial and anti-biofilm *Escherichia coli*, *Pseudomonas aeruginosa* and *Klebsiella pneumoniae.* Nosocomial infections are the infection caused by bacteria or viruses inhabiting hospitals and other clinical settings. Of the total 1.7 million Hospital acquired infections every year, two-third of them is due to gram-negative infections. This nickel oxide-based coating provides a cost effective and new alternative by giving two properties of self-cleaning and antibacterial in a single assembly and thin film prepared by spin coating can be employed as an efficient coating on glass for self-cleaning properties.

CHAPTER 1: INTRODUCTION

In the proposed study, efforts were made to fabricate a coated glass based on nickel oxide nanoparticles, to combine antimicrobial and anti-adhesive aspects in one. Nickel oxide nanoparticle was chosen because of his antibacterial and hydrophilic nature. The antibacterial activity of nickel oxide has not been studied in detail yet but the proposed mechanism of action of nickel oxide is based on the generation of reactive oxygen species (ROS) (Aranda, Sequedo et al. 2013). In this study, the synthesized nanoparticles had been assessed for antibacterial activity prior to coating procedure. Also, the origin of the nickel oxide nanoparticles used is biological. The nickel oxide nanoparticles were synthesized in and characterized using algae extract. These nanoparticles have functional groups on its surface from the flavonoids, proteins and phenols present in the extract which have been used as stabilizing and reducing agents during nanoparticle synthesis. The coating emulsion used was also hydrophilic in nature in order to produce a coating annealed on a glass substrate that it imparts overall hydrophilic character to the surface with good mechanical properties. Added benefit of this coating were antireflective nature along with the need self-cleaning and antibacterial character.

Nosocomial or Hospital acquired infections are broadly defined as those health care-associated infections (HAI) which were not present in a patient at the time of admission and appear after admission or immediately after discharge. The sources of nosocomial infections are broadly classified into two types; direct contact transmission and indirect contact transmission. Direct contact transmission is through invasive devices and procedures that are used to treat the patient whereas the indirect contact transmission involves the transmission of HAI through contact of susceptible host with inanimate intermediate surfaces such as glass surfaces, equipment buttons, handles, computers, patient charts, and hand lotion dispensers (Chinn and Sehulster 2003). According to CDC, 1 in 31 patients have one HAI in one day. CDC estimated statistics reveal that yearly 1.7 million hospital acquired infections from all microorganisms are reported. In United States, 99000 deaths each year result from HAI whereas in Europe the HAI affected death rate per year is 25000. Out of this 25000, two third of the nosocomial infections are from Gram negative bacteria. HAI is a foremost problem in clinical settings throughout the world and the frequency is two- to threefold higher in emerging countries compared to Europe or USA.

There is a wide range of microorganisms that are frequently associated with hospital acquired infections such as Ventilator-associated pneumonia, *Pseudomonas aeruginosa*, Gastroenteritis, Hospital-acquired pneumonia, Staphylococcus aureus, *Methicillin resistant, Staphylococcus aureus, Candida Albicans*, *Vancomycin-resistant Enterococcus, Closterium difficile, Aspergillu*s and *Zygomycetes* species (Xi, Huang et al. 2009)

The common cleaning practices include the use of water, detergents and disinfectants on routine basis. The performance of disinfectant is better than detergents in killing environmental organisms but some pathogens are able to survive the exposure of specific biocides (Bogusz, Stewart et al. 2013). The prolonged use of detergents causes the environmental bacteria to become resistant. Other cleaning techniques in the same line include steam cleaning, ozone treatment, UV light treatment and hydrogen peroxide treatment. The steam cleaning system achieves 90% cleaning rate but the steam cleaning treatment has a major limitation that it cannot be used for all kind of surfaces (Berrington and Pedler 1998). Ozone based cleaning systems are well in use because of the oxidizing potential of ozone, it is highly effective on vegetative cells but has very limited application against bacterial spore and fungi (Berrington and Pedler 1998). The ozone treatment also has impact on human health since it is potentially toxic and highly corrosive in nature. UV light treatment is promising because of its ability to cause lethal damage to bacterial cells by damaging the chemical bonds in DNA at molecular level. The UV light system has limitations in terms of cost, installation and operation. The UV light has limited activity in areas with corners and in areas shielded by solid objects which change the penetration power of the UV light (Boyce, Havill et al. 2011). The stated cleaning systems have higher costs, difficult management, cleaning area limitations and need professional trainings for management of these systems (Sattar and Maillard 2013). In general, using the routine cleaning approaches repetitively, rapid disinfection can be effectively achieved but premature incorporation of microorganisms into sanitization schedule can be a serious concern (Davies, Pottage et al. 2011).

Microorganisms are known for their ability to survive on inanimate surfaces for extended times, in one case study, Pseudomonas aeruginosa sample collected from contaminated sink drains was seen to be able to survive on glass slide for seven hours (Hirai 1991). *Pseudomonas aeruginosa* and *Acinetobacter baumannii* are strongly associated with environmental contamination (Olson, Weinstein et al. 1984).

Since these cleaning techniques are a regular part of cleaning programs at the hospitals and healthcare facilities, great attention has been diverted towards 'self-sanitizing' surfaces, high-tech solution to overcome current limitations in cleaning choices (Kingston and Noble 1964). This technology was first proposed in 1964 but the potential use of antimicrobial surfaces is still in the discussion phase due to the long-held view that these antimicrobial surfaces are not suitable for prevention of hospital acquired infections (Page, Wilson et al. 2009).

The development of functionalized antimicrobial surface coatings could intrude on the risk of recurring spread of pathogens. Coating of hospital surfaces which are prone to microbial contamination could lead to killing or inhibition of microorganisms in order to disrupt transmission to patients. These coatings might prevent the buildup of microbial load on a surface without additional cleaning and would therefore contribute towards cleaning practices in the hospital environment (Page, Wilson et al. 2009). Preventing a surface from functioning as a microbial reservoir efficiently lessens the risk of further transmission in health care environments. There remains the risk for pathogen transmission from one person to another, but this issue can be solved by adopting hand hygiene practices for the nursing staff, patients and visitors. In his review, Kristopher Page et al. 2009, classified these antimicrobial surfaces into two types; namely, anti-adhesive coatings and antimicrobial coatings (Page, Wilson et al. 2009).

In anti-adhesive coatings the microbial contamination is inhibited by engineering the surface in a way that it averts the microbial adhesion to the surface. These coatings are easy-clean surfaces based on extraordinary hydrophilic or hydrophobic behavior. PEG-coated surface and Diamond like carbon (DLC) coatings are based on extreme hydrophilicity. These hydrophilic coating surfaces prevent the hydrophobic bacterial attachment. PEG and DLC assisted coatings deter microbial interactions and are non-toxic in nature. The hydrophilic surfaces make a sheet of water which causes the ease of cleaning. Another example is the polymer embedded with zwitterion head groups, the zwitterion absorbs water and makes the coating hydrophilic. This and all other coatings have good property of hydrophilicity which makes them self-cleaning but these coatings have no inherent microbial property (Hauert 2003).

In antimicrobial coatings, the antimicrobial functionality is based on the organic antimicrobial materials impregnated into the coating (Kingston and Noble 1964). Various antimicrobial coatings are commercially available, and many are in the research phase. The examples of antimicrobial coatings include Triclosan, silver, Copper, bacteriophage-modified surfaces and light-activated anti-microbial surfaces. In triclosan's inorganic antimicrobial materials are embedded such as Copper and silver, these materials have profound antibacterial activity, but these materials do not show the same antimicrobial efficacy each time. These compounds can induce resistance in the environmental microorganisms and are continuously leached out into the environment (Syed, Ghosh et al. 2014).

In bacteriophage modified surfaces, bacteriophage is applied on the inanimate surfaces as an antimicrobial coating. Since only one phage can infect the bacteria leading to the production of multiple phages. This can be used as an efficient antibacterial technique but is presented with a complication that one phage can act against only one type of bacteria, so these coated bacteriophages are less effective for open surfaces where a dynamic microbial load is present. Open surfaces would need a mixture of bacteriophages as a potent coating but another problem is the difficulty in spread of phage suspension on large areas and uneven surfaces (Chen, Liu et al. 2013).

In Polycationic antimicrobial surfaces, the surfaces are coated with negatively charged polycations which are hydrophobic in nature. These polycations kill bacteria by causing physical impairment of the cellular envelope. This Hydrophobic polycation based coating attract bacteria toward its surface, causing in rupture of the cell wall and consequent cell death (Klibanov 2007).

Another type of microbial coating is the light activated coating. This type of surface produces reactive radicals which causes nonselective antimicrobial influence on a range of microorganisms thus avoiding the potential problem of developing resistance towards the treatment. There are two types of such antimicrobial coatings; photosensitizer-based coating and catalyst-based coatings e.g. TiO_2 based coating. The effectiveness of the coating depends upon the rate of hydroxyl or any other free radicals produced and the energy of light illuminated (Klibanov 2007)

1.1 Aims and Objectives of the Project

The aim of this project is to synthesize an antibacterial and self-cleaning glass. For achieving this aim, the following objectives were set;

- Synthesis and characterization of Nickel Oxide Nanoparticle using algal extract and its Characterization.

- Preparation and characterization of Nickel Oxide thin film as an antibacterial and self-cleaning glass.
- Biomechanical testing of Nickel Oxide nanoparticles and thin film

CHAPTER 2: LITERATURE REVIEW

2.1 Background

Spread of nosocomial infections is causing increase in the death rate worldwide. Due to ever spreading risk hospital acquired infections, scientific community is proficiently working on developing new antimicrobial coatings. Cleaning, sterilizing and coating methods have been proven through research for their capacity to reduce nosocomial infections (Stickler Ifrah thesis). Nickel oxide thin film has a potential for being used as an antibacterial layer against a vast range of bacteria (Lalithambika, Thayumanavan et al. 2017) and also has proven potential to be used as a self-cleaning surface by means of superhydrophilicity (Xi, Huang et al. 2009).

2.2 Nickel oxide Synthesis

With the advent of nanotechnology, scientists are searching for solutions to various environmental problems using different types of nanoparticles. Among them, serious attention has been given to metal oxide nanoparticles due to ease of their synthesis and vast range of functionality. Nickel oxide nanoparticles have been used for so many years for the synthesis of electrochromic films, smart windows, as a photocatalyst, magnetic material, antimicrobial agent etc. (Rakshit, Ghosh et al. 2013). Nanoparticles can be synthesized using various methods of physical biological and chemical ways. Physical and chemical methods are frequently used methods for the synthesis of different nanoparticles, but the use of NiO using chemical precipitation solution of Nickel salt using hypochlorite solution. Biological methods of nanoparticle synthesis are safer and non-toxic with no use of harsh chemicals and the simplicity of procedures make them a great area of interest (Imran Din and Rani 2016).

(Naidu, Nabose et al. 2014). Nickel oxide nanoparticles have high chemical stability, super conductance, and electron transfer capability and are able to perform electro catalysis function which compelled the scientist to work on NiO applications for environmental benefits (Haider, Al-Anbari et al. 2019). Nanoparticles synthesized using physical or chemical techniques include, sol-gel, microemulsion, hydrothermal reaction, electrospray synthesis, and laser ablation but these nanoparticles are compromised in terms of productivity antioxidant potential and antimicrobial activity. The cytoxicity of these nanoparticles is higher and are not suitable for the environment(Imran Din and Rani 2016) therefore the need of time is to find benign methods for production of safe nanoparticles with better productivity . Biological systems such as algae, bacteria, fungi, algae and plant are being used to synthesize nanoparticles, in these systems, the secondary metabolites as sugars, proteins, vitamins and peptide (Ezhilarasi, Vijaya et al. 2018) act as reducing agents converting metal ions into metal atoms (Mittal, Chisti et al. 2013). Biological synthesis methods are bottom-up approaches since the major reactions involved are oxidation and reduction (Lee, Lee et al. 2006). For the synthesis of nanoparticle through biological means the choice of appropriate solvent, appropriate reducing and stabilizing agent are the main requisites (Salvadori, Nascimento et al. 2014) which ensure the synthesis of nanoparticles with control morphology and low toxicity (Lalithambika, Thayumanavan et al. 2017). For the synthesis of nanoparticle through biological means the choice of appropriate solvent, appropriate reducing and stabilizing agent are the main requisites (Yuvakkumar, Suresh et al. 2014) which ensure the synthesis of nanoparticles with control morphology and low toxicity (Yuvakkumar, Suresh et al. 2014). Rambutan peel was used to synthesize NiO nanoparticles from nickel nitrate as a reducing and stabilizing agent which were later used as antibacterial coating on fabric (Yuvakkumar, Suresh et al. 2014). Dead biomass of *Aspergillus aculeatus* was used by Salvadori and his team to synthesis nickel oxide nanoparticles (Salvadori, Nascimento et al. 2014). Sathyavathi and his team reduced NiSO4 into nickel oxide nanoparticles using nickel resistant Mycobacterium specie (Sathyavathi, Manjula et al. 2014). Khalid et al reported successful synthesis of nanoparticles from fresh water microalgae (Khalil, Ovais et al. 2018).

2.3 Nickel Oxide as Antimicrobial Agent

The strategies are proposed to explain the damage caused by metal oxides to microorganisms which include the generation of reactive oxygen species which cause oxidative damage of the membrane and electrostatic interaction which also causes damage to the membrane surface (Wilson 2003). (Khalil, Ovais et al. 2018) reported that biologically synthesized nickel oxide nanoparticles are effective antibacterial and antifungal agents. They tested the activity of NiO against *Pseudomonas aeruginosa, Bacillus subtilis, Staphylococcus aureus, Staphylococcus epidermidis, Klebsiella pneumoniae, Aspergillus niger, Aspergillus flavus* and *Aspergillus fumigatus* (Khalil, Ovais et al. 2018). These all microorganisms are notable causative agents for the nosocomial infections worldwide. The actual mechanism of action of antimicrobial activity of nickel oxide nanoparticles is still under discussion (Baek and An 2011) proposed that the possible mechanism of action of NiO antibacterial activity is the electrostatic interaction between the positively charge nickel ions (Ni ++) and negatively charged cell membrane of bacteria. This interaction of the bacterial cell membrane with nickel ions which are released from nickel oxide upon penetration into the bacterial cell causes its disruption because of change in cell physiology.

(Wong and Liu 2010) proposed that nickel oxide nanoparticles can alter the permeability of bacterial cell membrane leading to protein leakage.

2.4 Nosocomial Infection

Nosocomial infections are a worldwide problem in the hospital around the globe (Weinstein and Hota 2004). HAIs inflict an important health challenge and is the major cause of deaths worldwide (Lozano, Naghavi et al. 2012). Nosocomial infections are responsible for 7% of deaths in developed countries and 10% of deaths in developing countries which lead to increase in socio-economic encumbrance. (Saloojee and Steenhoff 2001)

2.5 Sites of Nosocomial Infections

The infection sites in the patients are the major cause of fluctuation in the rate of environmental contamination (Dancer 2014). The contamination level will be higher in rooms with patients with urine infection or open wounds then the patients with bacteremia *(Doll, Stevens et al. 2018) P. aeruginosa, vancomycin- resistant enterococci* [VRE], *Acinetobacter* species and *S. aureus* have been cultured form mattresses, mattress paddings and leaks in mattress covers (Dancer 2014) MRSA has also been collected from mops, gowns, and gloves of health care providers. VRE has been seen to be present in environmental sites such as gowns worn by patients and health service providers, medical equipment's, bed railings, environmental surfaces (Ahoyo, Bankolé et al. 2014). *Enterococcus* was seen to survive on experimentally inoculated counter tops for 58 days (Dancer 2014)but these bacteria are easily removed using disinfectants and vancomycin resistance doesn't confer any added gain for survival (Allegranzi, Nejad et al. 2011).

2.6 Pathogens causing Nosocomial Infections

The source of nosocomial infections can be endogenous or exogenous, endogenous HAI are originated from microorganism inhabiting the patient's skin and may cause infection upon physical changes in bodily organs in response to any invasive treatment. The exogenous HAI have their origin in the environment, when the patient is exposed to the hospital environment, their compromised bodies tend to catch infection from the microorganisms inhabiting the inanimate surfaces. According to CDC the most frequent HAIs reported are central line-associated bloodstream infections, which account for a total of 12-25% (Weinstein and Hota 2004)of deaths Catheter associated urinary tract infection are the most common form among the nosocomial infections and accounts for a total of 11% HAIs reported Ventilator-assisted pneumonia, gastroenteritis and methicillin resistant staphylococcus aureus infection are also major reasons of HAIs (Ahoyo, Bankolé et al. 2014). The spectrum of microorganisms causing nosocomial infections is very broad and it also includes various species of fungi and viruses as well (Ahoyo, Bankolé et al. 2014).The pathogens responsible for these and other nosocomial infections include *Pseudomonas aeruginosa, Escherichia coli, Klebsiella pneumonia, Staphylococcus aureus, Closterium diffcile, Candida albicans, Acinetobacter baumannii*, Noroviruses, Hepatitis B virus, *Influenza virus, Ventilator-associated enterococcus* etc. (Weinstein and Hota 2004).

The risk factor for the spread of HAIs are associated with the condition of patient, the nature of therapy given and the hospital environment.(Mehta, Gupta et al. 2014)the most reported risk factors include; age more than 70 years, shock, major trauma, acute renal failure, Coma, prior antibiotics, mechanical ventilation, drugs affecting the immune system (steroids, chemotherapy), indwelling catheters, prolonged ICU stay for more than three days, duration of hospital stay, indwelling catheters, mechanical ventilation, use of total parenteral nutrition, antibiotic usage, use of histamine (H2) receptor blockers (owing to relative bacterial overgrowth) and immune deficiency (Mehta, Gupta et al. 2014).

Various modes of transmission of common causative agents of nosocomial infections have been reported. S.*aureus* is transmitted through contact with the infected individual’s skin or the surfaces touched by the individual such as door handles, benches, towels and taps etc. (Weinstein and Hota 2004). E.coli transmits from person to person and from consumption of contaminated food and water (Saloojee and Steenhoff 2001). P.*aerugionsa* transmission is through breast pump, incubators, sinks, glass surfaces as windows and doors, hands of hospital (Hirai 1991). *Clostridium difficle* can stay on inanimate surfaces for months. Patients infected with *C. difficile* and hospital staff treating these patients act as major reservoirs (Boyce, Havill et al. 2011). *Vancomycin resistant enterococci* is transmitted through contamination from stool of the infected patients. The survival of *VRE* on inanimate objects is longer and can survive there for up to weeks (Syed, Ghosh et al. 2014). The transmission of *K, pneumoniae* is through person to person contact and stool contamination. The major reservoirs of *K. pneumoniae* include, respiratory machine, open wounds and catheters (Naidu, Nabose et al. 2014).

2.7 Strategies for Avoidance of Nosocomial Infections

Two major broader techniques for cleaning exist; sterilization and disinfection. Sterilization tend to destruct the surface lying microbes using methods based on heat, chemicals or pressure. Disinfection involves the use of chemicals to destroy microbes including spores (Doll, Stevens et al. 2018).

Commonly used strategy which is non-toxic to the staff and the environment includes the use of detergents based surface cleaning agents but these detergents are inferior at killing microorganisms as compared to disinfectants, the detergent cleaned area can become contaminated with bacteria (Park, Kim et al. 1998).

Rutala and Weber reported that the use of surface disinfectants can reduce the bacterial colonies to a greater extent as compared to common detergents but the efficiency of the disinfectants depends on the concentration, contact time with the surface and also special training is required for using detergents in proper way. The use of disinfectants also leads to production of toxic fumes and waste in the environment (Rutala and Weber 2008).

Cleaning systems using UV-light, ozone, steam- cleaning and HINS light are also being used worldwide as part of routine cleaning and sterilization schedule, these are effective at lessening the microbial load off the surfaces but these techniques also involve potential limitations and disadvantages such as toxicity, corrosiveness, chance of missing high risk sites, residual moisture and irradiation barriers etc. (Page, Wilson et al. 2009).

. Fluorescent markers used these days act as surrogates of residual contamination, or quantification of adenosine triphosphate (ATP) echelons representing perseverance of organic material after cleaning of surfaces. The limitation of the use of ATP markers is that these cannot properly correlate the actual colony count on the surface. This process requires hefty purchase of monitoring supplies (Doll, Stevens et al. 2018).

Labor-intensive cleaning that is performed optimally can efficiently clean hospital surfaces. However, it is dependent on variable real world practices and human behavior factors (Doll, Stevens et al. 2018)

Other cleaning strategies proposed with the advent of time include antimicrobial self-cleaning surfaces (Page, Wilson et al. 2009).

2.8 Newer alternatives for Cleaning

In lieu of existing discrepancies of the common cleaning strategies, alternative technologies are being searched and adopted. Preventive strategies are being adopted to reduce microbial contamination by fabricating surfaces which makes the adhesion of microbes to their surface unsuccessful (Dancer 2014). Antimicrobial surfaces are now being used greatly as covering material for surfaces that are greatly exposed to touch (Page, Wilson et al. 2009). there are briefly two types of antimicrobial surfaces, anti-adhesive surfaces are being established by change the water contact angle of the surface to either extremes to make them work as super hydrophilic or superhydrophobic which assists in providing self-cleaning factor to the surface which also includes the inability of microorganisms, DNA, proteins and other bio components to attach to these surfaces. Antimicrobial coatings on the other hand, are based on the incorporation anti-microbial materials on various surfaces which cause damage to the physiological structure of the microorganisms (Page, Wilson et al. 2009). Water contact angle measurement is used to measure surface energy of the coated material which indicates whether a material is hydrophobic or hydrophilic. For self-cleaning surfaces water contact angle less than 10° or higher than 140° is required. Surfaces with water contact angle between 30° to 100° do not possess self-cleaning features and are prone to biofilm formation (Page, Wilson et al. 2009).

2.9 Hydrophilic Coating

Hydrophilic coatings are gaining attention recently for their use as anti-adhesive materials. PEG coating on polyurethane surface was first introduced in 1990s and was shown to inhibit bacterial adhesion (Park, Kim et al. 1998) further research was then conducted for improvements in this coating. Another example of hydrophilic coating was Diamond like carbon coating. These coatings have been fabricated using metastable form of sp3 amorphous carbon using ion beam epitaxy and plasma assisted methods (Hauert 2003), cathode arc method, sputtering and pulsed laser (Dancer

2014). Hydrophilic zwitterionic heads are being applied on surfaces to prevent adhesion of bacteria at all thus leading to detention of biofilm formation (Cheng, Zhang et al. 2007).

2.10 Hydrophobic Coating

Hydrophobic coatings are another promising area in self-cleaning surfaces. Polycationic antimicrobial surfaces are the ones which treat their bacterial population by physical damage to their cellular envelop which is a result of the incorporated negatively charged polycations such as polyethyleneimine (Klibanov 2007). PDMS-ZnO-Nano triangle based super hydrophobic surface was developed using spray coating and UV techniques, it is a promising self-cleaning surface which may have potential to reduce biofilm formation. This coating is chemically stable at acidic and neutral pH. (Basiron, Sreekantan et al. 2018). Nano/micro silica nanoparticles based super hydrophilic coating was made using dip-coating method in silica-THF emulsion. This chemically robust coating may cause reduction in microbial attachment to coated surface (Cholewinski, Trinidad et al. 2014).

2.11 Antimicrobial Coatings

Antimicrobial coatings are mostly in research phase. Only a few are available on commercial basis. (Dancer 2014). These coatings are based on impregnated organic antimicrobials or copper formulations (Medlin 1997). Microban, a type of triclosan, relies on inorganic silver or copper. The efficacy of these coatings decreases with time as the diffuse into environment and leach out. Such triclosan's produce poisonous dioxins upon exposure to UV light (Syed, Ghosh et al. 2014). Silver coatings are effective initially but not permanent and bacteria can gain resistance to silver coating (Sütterlin, Molin et al. 2014). Such coatings rely on additional diffusible materials such as rifampin (Taylor, Phillips et al. 2009, Stobie, Duffy et al. 2010). Light activated coatings produce reactive radicals which are bio toxic and exert nonspecific effect on a wide range of microorganisms (Wilson 2003) thus avoiding the problem of resistance. The photosensitizer type of coting has a photosensitizer embedded in it (Dancer 2014). The second type of coating is based on TiO_2 catalyst (Matsunaga, Tomoda et al. 1988). The mechanism of photocatalysis is based on the production of hydroxyl radicals at the surface of TiO2 which is dependent on energy from light illumination (Leng, Soe et al. 2013). Photocatalysis based disinfection is less toxic and better alternative than chemical disinfectants (Dancer 2014).

2.12 Surface Coatings with Nickel Oxide

Chtouki, Soumahoro et al. 2017 prepared NiO thin film using $NiCl_2.6H_2O$ based sol-gel of two different molarities through spin coating and spray pyrolysis which were then annealed at 350°C for 45 minutes. The spin coated films yielded better results than the sprayed ones in terms of surface topology (Jlassi, Sta et al. 2014) proposed the synthesis of thin film using spin coating technique at 3000 rpm for 30 seconds and the morphology of the annealed film was shown to vary with varying annealing temperature. The 24 hours aged sol-gel prepared for the coating had a concentration of 0.5M nickel acetate. The spin coated film proposed best result with annealing at 600°C under nitrogen atmosphere (Haider, Al-Anbari et al. 2019) synthesized NiO thin film through spin coating using sol-gel prepared form nickel acetate dissolved in 2-Methhoxethanol with nano-ethanolamine as a catalyst. The thin film annealed at a range of 450°C-650°C result with water contact angle of 0°C, the super hydrophilic nature of the thin film makes it suitable for self-cleaning application. NiO thin film was prepared through dip coating method using nickel nitrate-based sol in methanol. Antibacterial activity conducted using drip method under UV light and dark yielded good antibacterial activity against *E. coli* (Adekunle, Oyekunle et al. 2014).

CHAPTER 3: MATERIALS AND METHODS

3.1 Materials

3.1.1 For Algae Growth Culture

Algae culture of strain *Dictyosphaerium sp.* Strain DHM 2(LC159306) taken from lab mate, Muneeba Khalid (Khalid, et al. 2017) , Air pumps, Bold's Basal media, $NaNO_3$ (Sodium nitrate from Uni-Chem), MgSO4·7H2O, (Magnesium Sulphate from Daejung) NaCl (Sodium Chloride from Merck), K2HPO4, (Dipotassium Hydrogen Phosphate from Panreac) KH_2PO_4 (Potassium Dihydrogen Phosphate from Panreac) $CaCl_2 \cdot 2H_2O$ (Calcium Chloride from Daejung), H_3BO_3 (Boric acid from Merck) , $ZnSO_4 \cdot 7H_2O$ (Zinc Sulphate from Sigma-Aldrich), $MnCl_2 \cdot 4H_2O$ (Manganese Chloride from Duksan|), MoO_3 (Molybdenum Trioxide from Daejung), $CuSO_4 \cdot 5H_2O$ (Copper Sulphate from Riedal-de-Haen), Co(NO3)2 from Uni-Chem, Biomass, Deionized water, Ethanol from Riedal-de-Haen, paraffin oil from Sigma-Aldrich, distilled water, chloroform from Riedal-de-Haen, H_2SO_4 from Riedal-de-Haen, NaOH from Riedal-de-Haen, Ammonium Chloride (NH_4Cl) from Riedal-de-Haen, HCL, Marquis Reagent from Merck, Formaldehyde from Riedal-de-Haen, Ferric Chloride $(FeCl_2)_3$ from Panreac Glacial Acetic Acid from Riedal-de-Haen, Molish Reagent from Merck, Fehling A solution, Fehling B solution from Merck and Filter paper.

3.1.2 For Algae Extract and Phytochemical Analysis

Algae Biomass, Deionized water, Ethanol, paraffin oil, distilled water, chloroform, H_2SO_4, NaOH, Ammonium Chloride (NH_4Cl), HCL, Marquis Reagent, Formaldehyde, Ferric Chloride (Fe $(Cl_2)_3$), Glacial Acetic Acid, Molish Reagent, Fehling A solution, Fehling B solution and Filter paper.

3.1.3 For Nickel Oxide

$NiCl_2.6H_2O$ from Daejung, Ethanol from Riedal-de-Haen, Deionized water, Algae extract.

3.1.4 For Nickel Oxide Thin Film

Nickel oxide nanoparticles, Tetrahydrofuran from Sigma-Aldrich, Deionized water, Soda lime glass, Acetone from Riedal-de-Haen, Ethanol from Riedal-de-Haen

3.1.5 For Characterization Studies

Muller Hinton Agar from Oxoid, Tryptone soy broth from Oxoid,, NaCl form Merck, Distilled Water, Acetone from Riedal-de-Haen, ethanol from Riedal-de-Haen

3.1.6 For Antibacterial Activity

Nutrient broth from Oxoid, Nutrient agar media from Oxoid, Muller Hinton agar media from Oxoid, 0.85% normal saline, NiO nanoparticles, deionized water, Nickel oxide thin film, $BaCl_2$ (Barium Chloride from Sigma-Aldrich), H_2SO_4 from Riedal-de-Haen, Dimethyl sulphoxide (DMSO) from Panreac, Ciprofloxacin drug from Oxoid, Sterile cotton swab, bacterial inoculums *(P. aeruginosa, E. coli, K. pneumoniae)*

3.1.7 For Ring Test Assay

Crystal Violet 1% from Merck, Tryptone Soy Broth (TSB) media from Oxoid, Distilled water, 0.85% Saline, Bacterial inoculums *(P. aeruginosa, E. coli, K. pneumoniae)*

3.1.8 For Antibiofilm Assay

TSB media from Oxoid, inoculums (*P. aeruginosa, E. coli)*, Phosphate Buffer Saline (PBS) from Sigma-Aldrich, Paraformaldehyde from Icon Chemicals, Chilled Ethanol from Riedal-de-Haen (concentrations 25%, 50%, 75%, 95%, 100%),

3.1.9 For Self-Cleaning Assay

Diluent-ketchup solution (2:5 ketchup and water).

3.2 Methods

3.2.1 Algae Culturing for Growth

For algal biomass collection, a previously identified strain *Dictyosphaerium sp.* Strain DHM 2 (LC159306 (Khalid et al., 2017) was used as an inoculum. The strain was grown in a 1L culture bottle in which distilled water, Bold's Basal Media (BBM) were added. The culture bottles are provided with air pumps to provide continuous mixing and aeration of algal components. The whole culture set up was placed in an algal growth rack with white florescent lamp at 10µmol photons m-^{2}s^{-1} with a 24hour light cycle, as shown in Fig 3.1.

Figure 3.1: **Algae growth culture setup at 25◦C, white florescent lamp at 10µmol photons m-^{2}s-^{1} with a 24hour light cycle**

The total span of one algal culture to give required biomass is 30 days. For setting up an algal culture for the purpose of biomass, we add 20-50ml of inoculum, 50-100ml of BBM and then filled with distilled water to make 1L (Khalid et al., 2017).

3.2.2 Biomass Collection

After 30-day cycle, the culture bottles were taken out of the system and were kept aside for a few hours to let all the algal biomass sediment. After sedimentation, the above water was discarded, and the thick algal biomass was washed using distilled water. In the first step, centrifugation at 5000rpm for 10 minutes was done to make a pellet and the supernatant containing salts was discarded and then the pellet was suspended in distilled water for washing at 6000 rpm for 10 minutes. The washed pellets were collected in china dish and dried in hot air oven at 55°C. The dried biomass is then crushed into a fine powder and used for extract preparation (Sierra, Dixon, & Wilken, 2017).

3.3 Preparation of Algae Extract for Nickel Oxide Synthesis

Powdered biomass of algae (3g) was added to 1:2 ethanol and water mixture and refluxed for 4 hours at 60°C, shown in Fig 3.2. After 4 hours of reflux, the mixture was kept at 4°C overnight

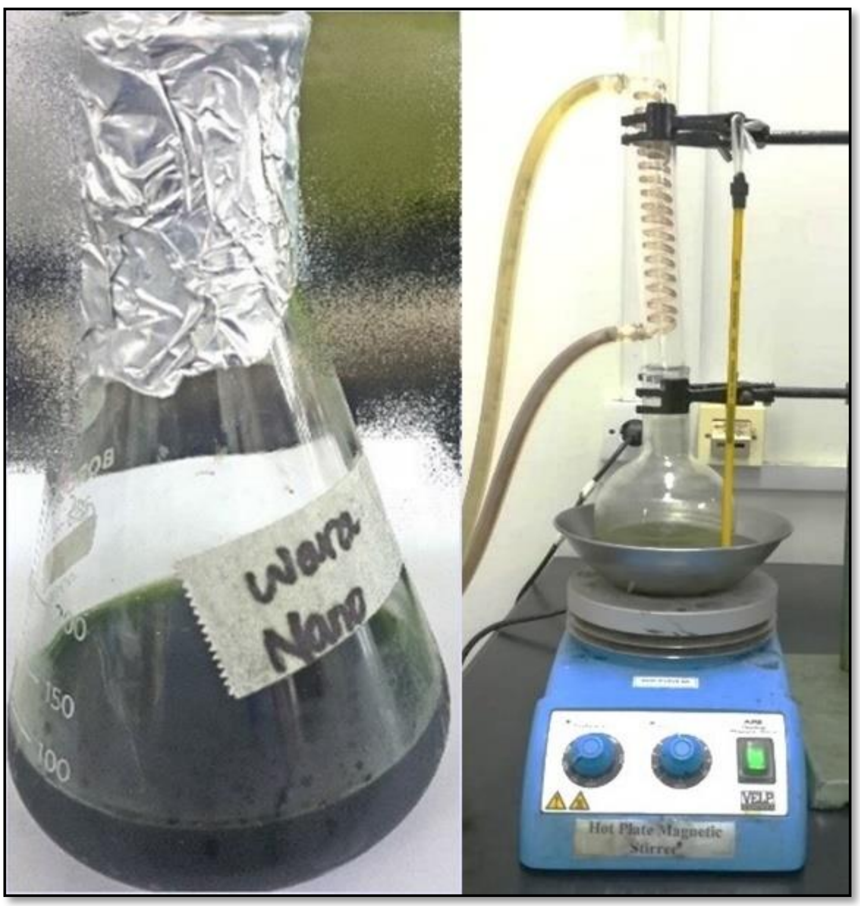

Figure 3.2:**Algae extract using mixture of water and ethanol**

.

The refluxed algae extract was then filtered twice using wattmann No. 1 and later used in reaction for Nickel oxide nanoparticle synthesis. Any leftover algae extract can be kept at 4°C for up to a week (Khalil et al., 2018).

3.3.1 Phytochemical Analysis of Algae Extract

For the identifying the constituents of extract that may act as a possible reducing agent i.e. Alkaloids, Carbohydrates, Cardiac glycosides, Flavonoid, Phenols, Saponins, Tannins, Terpenoids, Quinones, and Proteins etc. during the synthesis for nanoparticles were assessed by phytochemical analysis (Tayade, Borse, & Meshram, 2018). For phytochemical analysis, following tests were performed; The methodology for phytochemical tests stated in the table 3-1 was adopted from (Tayade, Borse, & Meshram, 2018).

Table 3-1: **Tests for phytochemical analysis of extracts**

Saponins	2 ml of extract+6 ml of distilled water was added and shaken vigorously Formation of bubbles or persistent foam= Saponins.
Steroids	2ml chloroform+ 1ml Sulphuric acid+ 0.5ml extract = Formation of reddish-brown ring at interface
Coumarins	1 mL of 10 % NaOH +1 mL of algal extract = Formation of yellow color
Quinones	1 mL of concentrated sulphuric acid +1 mL algal extract = Formation of red color
Flavonoids	2 ml of each extract + few drops of 20% NaOH, the formation of intense yellow color is observed. To this, few drops of 70% dilute hydrochloric acid was added and yellow color was disappeared which indicates the presence of flavonoids in the sample extract
Tannins	2 ml of each extract + 10% of alcoholic ferric chloride = formation of brownish blue or black color.
Phenol	2 ml of each extract+2 ml of 5% aqueous ferric chloride = formation of a blue color indicates the presence of phenols
Proteins	2 ml of each extract + 1 ml of 40% sodium hydroxide + few drops of 1% copper sulfate= formation of violet color
Cardiac Glycosides	1 ml of each extract +0.5ml of glacial acetic acid + 3 drops of 1% aqueous ferric chloride solution was added = brown ring at the interface indicates the presence of cardiac glycosides
Terpenoids	1ml of extract + 0.5 ml of chloroform followed by a few drops of concentrated sulphuric acid= the formation of reddish-brown precipitate indicates the presence of Terpenoids.
Carbohydrates	1 ml of extract+ few drops of Molish reagent + 1 ml of concentrated sulphuric acid at the side of the tube. Allowed to stand for 2 to 3 minutes. Formation of red or dull violet color
Oils and Resins	Apply a drop of extract on filter paper, it indicates the presence of oils and resins.

3.4 Synthesis of Nickel Oxide Nanoparticles from *Dictyosphrium sp*

0.5M of $NiCl_2.6H_2O$ was added to 25ml of algal extract and stirred for 2.5 hours at room temperature (25°C) until color change was observed. The precipitated solution was dried on a hot plate at 100°C to remove water content the dried nanoparticles were then sonicated for one hour in pure ethanol once for washing using centrifugation at 6000rpm for 10 minutes (Lalithambika, Thayumanavan, Ravichandran, & Sriram, 2017). The dried nanoparticles were then powdered and calcined at 550 °C in muffle furnace for 2 hours. Schematic representation of NiO nanoparticle synthesis is shown in Fig 3.3.

3.5 Characterization of Nickel Oxide Nanoparticles

3.5.1 X-ray Diffraction Study

XRD is a non-destructive analytical technique which is used to analyze the crystalline phases of material under question. The size and intensity of the peaks in XRD shows the crystalline or amorphous nature of the sample. During XRD analysis the two-theta range selected was 5°- 80° along with Cu K-alpha radiation (λ= 0.15418 nm). The step size for the XRD scan was at 0.020° and analysis was performed at voltage 20kV with current set at 5mA and at 25°C. The XRD results were further analyzed using "Origin Pro 8" and "Xpert High score" analysis software.

3.5.2 Scanning Electron Microscopy

Veg 3 Tescan Tungsten thermionic emission SEM was used for analyzing the morphology, microstructure and topography of Nickel oxide sample. It generates 2D images and gives qualitative information about the appearance of the sample.

The sample preparation is as further, very thin layer of Nickel oxide nanoparticle powder sample was placed directly on the sample holder with the aid of carbon tape, the sample was then sputter coated with gold under Argon purging using Quorum Sputter Coater.

The samples were analyzed at voltage 20kV, magnification up to 44.3kx with the scale of 0.5nm, 1um and 2um. The working distance was maintained at 9.55mm with the field view range between 3.1um to 7.65um.

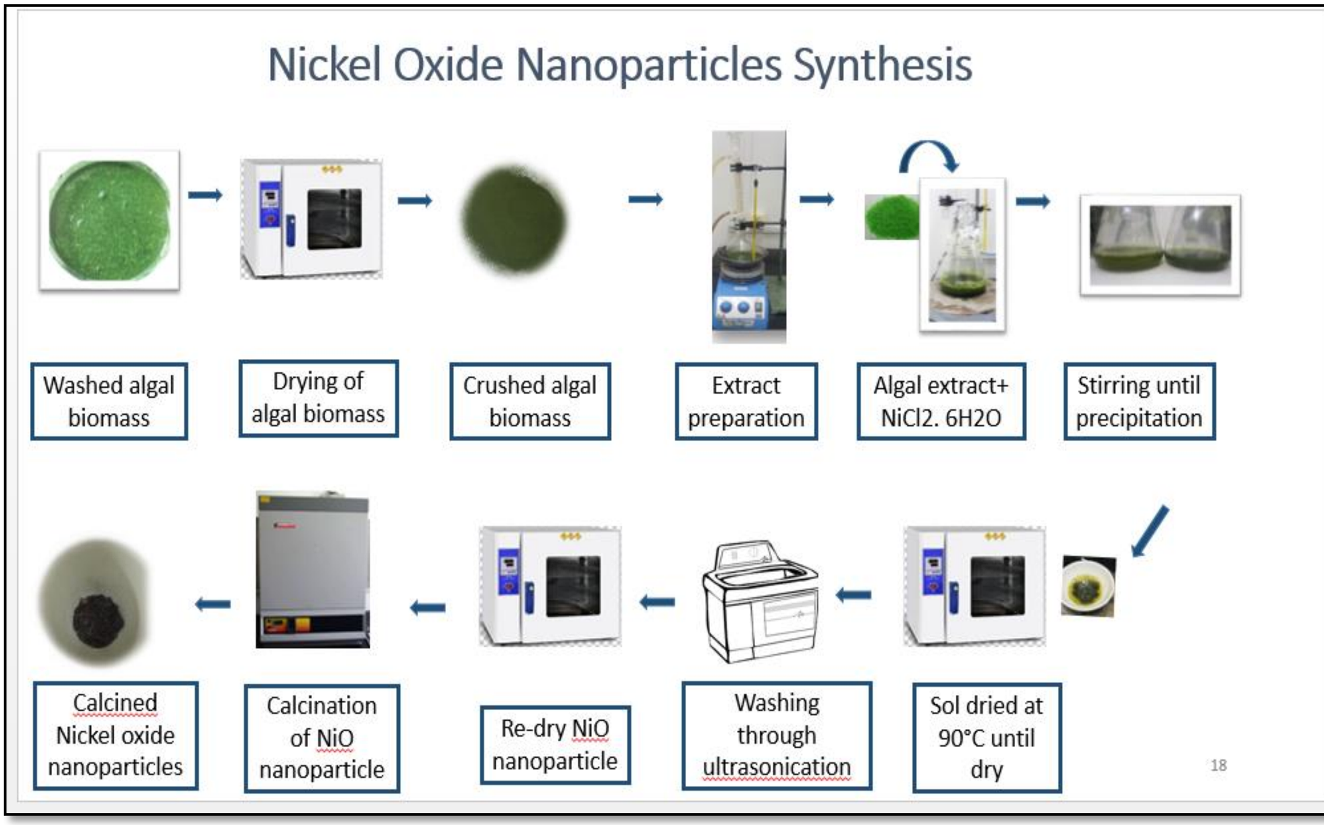

Figure 3.3: **Schematic representation for synthesis of Nickel Oxide Nanoparticles**

3.5.3 Energy Dispersive Spectroscopy

EDS extends the validation of SEM analysis. It is a chemical microanalysis technique which shows the elemental composition of the sample. In EDS a line or point spectrum is analyzed which is considered as representative of the whole sample under analysis. EDS is based on the interaction between the sample and source of X-rays. Voltage of 20keV at a scale of 5um was set for EDS analysis of NiO nanoparticle using Veg 3 Tescan EDS.

3.5.4 UV-visible Spectroscopy

UV-visible spectroscopy makes use of Ultraviolet light for analyzing samples, the ultraviolet light excites the atoms in the sample which is recorded as peaks of absorbed light beam on a spectrum. Absorbance and transmittance properties of the samples can be studied using UV-visible spectrophotometry. The absorbance of sample can be in the form of single wavelength or spectrum of extended range.

The spectrometer of the instrument records the degree of absorbance at different wavelength and the graph is generated between absorbance (A) versus wavelength (ƛ). The obtained graph is called as spectrum and is recorded in the range between 200-800nm. For nickel oxide the UV range is between 370nm-450nm (Adekunle, Oyekunle, *et al.*2014).

3.5.5 Atomic Force Microscopy

AFM is a more powerful instrument in presenting images with 3D topography of the sample where we can measure the height and thickness of the nano compounds. It generates images with atomic resolution. The NiO nanoparticles to be analyzed were deposited on a clean glass slide and the sample was dried under UV lamp. The sample is scanned through microfabricated cantilever tip of AFM machine and provides information about the morphology and uniformity of the object. Flex AFM C3000 was used for the analysis of Nickel oxide nanoparticles and the value of cantilever spring constant is 0.2 N/m with resonance frequency of 179 KHz.

3.5.6 Thermo Gravimetric Analysis

Thermo gravitational analysis (TGA) is a technique used for the characterization of various materials for application in nanomaterial, food, pharmaceuticals and petrochemicals etc. The increase or decrease in the weight of sample upon heating is monitored in TGA, as a function of time or temperature, under controlled atmosphere (Bi & He, 2013)

The analysis of Nickel oxide nanoparticle precursor was carried out on Ascii DTG-60H analyzer system in nitrogen atmosphere, at a temperature range of 25°C to 800°C with 10°C/min.

The TGA analyzer has an alumina pan of 15mg weight capacity for holding samples. Nitrogen gas is used as carrier for protection of samples from oxidation. The TGA results for nickel oxide nanoparticle precursor are analyzed through literature and graphs of TGA have been plotted using "Origin Pro8" software.

3.5.7 Fourier Transform Infrared Spectroscopy

FTIR spectroscopy is based on Infrared radiations where the frequencies vary among different functional groups. Spectrum 100 FTIR spectrometer was used for the analysis of NiO nanoparticle and algae extract so that an analysis for the presence of algal functional groups on the surface of Nickel oxide nanoparticles can be made. This instrument can analyze all types of samples using solid, liquid and gas.

For FTIR analysis, the sample is prepared using Specac Manual Hydraulic press/ FTIR-Pellet-press where Potassium Bromide (KBr) is used as a carrier for the sample in FTIR since KBr is optically transparent in the IR region ranged 4000-400cm^{-1}. Added ability of KBr is to form plastic sheet like structure under pressure.

For sample preparation, 1% of the sample, solid or liquid, is mixed well with 200-250mg KBr inside the sample holder of FTIR-Pellet-press and a pressure of approximately 5-8 tons is applied by the hydraulic press turning it into a pellet. The prepared sample pellet is then subjected to FTIR analysis, in range selected between 4000-400cm^{-1}, for the presence of various bond interactions. The chemical composition of the obtained FTIR result is analyzed using "Origin Pro 8" software whereas the peak values for different functional groups are matched using literature.

3.5.8 Zeta Potential Analysis

Malvern Zetasizer, verion 7.10 was used for analyzing the zeta potential of NiO nanoparticles at 25°C. Zeta analyzer is used for the analysis of charge distribution of our sample for the sake of measuring stability of the material. Higher stability of the material depends upon how higher the positive or negative value in its magnitude is. For sample preparation, NiO dispersion in deionized water was made after hour long sonication and the sample was then poured in clean cell of zeta analyzer.

3.6 Nickel Oxide Thin Film Synthesis

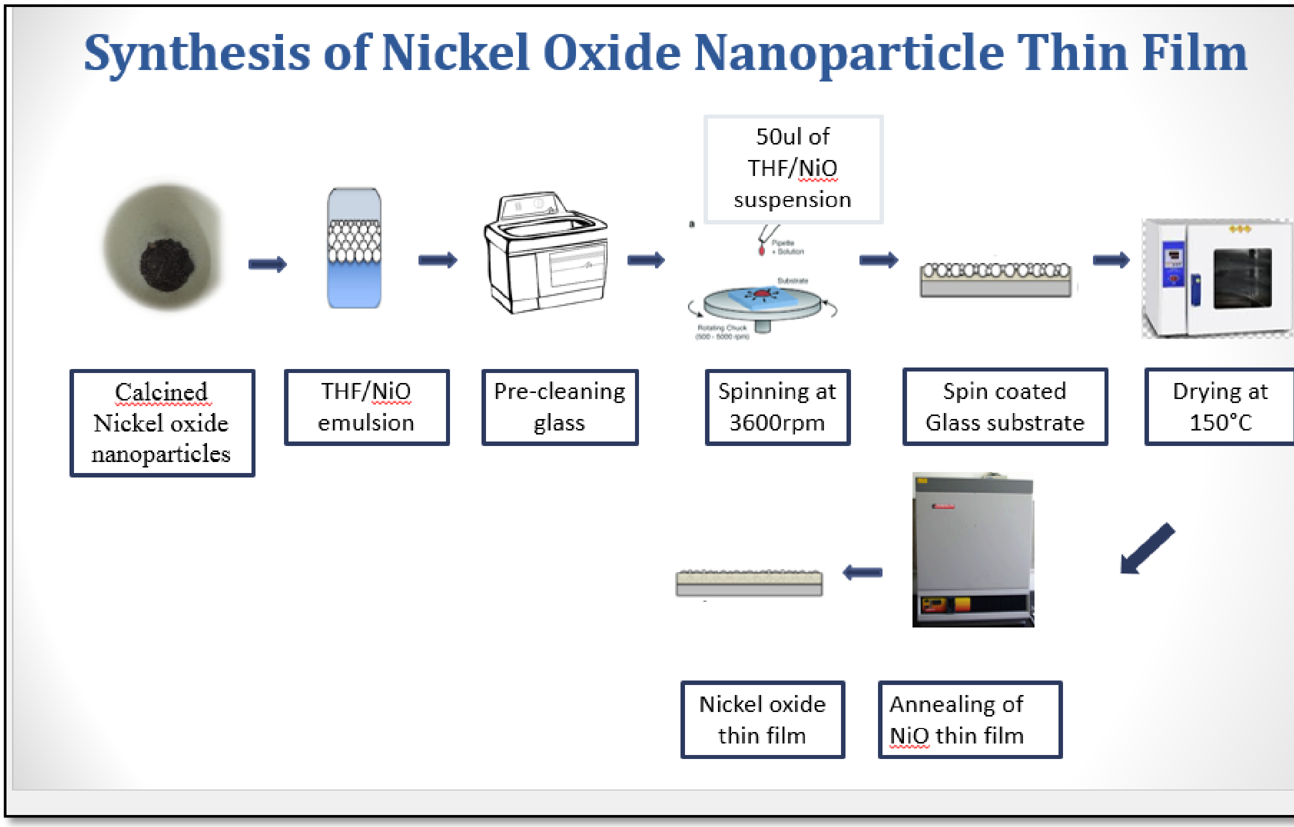

Figure 3.4: **Schematic representation for the formation of Nickel Oxide thin film using spin coating technique**

3.6.1 Tetrahydrofuran/Nickel Oxide Emulsion Preparation

The NiO nanoparticles were added in 20ml of Tetrahydrofuran (THF) in range from 0.5%-6% by weight percentage. This mixture was vortexed for 1-5 minute to ensure good dispersion. NiO and THF mixture was added with 70ml of ultrapure water and vortexed again for 1 minute. After vertexing the mixture was sonicated for 10 hours at room temperature in order to get a uniform dispersion of NiO nanoparticles in NiO-THF emulsion. The prepared emulsion was then used for nickel oxide thin film synthesis (Cholewinski, Trinidad, McDonald, & Zhao, 2014).

3.6.2 Pre-treatment of Glass

The Soda lime glass (SLG) was pre-cleaned thoroughly prior to coating. The SLG was washed in soap and then proceeded through steps of further sonication-based cleaning to ensure maximum effectiveness of the coating procedure. Firstly, the SLG was sonicated in absolute ethanol for 10 minutes. After that the SLG was sonicated in deionized water for the next 10 minutes. After making sure that the surface of SLG was cleaned enough, one last sonication of SLG was done in absolute acetone for 5 minutes to ensure absence of all water marks and any possible grim (Marques, Mansur, & Mansur, 2013).

3.6.3 Spin-Coating of Tetrahydrofuran/Nickel Oxide Emulsion on Glass

For spin coating the NiO-THF emulsion was kept on a hotplate at 125°C for 20 seconds, to make sure that the NiO nanoparticles rose up to the top layer. Form the top layer of NiO-THF emulsion 50 microliter of the emulsion was picked up and placed on the pre-cleaned glass which had been placed on the spin coater SCS G3-8 Spin coat with the help of double-sided sticking tape. THF emulsion was constantly kept at 125°C to ensure maximum nanoparticle transfer for coating and the THF solution was vortexed for 30 seconds at full speed before every coating procedure, this ensured the breakdown of bubbles in the emulsion which provided more uniformity to the coating procedure. The sample was spin coated on the glass for 30 seconds at 3600rpm (Chtouki et al., 2017). The schematic representation of NiO thin film is shown in Fig 3.4.

3.6.4 Annealing of Nickel Oxide Thin Film

After spin coating the coated SLG was kept in hot air oven at 150°C for 10 minutes to ensure removal of THF solvent (T. Chtouki, *et al.*2016). After drying procedure, the coated SLG was annealed in an open-air furnace at 400°C with ramp time of 2°C/minute and holding time of 1 hour. The annealed Nickel oxide thin film shown in Fig 3.5 was then characterized further (Haider *et al.*2019).

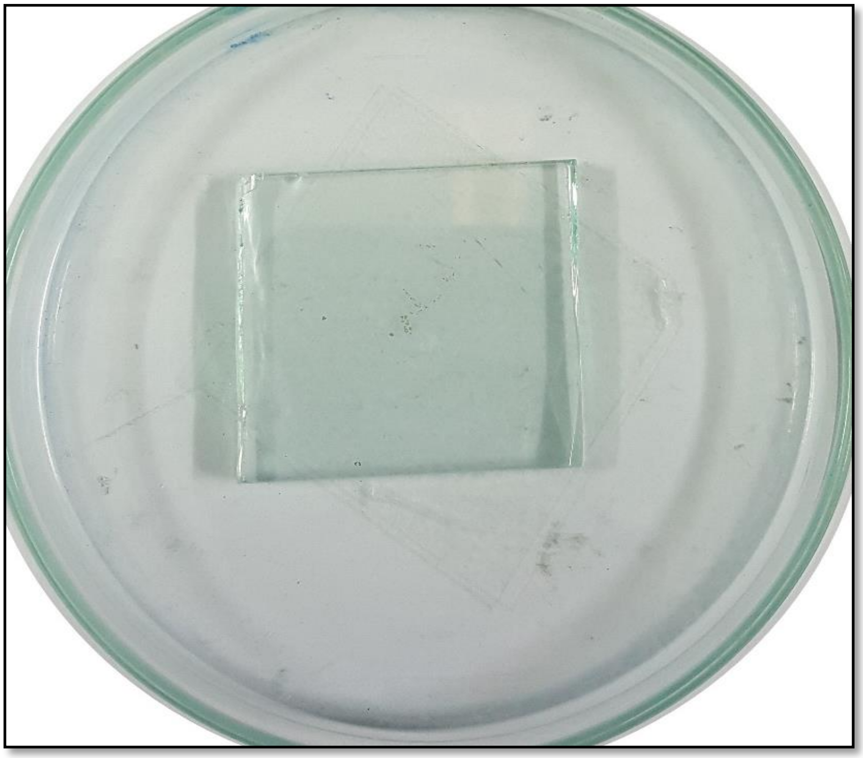

Figure 3.5: **Prepared Nickel Oxide thin film annealed at 550◦C**

3.6.5 Optimization of Nickel Oxide Thin Film

For the optimized synthesis of Nickel oxide based thin film, different concentrations of NiO nanoparticles in the emulsion ranging from 0.5% by weight to 6% by weight were prepared. After performing spin coating and annealing procedure on same condition i.e. 3600rpm for 30 seconds and annealing at 400°C. The nickel oxide thin film coated glass with the least contact angle was taken to further characterizations including XRD, UV-visible spectrophotometer and AFM (Chtouki et al., 2017).

3.7 Characterization of Nickel Oxide Thin Film

3.7.1 X-ray Diffraction Study

For XRD analysis of the Nickel oxide thin film the two-theta range was selected 5°- 80° along with Cu K-alpha radiation (λ= 0.15418 nm). The step size for the XRD scan was at 0.020° and the analysis was performed at voltage 20kV with current set at 5mA and at 25°C. The XRD results were further analyzed using “Origin Pro 8” and “Xpert High score” analysis software.

3.7.2 Scanning Electron Microscopy

For the morphological analysis of Nickel oxide thin films, the samples were sputtered with gold under Argon purging using JEOL JFC-1500 ion sputtering device. Roughly, it generates a coating of 50 nm over the sample. After sputtering, the samples were analyzed using JEOL 6490LA SEM. The samples were processed at voltage of 10kv, magnification range from 20kx-30kx at the scales of 0.5um, 1um and 2um with working distance of 9.05mm.

3.7.3 Energy Dispersive Spectroscopy

For the energy dispersive spectroscopy, Nickel oxide thin film was analyzed at the voltage of 20keV and scale of 10um.

3.7.4 Optical study of Nickel Oxide Thin Film using % Transmittance

After the coating of nickel oxide thin film over pre-cleaned glass substrate, there was a need to access the level of opacity induced by the thin film to the SLG. For this purpose, the absorbance and % Transmittance data of the nickel oxide thin film is recorded in the wavelength range of 200-800 nm. The instrument used for this analysis was "Jenway 7315 UV-spectrometer". The result files retrieved from UV-visible spectrophotometer were analyzed using "Microsoft excel 2013" and "Origin Pro 8".

3.7.5 Atomic Force Microscopy

Flex AFM C3000 with the value of cantilever spring constant at 0.2 N/m with resonance frequency of 179 KHz was used to analyze the average surface roughness of the nickel oxide thin film. The 3D images of AFM were analyzed using Nano surf 3000 software.

3.7.6 Water Drop Contact Angle Measurement

Drop Shape Analyzer DSA-25 was used to determine the contact angle of a droplet on the surface. A drop of water falls on a sample surface and then was measured through different means. A sessile drop was placed on the solid sample and image of this drop was analyzed using a Drop Shape Analysis software.

3.8 Antibacterial Activity of Nickel Oxide Nanoparticles

3.8.1 Collection of Bacterial Strains

Firstly, for antibacterial activity, three bacterial strains as representative of the frequent source of nosocomial infections namely, *P. aeruginosa ATCC* 9027, *E. coli* ATCC8739 *and K. pneumoniae* were selected for checking the antibacterial activity of NiO nanoparticles (Oberdorfer. P, *et al,* 2009). The strains were provided by Food Microbiology lab.

3.8.2 Preparation of Nanoparticle Concentration

The prepared NiO nanoparticles were weighed and added to DMSO for making bacterial concentrations for use in antibacterial activities. The concentrations chosen were 1.5mg, 2.5mg and 3.5mg and the prepared concentrations were sonicated for 1 hour at 25°C before antibacterial activity (Rakshit et al., 2013).

3.8.3 Preparation of McFarland Standard

McFarland 0.5 is a standard used for comparing the turbidity of the bacterial suspensions in saline. If the turbidity of the bacterial saline and McFarland standard matches, the bacterial saline is thought to be of optical density (OD) 0.5. For the preparation of the McFarland standard, 0.05ml of 1.17% Barium Chloride ($BaCl_2$) was added with 9.95% of 1% Sulfuric acid (H_2SO_4). The OD of the prepared McFarland was then calculated on spectrophotometer, 0.9 is the standard OD for the prepared suspension. The McFarland standard was vortexed well and stored in sealed tube at 4°C in dark (McFarland, 1907).

3.8.4 Antibacterial Well Diffusion Assay

For Antibacterial activity firstly, the Nutrient agar media, nutrient broth, Muller Hinton agar media, saline 0.85% were prepared and autoclaved along with petri dishes, test tubes and micropipette tips etc. Next the plates were poured with media inside laminar flow hood which had been previously treated with 75% ethanol and UV light source to keep the working environment sterilized.

After confirming the sterility of the plates, inoculums were streaked on the nutrient agar plates and grown over night. The next day, bacterial saline suspensions were made in saline by taking 5ml of 0.85% saline in sterilized test tube and a loop full bacterial colony was picked up using wire loop and mixed into the saline with the help of vortex mixer. The turbidity of the bacterial saline suspensions was compared with McFarland standard. For well diffusion assay, when the OD of bacterial saline suspension is considered as 0.5, 100ul of the suspension was dropped onto MHA plate with a help of micropipette. Bacterial lawn was then made from this inoculum using sterile cotton swab/ glass spreader. After lawn formation, 4 wells of 6mm were made inside the media using well borer (Heatley, 1944). 50ul of each NiO nanoparticle suspension was added in the labeled wells and 50ul of DMSO was used as a negative control. Here ciprofloxacin drug was chosen as positive control, diagrammatic process shown in Fig 3.6 The plates were incubated overnight at 37°C and the results were recorded by measuring the zones of inhibition and the data obtained was used to plot graph (Rakshit et al., 2013).

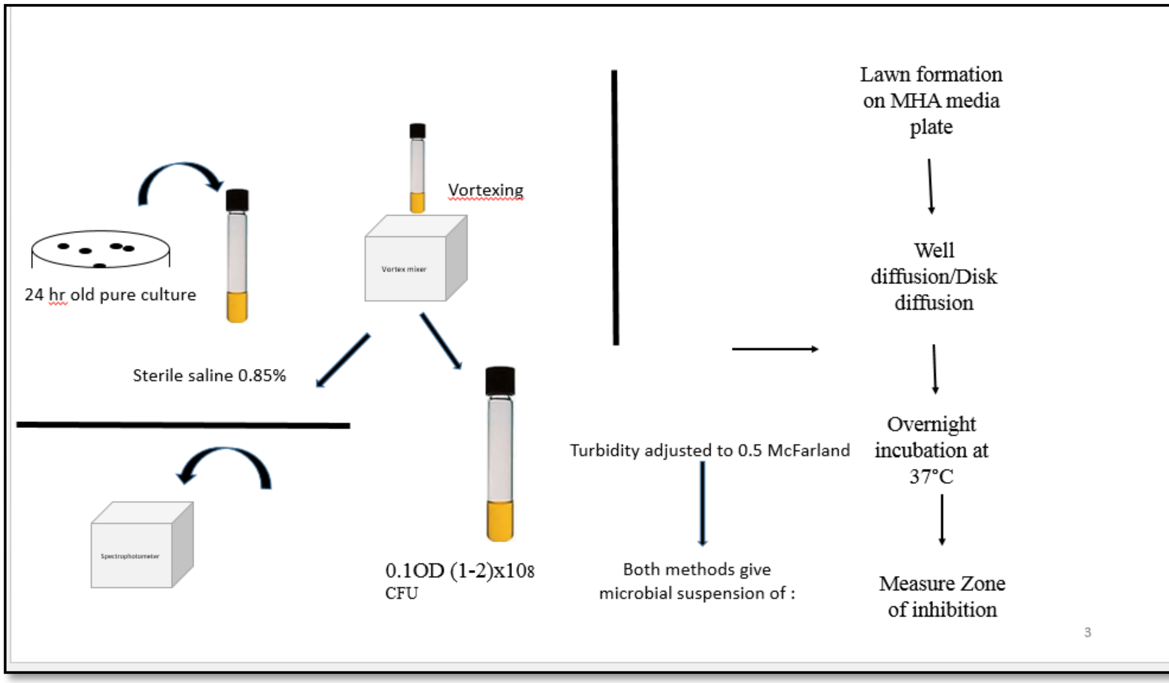

Figure 3.6: **Flow diagram for antibacterial activity**

3.9 Biomechanical Testing of Nickel Oxide Thin Film

3.9.1 Antibacterial Activity of Thin Film

3.9.1.1 Bacterial Culture

Three bacterial strains as representative of nosocomial infection causing bacteria i.e. *E. coli* ATCC8739, *P. aeruginosa* ATCC9027 and *K. pneumoniae* were used for antibacterial activity of the nickel oxide thin film using the same procedure.

3.9.1.2 Preparation of Media

For antibacterial activity, Nutrient agar media, nutrient broth media and Muller Hinton agar media were prepared as dissolving them in distilled water and autoclaving them. The autoclaved media was then poured into sterile petri dishes inside the sterilized environment of laminar flow hood.

3.9.1.3 Zones of Inhibition Assay

For the antibacterial activity of the nickel oxide thin film, bacterial lawn was made on the MHA plates as stated above and the nickel oxide thin film was placed on the media plate along with bare glass which acted as a negative control, both glass samples were cleaned under UV light for 10 minutes prior to their placement onto the MHA plates, the plates were then incubated overnight at 37°C and the results were then recorded by measuring the zones of inhibition (Karunanidhi et al., 2017).

3.9.2 Antibiofilm Activity of Nickel Oxide Thin Film

3.9.2.1 Ring Test Assay

For ring test assay the bacterial inoculum were added into 5ml of TSB broth media and their OD was checked after overnight growth, at 600nm using spectrophotometer. After adjusting the OD to 0.5, 100ul of each of the mother culture were added into new test tubes containing 5ml of sterile TSB broth media, diagrammatic process shown in Fig 3.7.

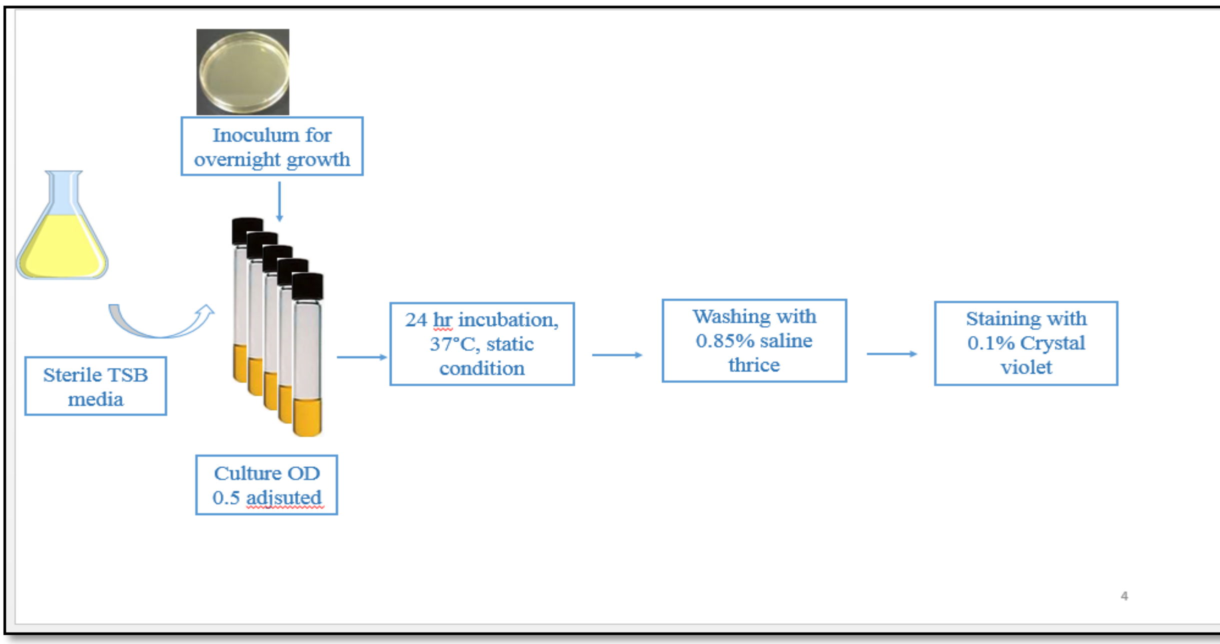

Figure 3.7: **Ring test assay methodology**

The inoculated TSB media tubes were vortexed well and incubated at 37°C under static condition for 24 hours (Di Domenico et al., 2016) After 24 hours, the bacterial cultures were discarded, and the tubes were washed twice with 0.85% saline solution. The washed tubes were dried in hot air oven. Once the tubes were dried, they were stained with 0.1% of crystal violet dye solution for 10 minutes.

The stained tubes were then washed thrice using 0.85% saline solution. The tubes were then dried in oven and ring formation was observed and recorded using a mobile camera lens.

The formula for setting OD is;

$$\frac{\text{Required OD x Required volume}}{\text{OD of Mother Culture}}$$

3.9.2.2 Biofilm Formation of Selected Bacteria

The selection of bacterial species for anti-biofilm studies i.e. *P. aeruginosa* and *E. coli* were collectively based on the results of antibacterial activity and ring test assay.

First the biofilm was formed by inoculating 5ml of Luria Bertani broth with 50ul of selected biofilm forming bacterial strains. After 48hours, these bacterial cultures were grown in TSB broth at 37°C overnight.

3.9.2.3 24 and 72Hours Treatment with Nickel Oxide Thin Film

Nickel oxide thin film coated glass was used for biofilm inhibition studies on two bacteria, i.e. *P. aeruginosa* and *E. coli* for two-time durations i.e. 24 hours and 72 hours. 50ul from the overnight bacterial culture was released onto the NiO thin film coated glass as well as on the bare glass which acted as a positive control, already placed inside the 6-well microtiter plates. The last two wells on the 6-well plate only contained 6ml of sterile TSB media which acted as a negative control, 6ml of sterile TSB media was also added to the wells containing NiO coated glass and bare glass, shown in Fig 3.8 (Coenye, Peeters, & Nelis, 2007).

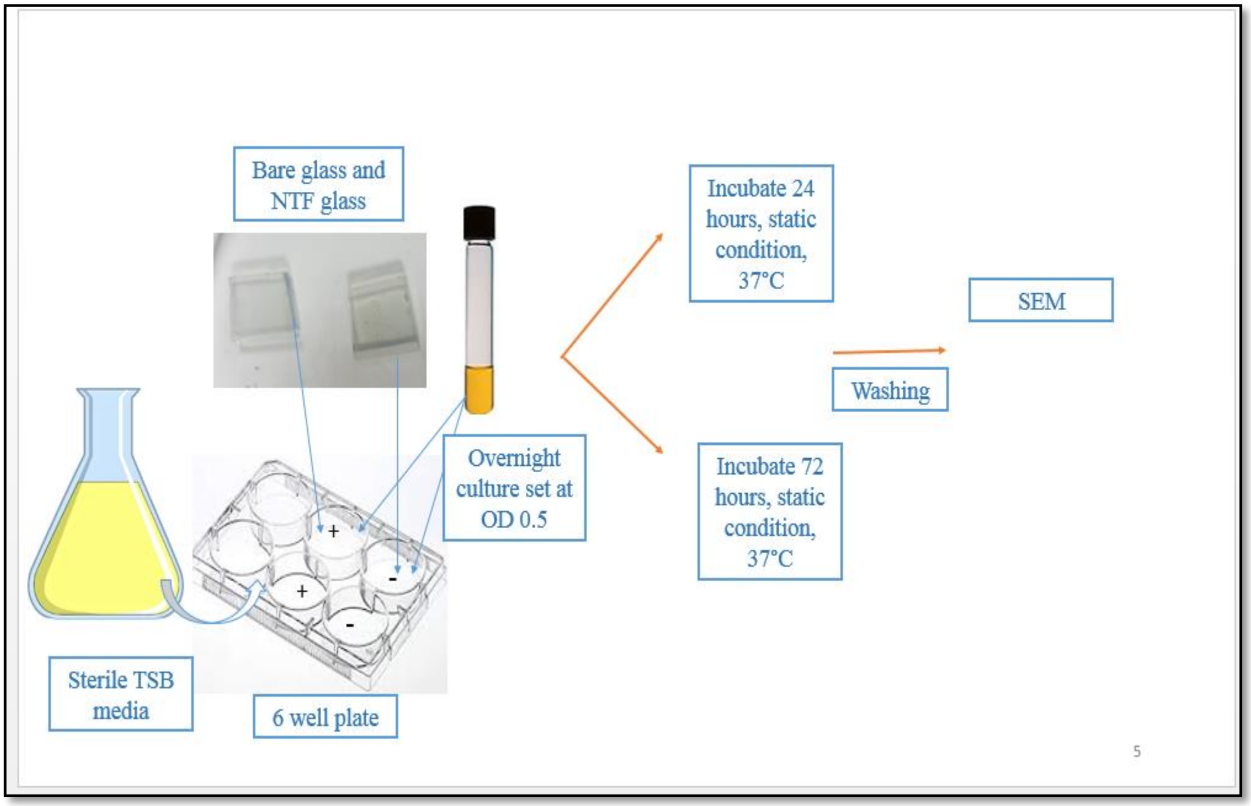

Figure 3.8: **Diagram for biofilm assay methodology**

The microtiter plates were incubated for 24 hours and 72 hours at 37ºC under static conditions. The coated and uncoated glass samples were carefully removed using sterile forceps after the completion of incubation period from the microtiter plate and washed thoroughly with 1X PBS to get rid of planktonic cells. The whole procedure was being carried out inside the laminar flow hood. The samples were then ready for SEM analysis.

3.9.2.4 Confirmation of Biofilm Inhibition through OD

In order to quantify the total number of bacteria, left over suspension in each well of the 6-well microtiter plate was analyzed through spectrophotometer and their OD were recorded (Di Domenico et al., 2016).

3.9.2.5 SEM Bacterial Biofilm Sample Preparation

The NiO thin film coated glass and bare glass exposed to biofilm inhibition assay were prepared for SEM analysis through a series of steps; firstly, the glass samples were organized and attached to petri dishes for

SEM analysis and initially washed with PBS solution. Next, a primary fixative, 4% paraformaldehyde (PFA) was made by dissolving 4% PFA in 50ml of PBS. 200ul of PFA was added onto coated and uncoated samples in a sterile environment. These samples were then allowed to set for 45minutes and air dried. These samples were subsequently picked up using forceps and dipped in various concentrations of chilled ethanol (25%, 50%, 75%, 95% and 100%) for 2-3 minutes (Vuong et al., 2004). The dried samples were then packed in sterile petri dish and stored at 4ºC until used for analysis under JSM 6490LA SEM.

3.10 UV Illumination Test

For checking the effect of sunlight on the Nickel oxide thin film coated glass, UV-A based photo catalytic chamber, shown in Fig 3.9, with four UV led lamps of 100 watts was used for performing UV illumination test, since UV-A rays in the sun reaches the most on surface of earth and have electromagnetic wavelength range of 340-400nm (Syafiq, Vengadaesvaran, Pandey, & Rahim, 2018).

Figure 3.9: **Photocatalytic reactor setup at ASAB-NUST with UVA range (400 Watts)**

Here the water contact angle of the nickel oxide thin film coated glass was checked before UV illumination. After that the coated glass was placed inside UV-A source at 25 ºC for 6 days. After 6 days, the water contact angle was checked again using Drop Shape Analyzer DSA-25 and the results were analyzed to check the change in the contact angle which indicates the capacity of hydrophilicity or hydrophobicity of the surface (Syafiq et al., 2018).

3.11 Water Contact Angle Analysis in Dark

In order to check the response of Nickel oxide thin film coated glass in dark, the NiO thin film coated glass was kept in dark for 6 days and water contact angle of the glass was calculated after every 48 hours by dispensing deionized water (5ul) using Drop Shape Analyzer DSA-25 goniometer (Syafiq et al., 2018).

3.12 Self-Cleaning Assay

3.12.1 Dirt Model Assay

Diluent-ketchup model was prepared by mixing water and ketchup in 2:5 as a dirt model for assessing the self-cleaning quality of NiO thin film coated glass. The dirt model was poured over bare glass and NiO thin film coated glass both and the response of self-cleaning was recorded using a mobile camera (Syafiq et al., 2018).

3.12.2 Rainfall Spray Test

Rain water and dust degrade the transparency of glass surface, advent of surfaces which able to retain their transparency would save time, energy and chemical cleaners spent in cleaning such surfaces .In rain fall spraying test, Deionized water was sprayed onto the bare glass and NiO thin film coated glass using an auto sprayer for 5 minutes. The horizontal distance between auto sprayer and the bare glass was kept at 10cm. After spraying, the presence of water droplets or streaks on both surfaces was observed using mobile camera (Syafiq et al., 2018).

3.12.3 Anti-Fog Analysis

In anti-fog test, both coated and uncoated glass samples were hung in air with the help of a stand over a beaker placed on hotplate with water boiling in it at 100°C. The glass samples were taken out and placed on white paper after 10 minutes. The glass samples were optically investigated for the presence of haze or tiny water droplets (Syafiq et al., 2018).

CHAPTER 4: RESULTS

4.1 Biomass Collection

After 30 days cycle, each liter of the algal culture provides 1-3g of biomass after complete water removal through centrifugation and drying. This biomass, shown in Fig 4.1, was collected for extract preparation which was used as a reducing and stabilizing agent for NiO nanoparticles synthesis.

Figure 4.1: **Dried and crushed algae powder**

4.2 Phytochemical Analysis of Algae Extract

Various phytochemical analysis tests are performed in order to know the nature of the extract and the possible reducing and stabilizing agents that may play role during nanoparticle synthesis. The phytochemical analysis of ethanol-based extract of algae was run for 12 tests which revealed the presence of saponins, steroids, quinones, flavonoids, phenol, protein, cardiac glycosides, terpenoids, carbohydrates and oils. Tannins and coumarins were absent in them, results shown in Fig 4.2. Any of these constituents of the algae extract may play a role in the reduction during the synthesis of NiO nanoparticles. FTIR analysis would give more details of the components the extract takes part in the synthesis process.

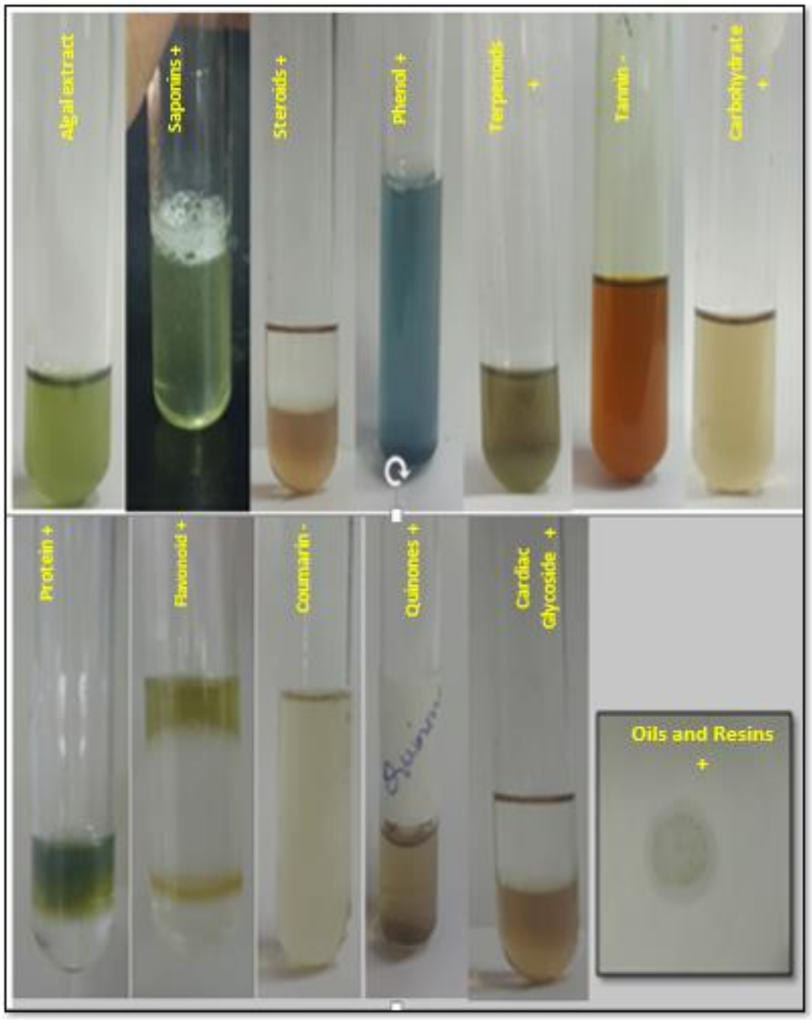

Figure 4.2: **Results of different phytochemical tests**

4.3 Synthesis of Nickel Oxide Nanoparticles from *Dictyosphrium* sp

Color change from bright green to blackish green with precipitate formation was observed after stirring of 2.5 hours. The quantity of the batch reduced various folds after second drying step which is done after ethanol wash. The final weight of one NiO synthesis batch from 25ml extract is 0.5gm. After calcination, the color of the NiO nanoparticles turned black as Ni (OH)2 got decomposed into NiO completely.

4.4 Characterization of Nickel Oxide Nanoparticles

4.4.1 X-ray Diffraction Study

XRD test was performed for the analysis of crystalline phases of NiO nanoparticles. The crystallographic structure of bio inspired nickel oxide nanoparticle was found using STOE diffractrometer at NUST. No other associated compounds were found in XRD peak analysis which indicated that the NiO nanoparticles synthesized were in pure phase. The Diffraction peaks corresponding to (111), (200), (220), (311) and (222) miller index values were matched to 2θ value of observed pattern through Xpert software analysis. These diffraction peaks form a crystallographic lattice plane of face centered cubic NiO. According to Xpert analysis software, the synthesized form of NiO are in bunsenite phase and match with JCPDS card No: 01-089-7130. The major peaks in the X-ray crystallography of NiO are at (111), (200), (220) with (200) being the preferred direction. The broader nature of the peak also indicated that nanoparticle size is agreeably small (A. T Khalil, et. 2017). The peaks comparison drawn between synthesized NiO nanoparticles and reference xrd pattern is represented in Fig 4.3 (a) and (b). This comparative image was generated using Xpert highscore analysis software. The synthesized NiO nanoparticles have a purity score of 84% as indicated by Xpert analysis software.

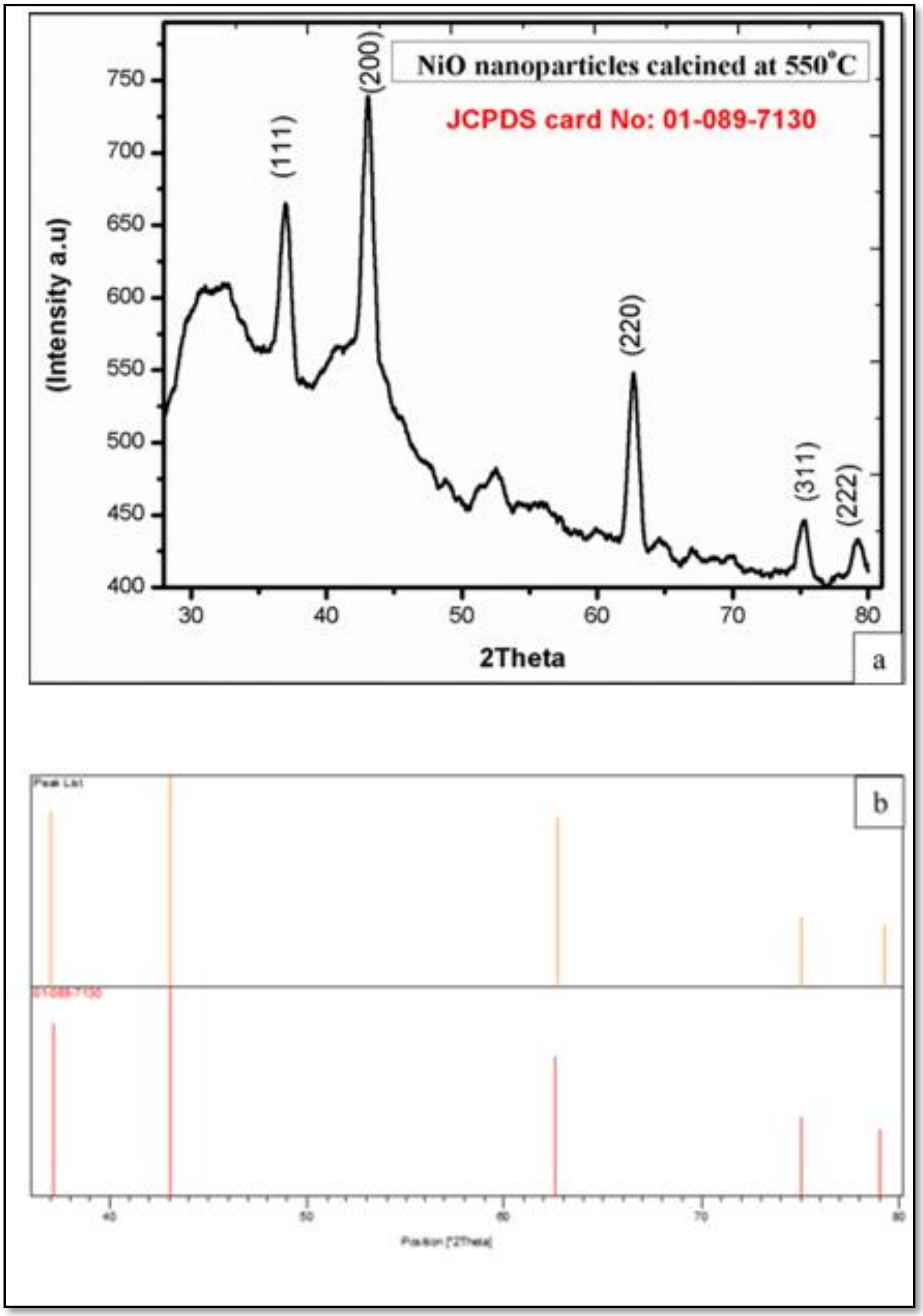

Figure 4.3: **XRD spectrum of NiO nanoparticles** (a) XRD spectra of Nickel Oxide Nanoparticles with miller index values at 111,200,220,311 and 222 with 200 being preferred direction for cubic structure (b) XRD stick patterns of Nickel Oxide Nanoparticles matching JCPDS No. 01-089-7130

4.4.2 Scanning Electron Microscopy

SEM techniques was used to analyze the morphology, topography and microstructure of NiO nanoparticles. The Scanning electron Micrograph shows successful synthesis of NiO nanoparticles. Electron micrograph in Fig 4.4 shows separated small cubic NiO nanoparticles with some particles seen as surface aggregates between them. The average size of NiO nanoparticles calculated from the electron micrographs in between 20-90nm. The size shown in SEM in Fig 4.4 is in good correlation with the calculations achieved through XRD and AFM.

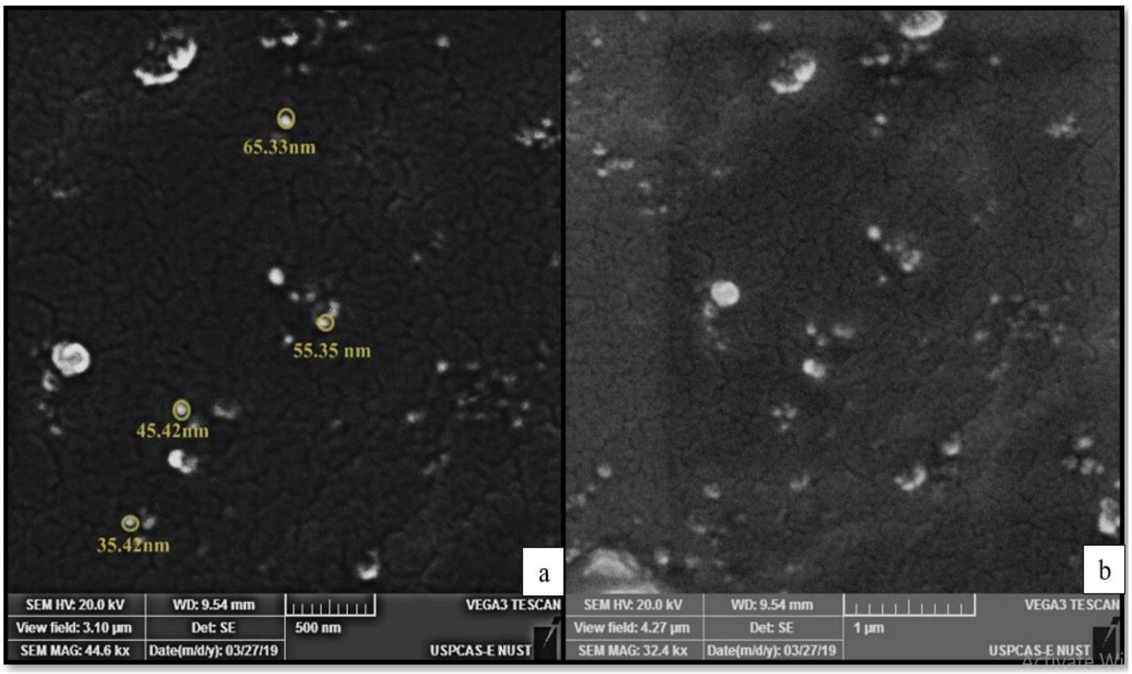

Figure 4.4:**SEM images of Nickel Oxide Nanoparticles** (a) 500nm(b) 1µm with nanoparticle range between 20-90 nm

4.4.3 Energy Dispersive Spectroscopy

EDS is performed for the analysis of elemental composition of sample. EDS techniques confirms information from SEM images further. EDS reveals strong spectrum peaks for Nickel at 1keV, 7.5keV and 8.5keV whereas there is oxygen peak at 0.5keV. This confirms successful synthesis of nickel oxide nanoparticles. The minor carbon peak is from the carbon tape which was used as base to fix nickel oxide nanoparticle sample to the sample holder. Chlorine peaks comes from functional group coated on the NiO nanoparticles from the algal extract. The weight percentages of nickel and oxygen are shown in Fig 4.5.

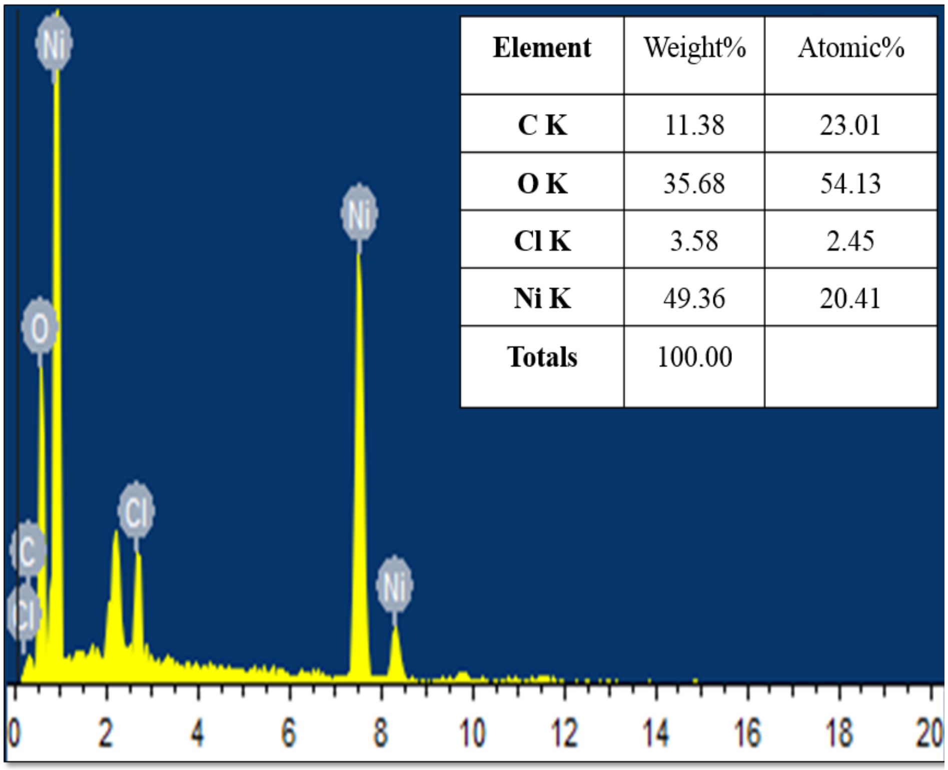

Element	Weight%	Atomic%
C K	11.38	23.01
O K	35.68	54.13
Cl K	3.58	2.45
Ni K	49.36	20.41
Totals	100.00	

Figure 4.5: **EDS spectrum of NiO nanoparticles showing presence of Nickel and Oxygen**

4.4.4 UV-visible Spectroscopy

The nickel oxide nanoparticles synthesized extracellularly have absorption spectrum in the range of 370-450 nm. From the shape of the resonance peak on the absorption spectrum in Fig 4.6, the nature of the nanoparticle can be concluded, sharp resonance peak would indicate the presence of small sized nanoparticles with uniform dispersion whereas the nanoparticles with aggregation in dispersion would tend to form small sized and wide peak. A wide peak at 387nm has been noticed on the absorption spectrum of NiO nanoparticle synthesized, which is in accordance with the reported peaks of nickel oxide nanoparticles (Sathyavathi, Manjula, Rajendhran, & Gunasekaran, 2014). The aggregation of NiO nanoparticles in dispersion is attributed to their magnetic nature.

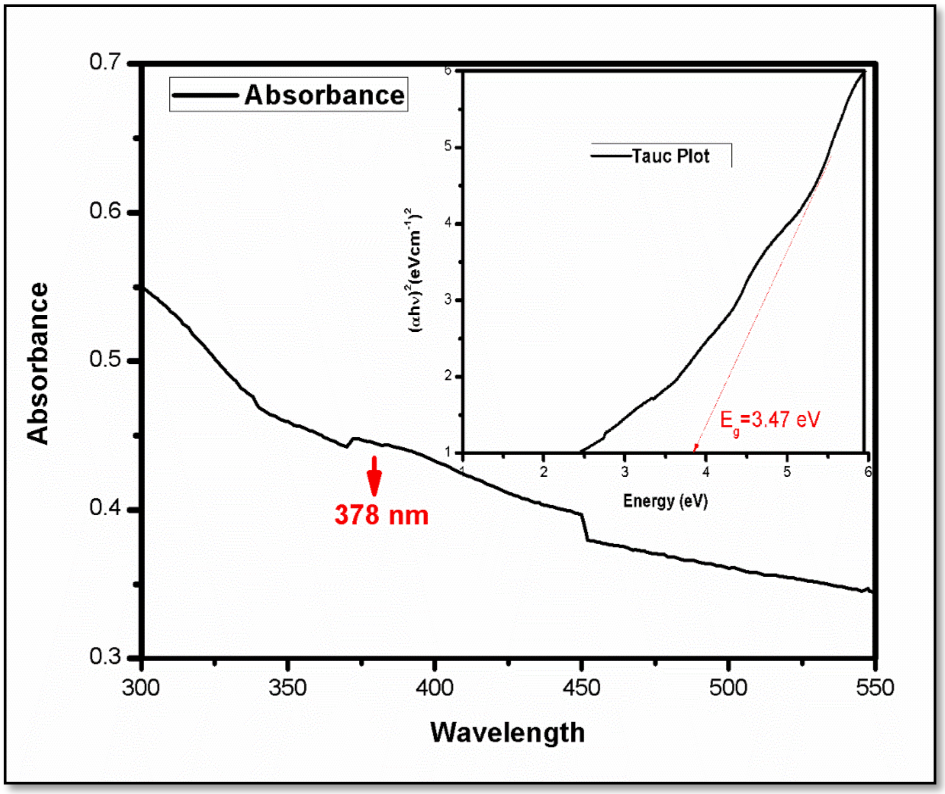

Figure 4.6: **UV visible spectra of Nickel oxide Nanoparticles showing NiO peak at 378 nm and energy band gap value of 3.47eV**

Tauc relation was used to calculate band gap value of NiO nanoparticle from the absorption spectrum. The Eg (energy band gap) value is evaluated by extrapolating an intercept at ($\alpha h\nu$) = A ($h\nu$-Eg) when α=0.

Where,

α= absorption co-efficient

Hν= energy in eV

The energy band (Eg) value for NiO nanoparticle calculated is 3.47 eV. The energy band gap value is the difference in energy between the valance and conduction band of solid material and is represented in eV (Chougule et al., 2011) which is a unit indicating the energy required by an electron to accelerate across the potential difference of 1 volt. The reported band gap value of NiO ranges from 3.4eV to 4.3 eV (Irwin, Buchholz, Hains, Chang, & Marks, 2008) depending upon the first point of absorption, midpoint of the first absorption and the end of slope of absorption which extrapolates to zero (Irwin et al., 2008) . The 3.47 eV indicates that the NiO nanoparticles are p-type semiconductors (Khalil et al., 2018) with low absorbance in the IR and visible region and higher absorbance seen in the UV region at 378 nm. Energy band gap value of 3.47eV indicates that the defect level was decreased after annealing at 550°C (Chougule et al., 2011) (Khalil et al., 2018).

4.4.5 Atomic Force Microscopy

Atomic Force microscopy is an advanced technique to confirm the images generated by SEM by confirming its surface topology through measurement of height of the nanoparticles present on the substrate. AFM generates 3D images and that's why it was used for the surface roughness and size estimation of nickel oxide nanoparticles. In AFM images the NiO nanoparticle size range is in commendation with the nanoparticle size marked on SEM images. The size of NiO nanoparticles measured by Nano surf 3000 software shows nanoparticle size range between 30-90 nm as stated in Fig 4.7. The NiO nanoparticle sample had been sonicated well before subjection to AFM imagining technique making the agglomeration of NiO nanoparticle to be negligible. The points of measurements labeled as A, B, C and D are shown in Fig 4.7 a to d.

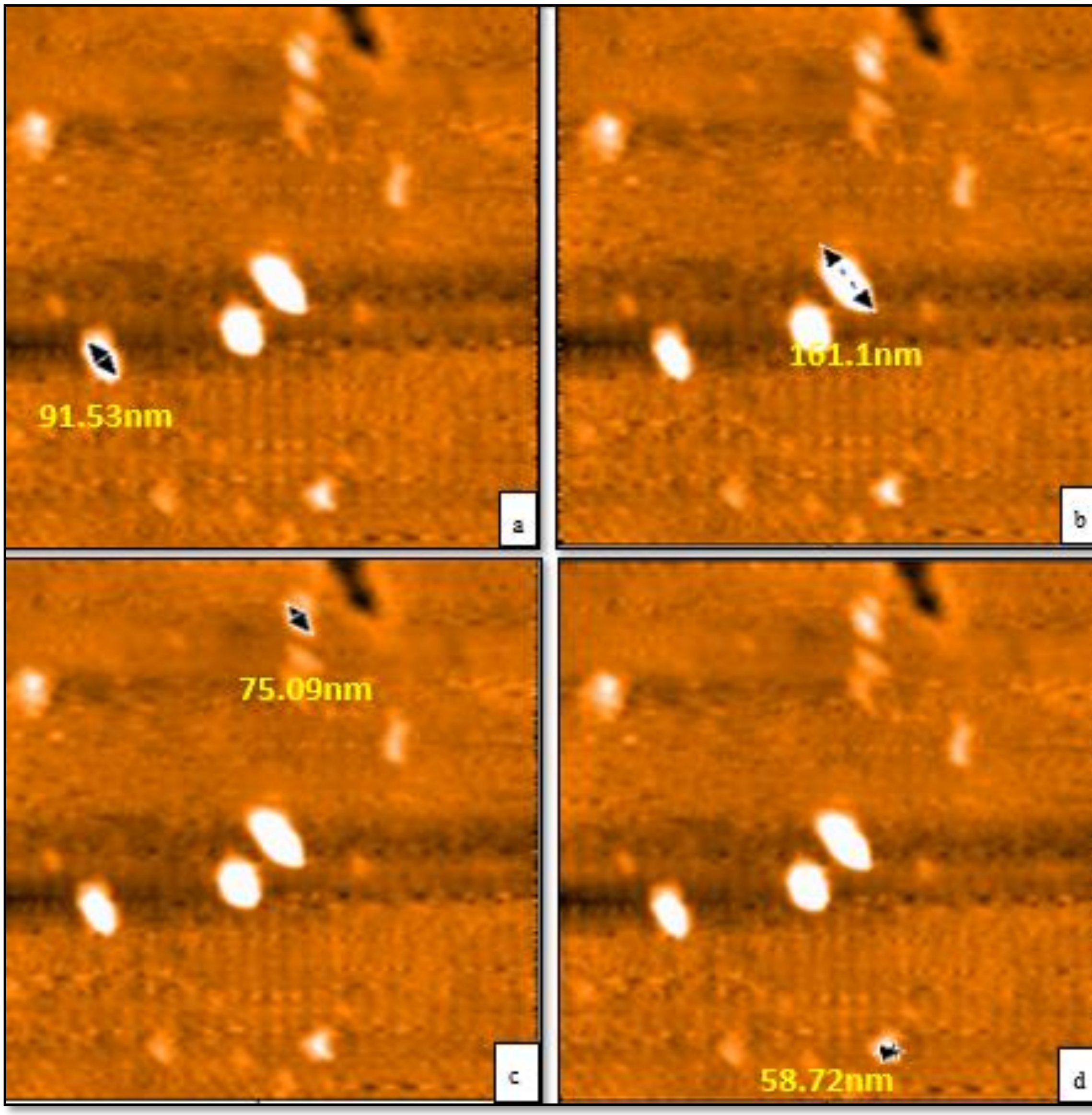

Figure 4.7: **AFM image of Nickel Oxide Nanoparticles at four different points** (a) Point A measures 91.53nm up size(b)Point B measures 30.11nm up size (c) Point C Measures 5.09nm up size (d) Point D measures 58.72nm up size

4.4.6 Thermogravimetric Analysis

Thermal gravimetric analysis was performed to analyze the thermal stability of NiO nanoparticles (Rakshit et al., 2013). TG and DSC graphs of NiO nanoparticles are presented in Fig 4.8 (a) and (b).

The TG graph is comprised of four distinct stages of weight loss. The first stage shows 14% weight loss, this stage lies in range between 25°C to 150°C. This stage signifies physical water loss from the sample. The second stage is between 150°C to 240°C and implies the loss of water of crystallization. This stage accounts for a total of 15% weight loss in NiO nanoparticle precursor.

The DSC graph, generated through origin Pro 8 software by combining TG-DT curves data of NiO nanoparticle, was meant to measure the flow of heat produced in NiO precursor sample at constant temperature. It defines the loss of different components of NiO precursor in terms of endothermic or exothermic change.

In the first part of DSC curve, there is one exothermic peak at about 40°C which indicates the start of physical water loss and one endothermic this peak at about 60°C, this relates to the loss of water of crystallization.

The third step in the TG curve implies the decomposition of $Ni(OH)_2$ into NiO, which is the final product. The highest percentage of weight loss is observed on this stage i.e. 22%. The DSC curve indicates that the decomposition of Nickel hydroxide to NiO begins at 497°C, which is an exothermic part of the process at constant temperature. The third step last between 240°C to 571°C. According to the DSC curve of NiO, the decomposition into NiO completes at 571°C, this temperature can be regarded as optimal calcination temperature of NiO synthesis using precursor. The completion of decomposition step marks an endothermic stage in the process. The last step in TG curve accounts for a total of 18% weight loss, which is attributed to volatile mass loss (Bi & He, 2013), the loss after this step become fairly slight and no loss is seen after 600°C. In the DSC curve, there is no major dip or rise after this temperature.

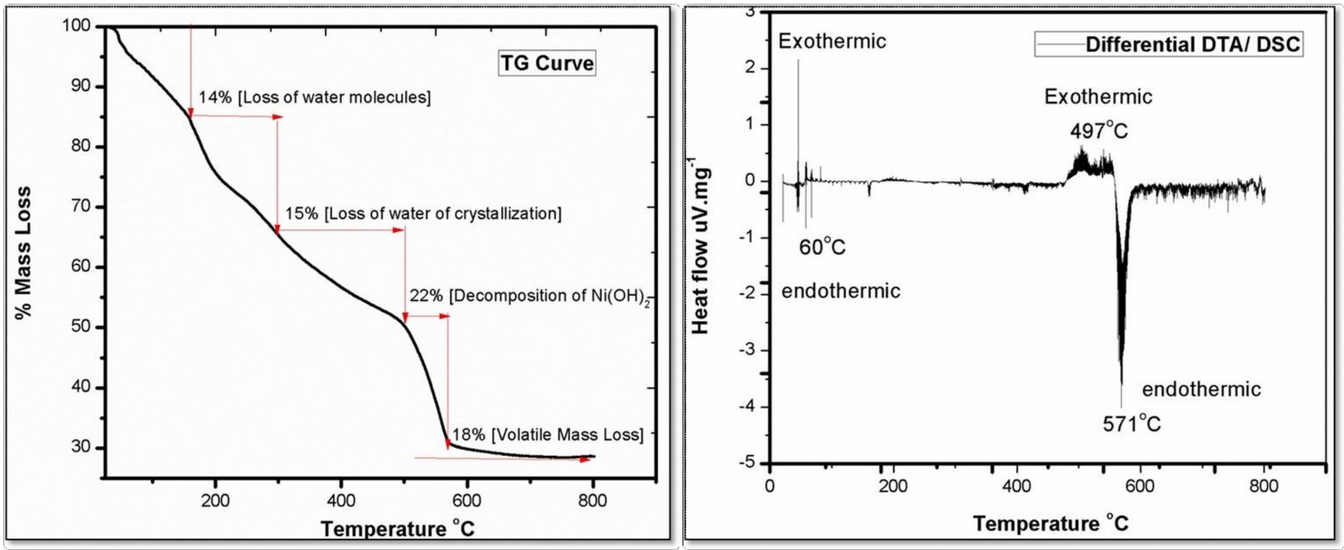

Figure 4.8: **Thermogravimetric analysis of NiO nanoparticles** (a) TGA curve of Nickel Oxide Nanoparticles (b) DSC curve of Nickel Oxide Nanoparticles

4.4.7 Fourier Transform Infrared Spectroscopy

FTIR analysis was performed in order to know the possible reducing agents taking part in the formation of nickel oxide nanoparticles. The FTIR spectrum of algal extract and nanoparticle are presented in Fig 4.9 (a) and (b). The peaks at 715, 2077.37 and 1033.77 corresponds to benzene derivative, allene functional group and amine group respectively which come from phenol, flavonoid (polyol) and protein parts of the algal extract. By comparative analysis between the spectrums of algal extract and NiO, their role as reducing and stabilizing agents is justified since these groups are missing in the absorption spectrum of NiO, the peaks at 1017.53 ad 1046.85 correspond to carbonyl group which represents aldehyde and ketone compounds of algal extract. The peak at 3428.22 correspond to water molecule since it represents hydroxyl group. The peak at 1410.85 also corresponds to hydroxyl group but is intramolecularly bonded, indicating its relation to the hydroxyl group originating from the ethanolic part of the extract.

The image in Fig 4.9 (b) represents FTIR spectrum of NiO nanoparticles. The peaks at 3779.48 and 3398.96 represent hydroxyl groups. The peak at 2311.96 is indicative of CO_2 which comes from the experiment conditions or atmospheric environment. The peaks at 568.38 and 458.93 are representative of Ni- O (Khalil et al., 2018) vibrations whereas the peaks at 1620.54 and 1036.21 are indicative of alkene and carbonyl groups. The FTIR peak analysis was done using IR table given by Sigma Aldrich.

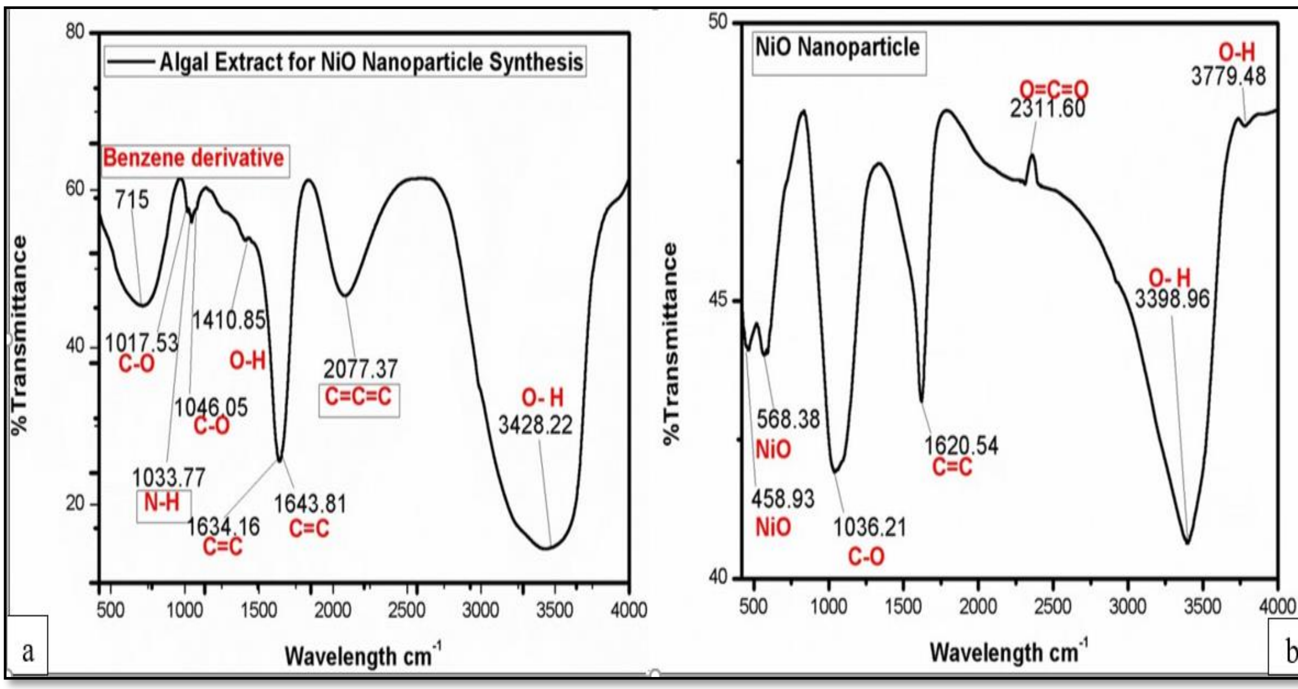

Figure 4.9: **FTIR analysis of NiO nanoparticles** (a) FTIR spectrum of Algae extract (b) FTIR spectrum of Nickel Oxide Nanoparticle

4.4.8 Zeta Potential Analysis

NiO nanoparticles are positively charged and one peak was obtained with the magnitude of 8.66, shown in Fig 4.10. The magnitude of the zeta potential stipulates the amount of electrostatic repulsion between neighboring, similarly, charged Nano sized particles in dispersion. Low value of Zeta potential means that attractive forces between the particles will exceed repulsive forces causing them to aggregate. Same is the case with NiO nanoparticles. NiO nps are more not much stabilized and repulsive forces between the particles are low which causes agglomeration of particles in colloidal therefore, zeta potential results indicate that NiO nanoparticles synthesized in the current project have a positive charge and tend to aggregate in suspension. Therefore, for coating application, prior sonication for long hours is a necessary in order to break the agglomeration or aggregation.

Nano dimension of NiO nanoparticles was not studied using zeta sizing since it shows the size of whole aggregate. Instead, AFM and therefore SEM techniques were used to measure the size of nanoparticles.

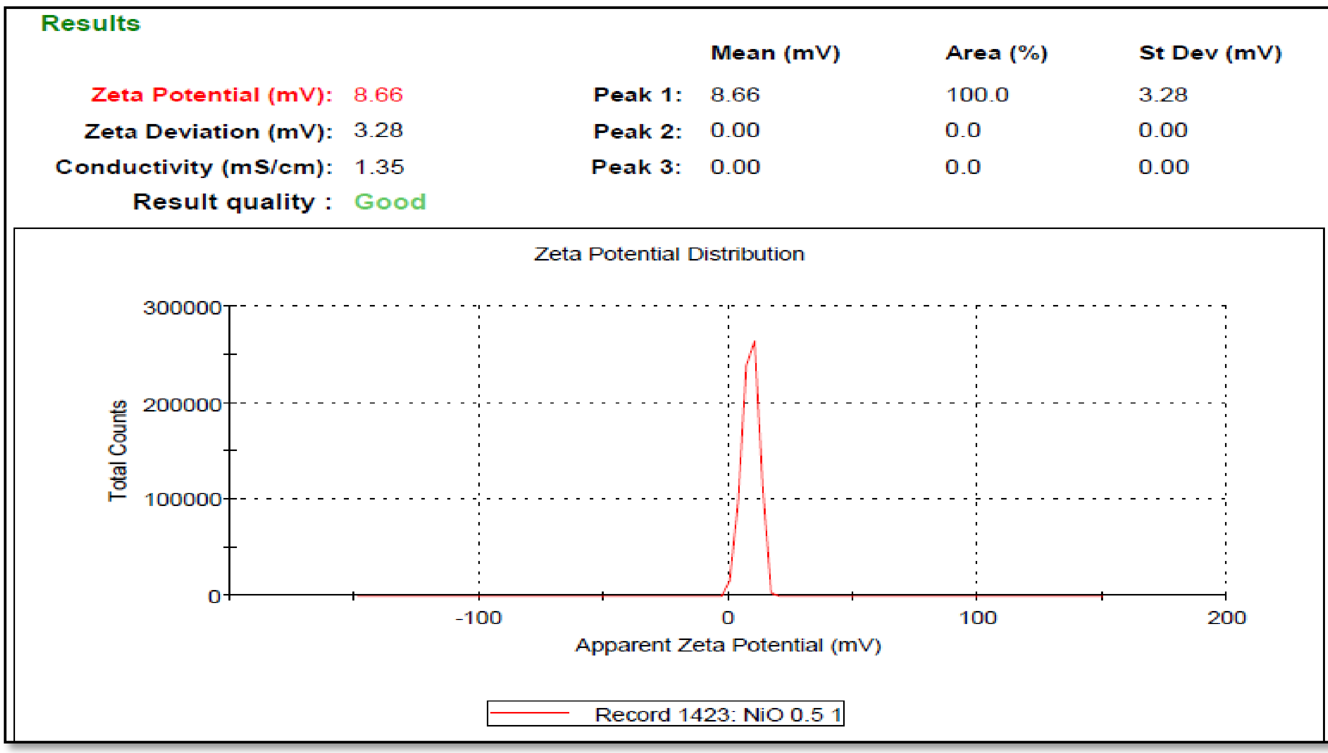

Figure 4.10: **Zeta potential spectrum of Nickel Oxide showing peak with 8.66 magnitude**

4.5 Nickel Oxide Thin Film Synthesis

4.5.1 Optimization of Nickel Oxide Thin Film

During Nickel oxide thin film synthesis, the NiO-THF emulsion was made in six concentrations and resulting NTF coated glasses with different NiO nanoparticle concentration were analyzed by checking their water contact angle through Drop Shape Analyzer DSA-25. As the concentration of nanoparticles incorporated increases from 0.5% to 4 % by weight the water contact angle decreases gradually from 36.7° to 19.3° for 0.5%, 18.1° for 1%, 17.8° for 2%, 15.8° for 3%, 10.0° for 4%, see Fig 4.11. However, after this point there is not decrease in contact angle upon increasing the NiO nanoparticle concentration in the NiO-THF emulsion used for coating, here the contact angle goes back to 14°. This shows that the best concentration for Nickel oxide thin film synthesis using spin coating is 4% by weight NiO-THF emulsion. The concentration of nanoparticles in coating emulsion has an impact on quality and performance of the coated glass (Cholewinski et al., 2014). In this optimization study the resolution was to confirm optimal concentration of NiO-THF emulsion which would produce good quality of Nickel oxide thin film coated glass, in terms of uniformity and performance.

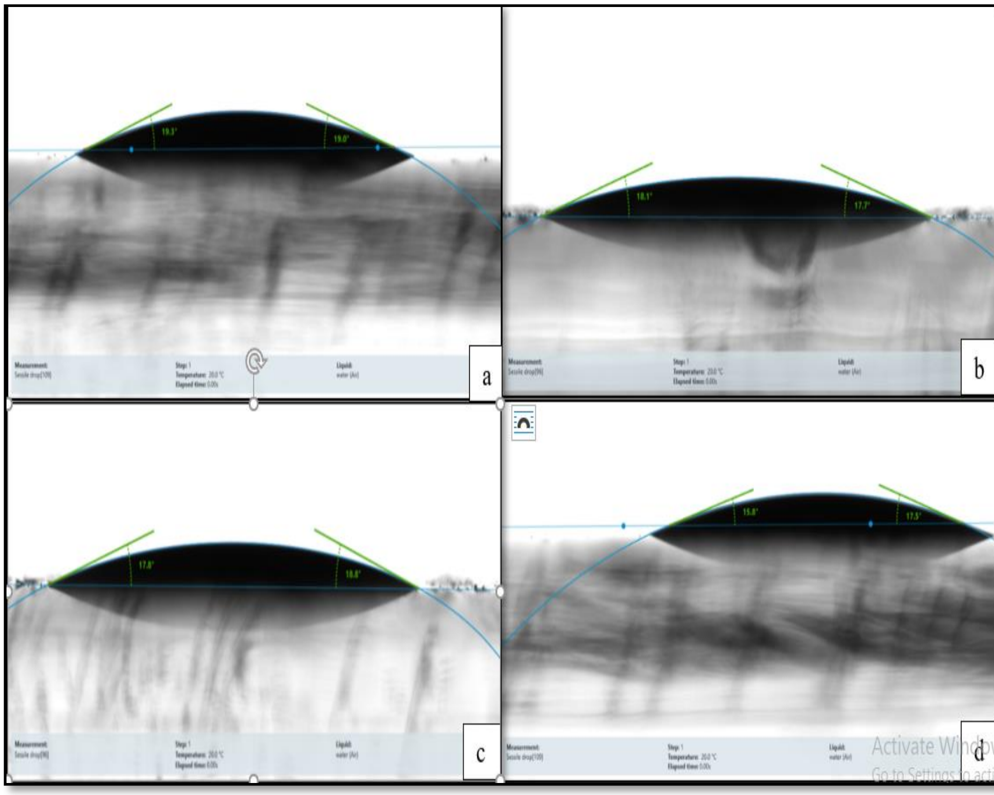

Figure 4.11: **Water contact angle of NiO thin film** (a) Water contact angle at Nio/THF concentration 0.5%, (b) Water contact angle at Nio/THF concentration 1% (c) Water contact angle at Nio/THF concentration 2% (d) Water contact angle at Nio/THF concentration 3%

The concentration of NiO nanoparticle was increased at a uniform rate of 1% at each step except at 0.5%. The NiO thin film with 0.5% was synthesized to verify NiO thin film remains functional even at low concentration, although the decrease in contact angle at 0.5% is not that low as it is on the higher concentrations. The CA at 0.5% emulsion is 19° which is near superhydrophilicity.

4.6 Synthesis of Nickel Oxide Thin Film

During Nickel oxide thin film synthesis, when NiO- THF emulsion drop is placed over pre-cleaned glass, it appears blackish due to the color imparted by NiO nanoparticles to the emulsion, upon spinning, the extra amount of THF emulsion gets removed by the action of centrifugal and centripetal force from spin coating and nickel oxide nanoparticles are spread evenly on the glass surface. The spread of NiO nanoparticles caused the reflection of the glass to get changed which acted as a preliminary confirmation that the coating has taken place. After calcination the glass appears transparent with a very thin completely see-through coating.

4.7 Characterization of Nickel Oxide Thin Film

4.7.1 X-ray Diffraction Study

The crystalline nature of the NiO thin film coated glass is revealed through XRD analysis, shown in Fig 4.12.

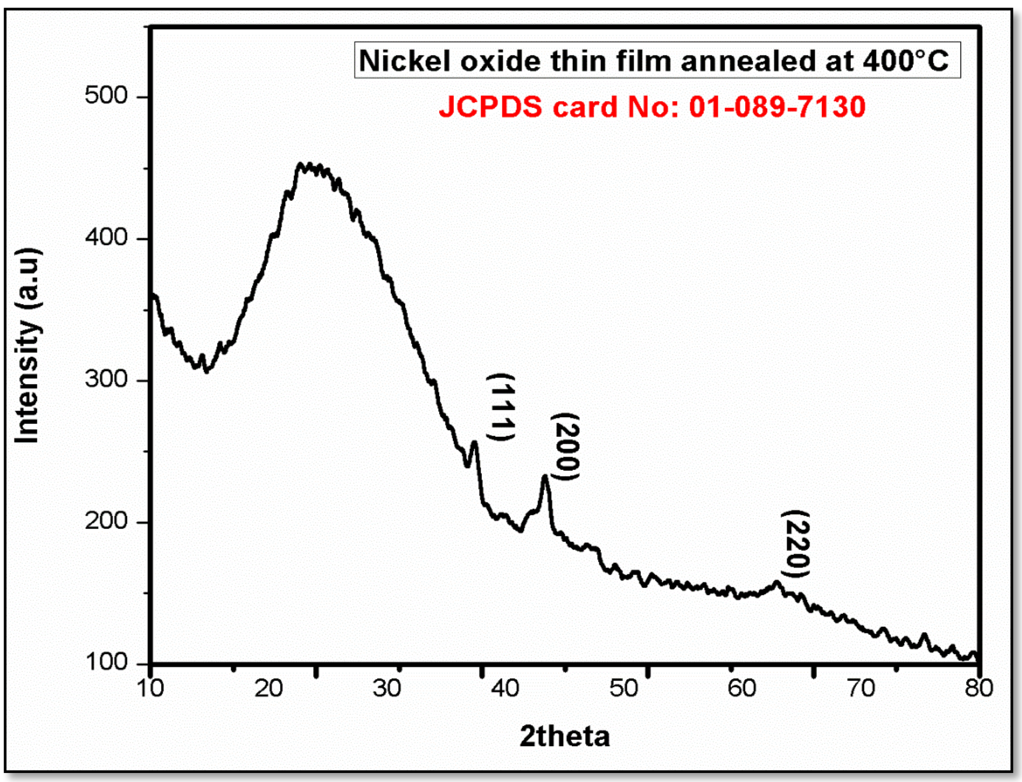

Figure 4.12: **XRD pattern of Nickel Oxide film showing major peak values at 111, 200 and 220 with 200 being the preferred direction**

The synthesized film has polycrystalline structure which approves well with the XRD of Ni|O nanoparticle with the same JCPDS card allotment number: 01-089-7130. Annealing at 400°C, reorientation of crystallite occurs which causes the secondary peaks to emerge, that's why this temperature has been chosen for annealing of NiO thin film (M. Jlassi, et al. 2014). The thin film has 2θ values 37.095° (111), 43.098° (200), 62.590° (220), 75.048° (311) and 79.015° (222) with 111, 200 and 220 being the major peaks with preferred peak being 200, this indicates the polycrystalline nature of the thin film. NiO thin films have cubic structure with purity score of 63% as predicted by Xpert analysis software report. The xrd peaks corresponding to 111, 220, 311 and 222 are present but their intensity is very small as compared to 200.

As the concentration chosen for NiO thin film formation was 4%, at higher concentration the intensity of the peak increases which is the reason for film thickness. XRD of NiO thin film demonstrates that annealing temperature has an important role in deciding the orientation of NiO and the XRD plot indicates that (200) is the most suitable direction for ion exchange (Chtouki et al., 2017).The Xpert analysis also proved that there are no other unwanted phases as all the peaks were matched perfectly to the allotted JCPDS card number.

4.7.2 Scanning Electron Microscopy

SEM is used to study the topography and microstructure of the thin film samples. This SEM was performed to know the uniformity of the synthesized thin film. SEM was used to confirm the presence of NiO nanoparticles coating on glass. The SEM images of the Nickel oxide thin film coated glass, in Fig 4.13 shows very uniform layer of NiO nanoparticles on the surface. SEM also explains the morphology of coating on glass surface.

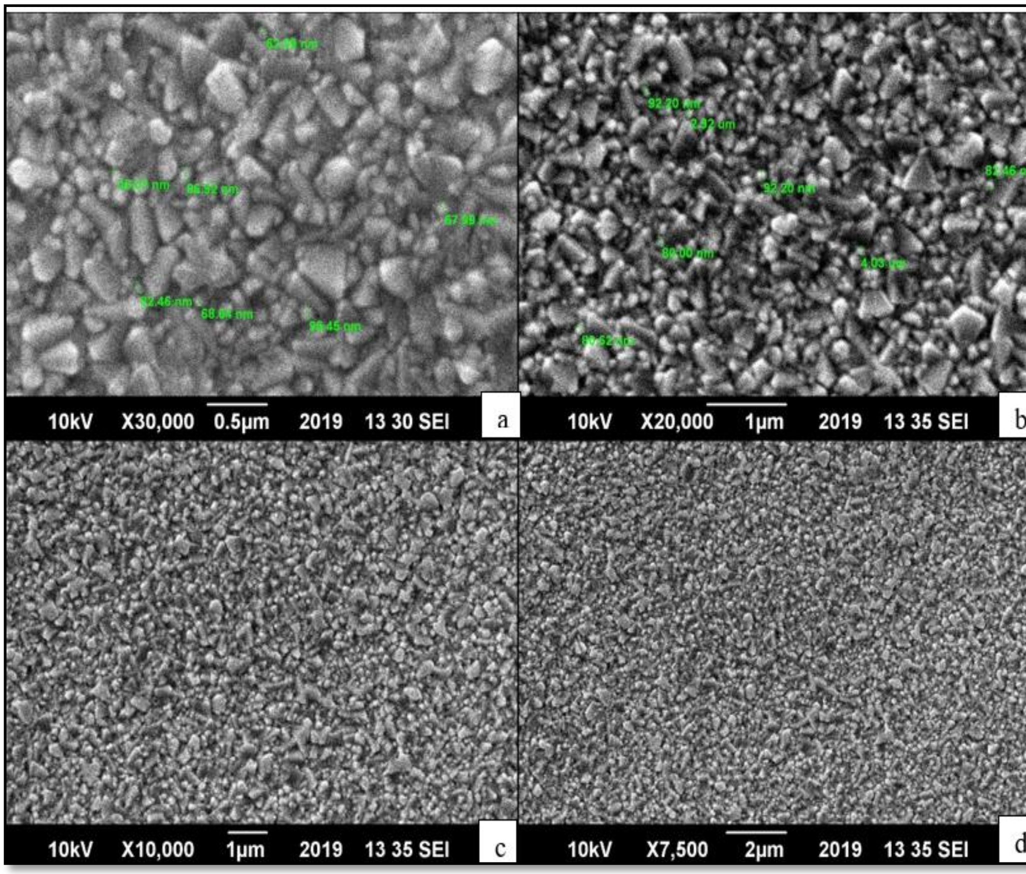

Figure 4.13: **SEM images of Nickel Oxide thin film at various magnifications, showing uniform, crack free and pinhole free coating** (a) 30,000X (b) 20,000X (c) 10,000 (d) 7500X

The coating is absolutely pin hole free and has nanoparticles in range of 80-90 nm. The increase in size is because of the temperature provided to the NiO coating during annealing process. 20X magnification image clearly exhibits the uniform presence of nanoparticles on glass surface. No cracks and phase depression were observed in the NiO thin film micrographs which tells us that the nanoparticles in the THF suspension were well dispersed and the quality of the SEM images has also been confirmed through AFM and XRD analysis of the thin film. The morphology of the nanoparticle here is also cubic which agrees well with the SEM images of the NiO nanoparticles.

4.7.3 Energy Dispersive Spectroscopy

EDS is used for microanalysis of the elemental composition of sample. EDS analysis of coated glass confirms the presence of nickel oxide nanoparticles on the glass surface, Fig 4.14. The EDS spectrum shows multiple nickel peaks at 1keV, 7.5keV and 8.5keV along with oxygen peak at 0.5keV. The peak positions in the EDS of the coated slide are the same as in the EDS spectrum of NiO nanoparticles. This further confirms the presence of NiO nanoparticles on the coated glass. Chlorine peak is also consistent with other NiO peaks in the EDS of coated glass. The EDS of the coated glass include, calcium, sodium, aluminum, silicon, phosphorus and calcium which are all constituents of glass (Couchman & Karasz, 1978). These are apparent in the EDS because the coated layer is very thin.

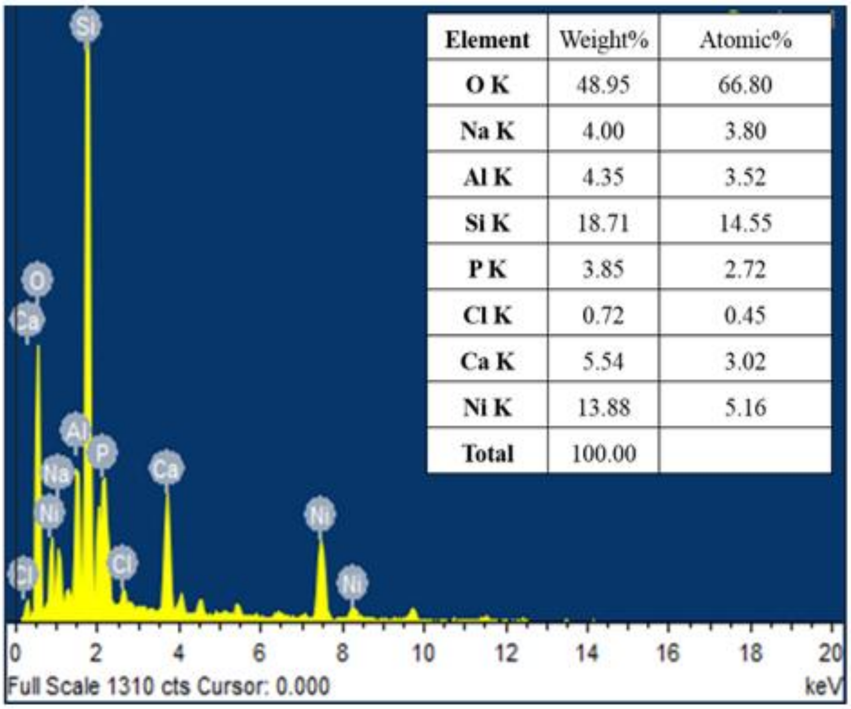

Figure 4.14: **EDS spectrum of Nickel Oxide thin film confirm the presence of nickel and oxygen along with impurities from glass base**

4.7.4 Optical study of Nickel Oxide Thin Film using % Transmittance

In order to know the impact of thin film coating on the transparency of the glass, optical studies are performed. In the optical study conducted for control glass and coated glass, it can be seen in Fig 4.15 that the transmittance of light through the control glass is 100% whereas the transmittance of light through control glass is nearly 90% which indicates that the nickel oxide thin film coating does not deteriorate the transparency of the glass substrate to an undesirable extent.

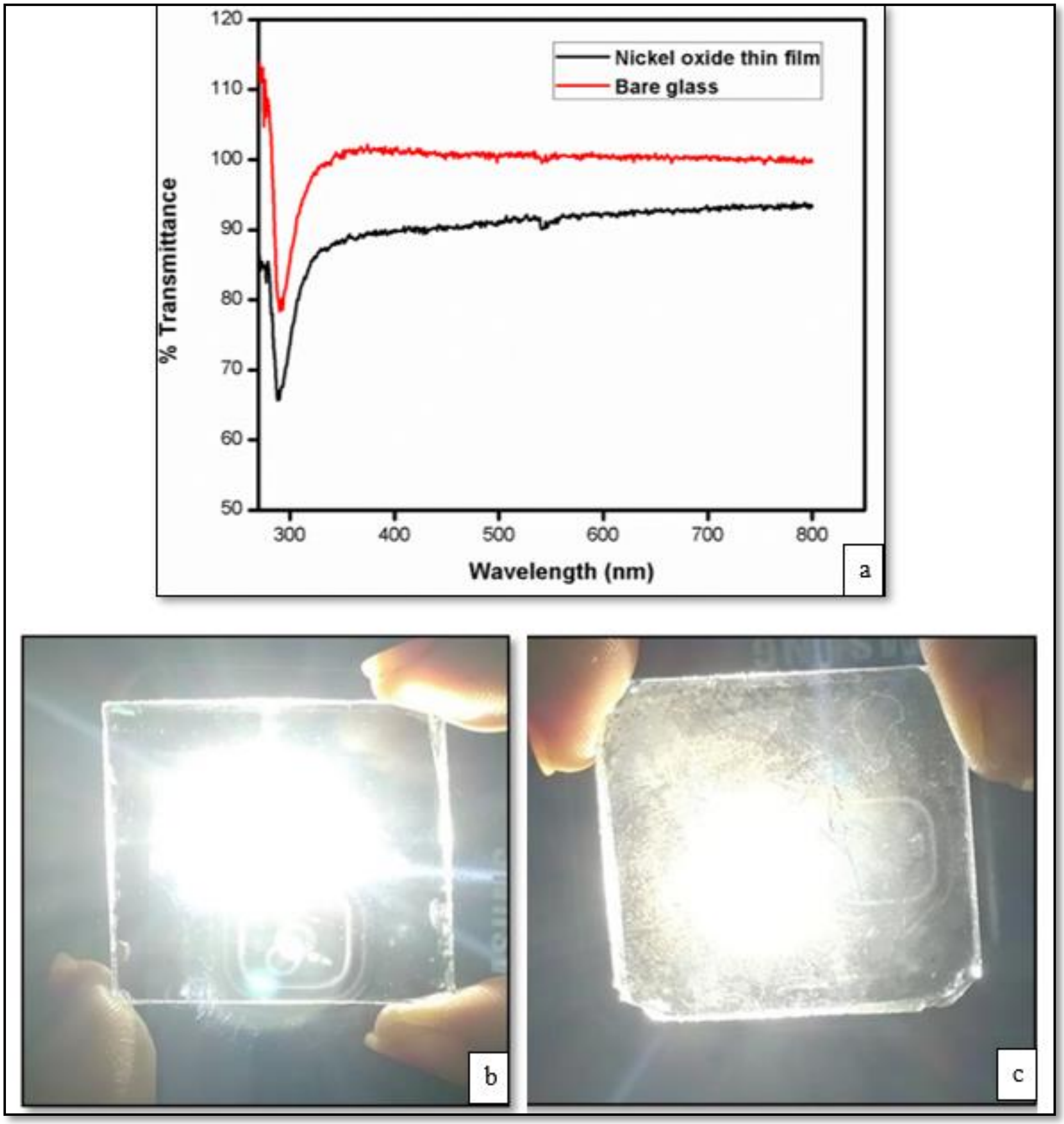

Figure 4.15**: Optical characteristics of nickel thin film coated glass** (a) % Transmittance spectrum of control glass and Nickel oxide thin film coated glass (b)100 % Transmittance of control glass (c) 90 % Transmittance of control glass

4.7.5 Atomic Force Microscopy

The 3D image of the Nickel oxide thin film confirms the morphology visualized by SEM. AFM was performed for NiO thin film sample to analyze the morphology of thin film after its thermal treatment in furnace under oxygen. The area of the NiO thin film scanned was 12.5um X 12.5um and the image acquisition was performed under tapping mode. The NiO thin film, annealed at 400°C is shown in Fig 4.16.

The application effectively of the designed NiO thin film depends upon its surface roughness. The roughness of thin films depends on the average size of the nanoparticles. Here NiO thin film reveals the nanoparticle size of 20-90 nm which agrees well with SEM results. Through Nanosurf 3000 software the NiO thin film membrane was analyzed by sectioning the thin film image into three sections. In each of these sections, line area roughness of three sites were measured by drawing measurement lines across the length and width of each sample. The line area roughness of the sections is stated in description of Fig 4.16 (b). The average roughness as calculated from all sections of the NiO thin film inclusive is 26 nm as indicated by the graph in Fig 4.16 (a).

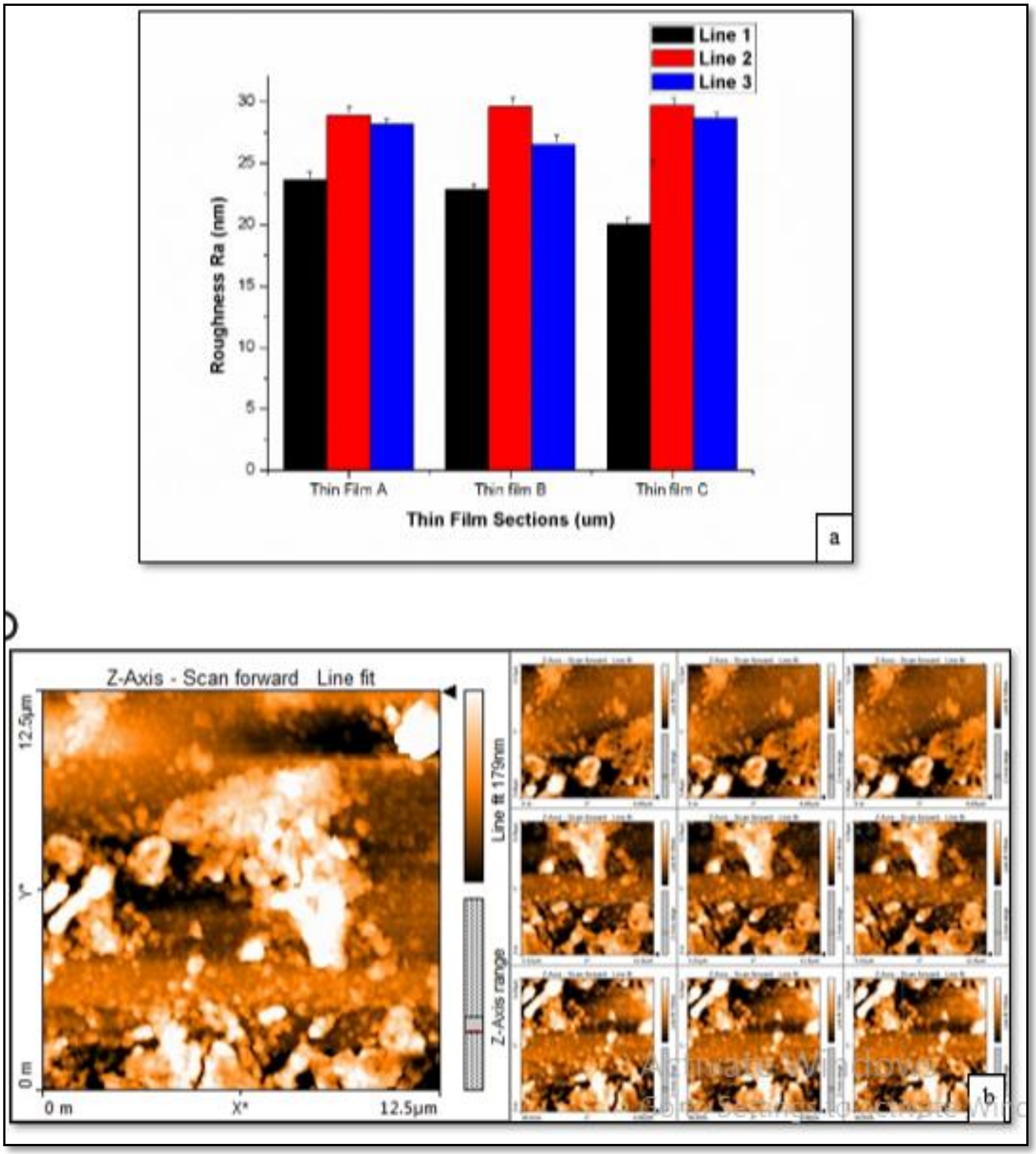

Figure 4.16: **Atomic Force Microscopy images of NiO thin film** (a) Graph representing surface roughness of NTF (b) AFM images of Nickel oxide thin film; line measurements at three points in each of the three sections of the image

4.7.6 Water Drop Contact Angle Measurement

The water contact angle of the Nickel oxide coated thin film was checked by dispensing 5ul of deionized water in the form of a sessile droplet from Drop Shape Analyzer DSA-25. The goniometer drops a steady drop on the coated surface and the point where water droplet makes physical contact with water is analyzed using a Drop Shape Analysis software. The comparison between coated and bare glass was is shown in Fig 4.17.

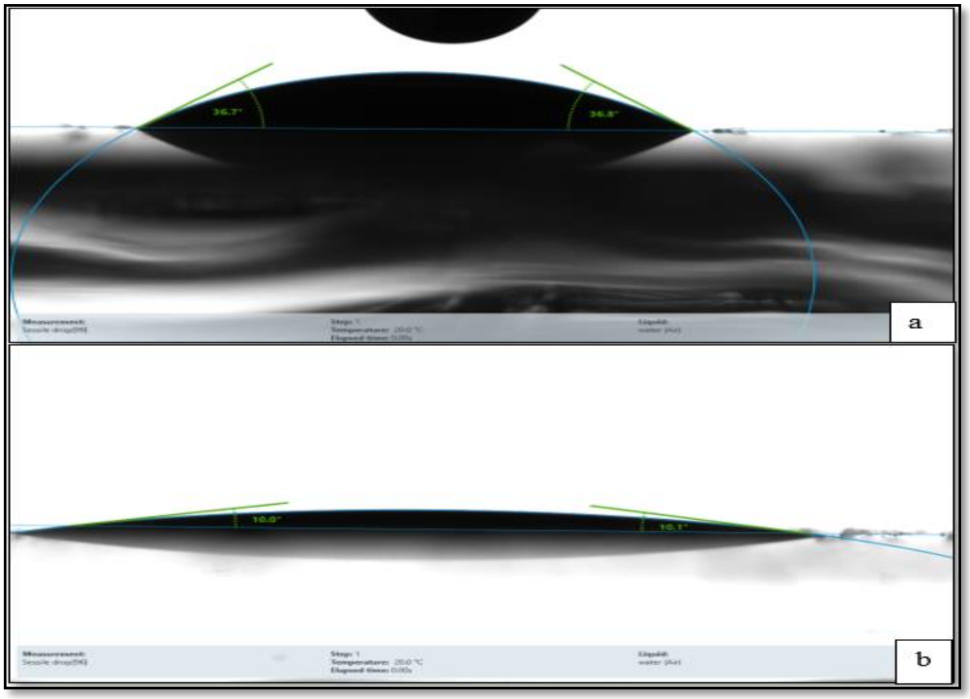

Figure 4.17: **Water Contact angle image of base glass and control glass**

(a) bare glass showing contact angle of 36.6◦, not suitable for self-cleaning
(b) applications (b) NiO thin film with 4% Nickel Oxide THF concentration
(c) showing contact angle of 10◦, good for self-cleaning application.

The uncoated glass showed a water contact angle (CA) of 36.7° whereas the finalized NiO thin film coated glass with 4% NiO concentration by weight showed a decreased contact angle of 10.0°.

4.8 Antibacterial Activity of Nickel Oxide Nanoparticles

The antibacterial activity of NiO nanoparticles was inspected through well-diffusion assay. Three bacterial species; *E, coli, P. aeruginosa* and *K. pneumoniae* were taken. NiO nanoparticles were taken in three concentrations (1.5mg/ml, 2.5mg/ml, and 3.5mg/ml) by making dispersion in DMSO through sonication. Ciprofloxacin (5ug) and DMSO were used as positive and negative control respectively.

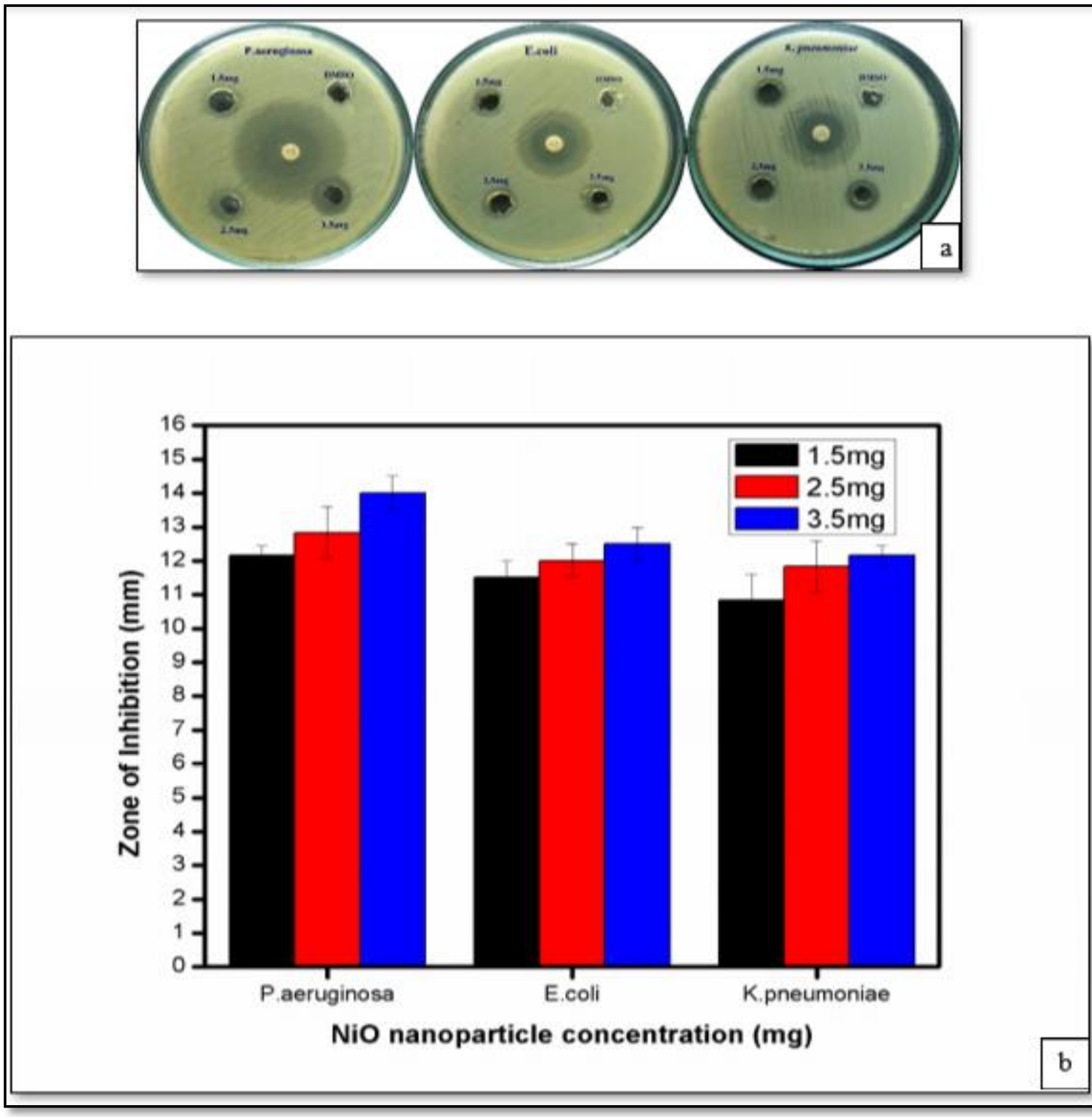

Figure 4.18: **Antibacterial activity of NiO nanoparticles** (a) Digital images of zone of inhibition of Nickel Oxide Nanoparticles (b) Graph representing zone of inhibition of Nickel Oxide Nanoparticles

The antibacterial activity of NiO nanoparticles tends to increase with increasing concentration, maximum activity at each concentration being recorded against *P. aeruginosa.* The reason for selecting these concentrations is that NiO nanoparticles synthesized for this study doesn't show significant antibacterial activity below 1.5mg/ml. The Fig 4.18 shows NiO nanoparticles are effective against all species. The minimal inhibitory concentration against *P. aeruginosa* is of 12mm at 1.5mg/ml. for *E. coli* and *K. pneumoniae*, the MIC is 11 mm at 1.5mg/ml.

4.9 Biomechanical Testing of Nickel Oxide Thin Film

4.9.1 Antibacterial Activity of Thin Film

The antibacterial activity of Nickel oxide thin film coated glass was investigated using disc-diffusion method. The NiO thin film used for this assay is the one formed using lowest concentration of NiO- THF emulsion (0.5% by weight). This selection was made in order to check the capacity of this thin film at lowest concentration. Here bare glass was taken as negative control which should have no inhibitory diameter. It was noted that the NiO thin film was active against all bacteria and its effectiveness was in accordance with the results obtained from the antibacterial assay of Nickel oxide nanoparticles.

The zone of inhibition around *P. aeruginosa*, as seen in Fig 4.19 was 4mm, *E. coli* and *K. pneumonia* showed zone of inhibition of 4mm and 3.5mm respectively.

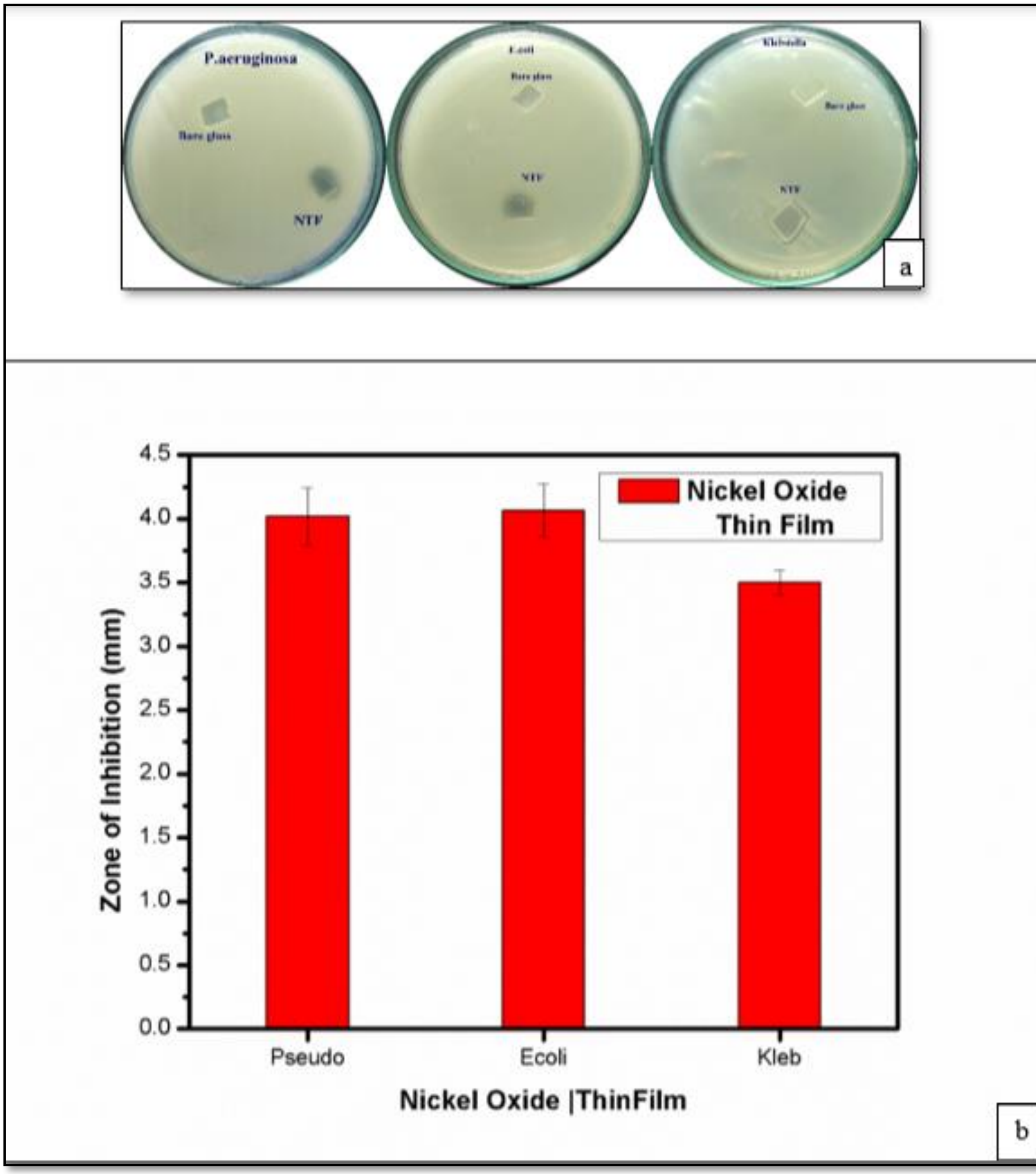

Figure 4.19: **Antibacterial activity of NiO thin film** (a) Digital images of zone of inhibition of Nickel Oxi de Thin film (b) Graph representing zone of inhibition of Nickel Oxide Thin film

4.9.2 Antibiofilm Activity of Nickel Oxide Thin Film

4.9.2.1 Ring Test

After 24 hours, when the tubes were washed and stained, ring appeared on all test tubes. The ring test assay came out positive for all three strains, which indicates that all three bacterial strains chosen for this study had the ability to form biofilm, shown in Fig 4.20. Anti-biofilm assay was then tested for *P. aeruginosa and E. coli* in 6- well plate for 24 and 72 hours for seeing the effect of NiO coated thin film on biofilm prevention through SEM analysis.

Figure 4.20: **Ring test assay of test organisms showing positive -ring formation for all three strains**

4.9.2.2 24 Hour and 72 Hour Treatment with Nickel Oxide Thin Film

Anti-biofilm activity of Nickel oxide thin film coated glass was tested separately for 24 and 72 hours on *E. coli* and *P. aeruginosa* to evaluate the efficacy of NiO coating in biofilm prevention. SEM images of NiO thin film coated glass and uncoated glass after 24- and 72-hours anti-biofilm assay are given in figure

4.21 and 4.22. The positive control of the 24 hours biofilm image shows preliminary stage of biofilm formation whereas the biofilm at 72 hours is fully formed which shows better biofilm demolition in the test image. Bacterial biofilm morphology remains intact in the uncoated samples in both assays whereas, biofilm disruption can be clearly observed in both sets of coated glass in case of E. *coli* as well as *P. aerugionsa*. This proves the capability of NiO thin film to act as antibacterial glass. The biofilm prevention ability of the NiO thin film was reconfirmed by checking the OD of leftover liquid in the 6- well plates.

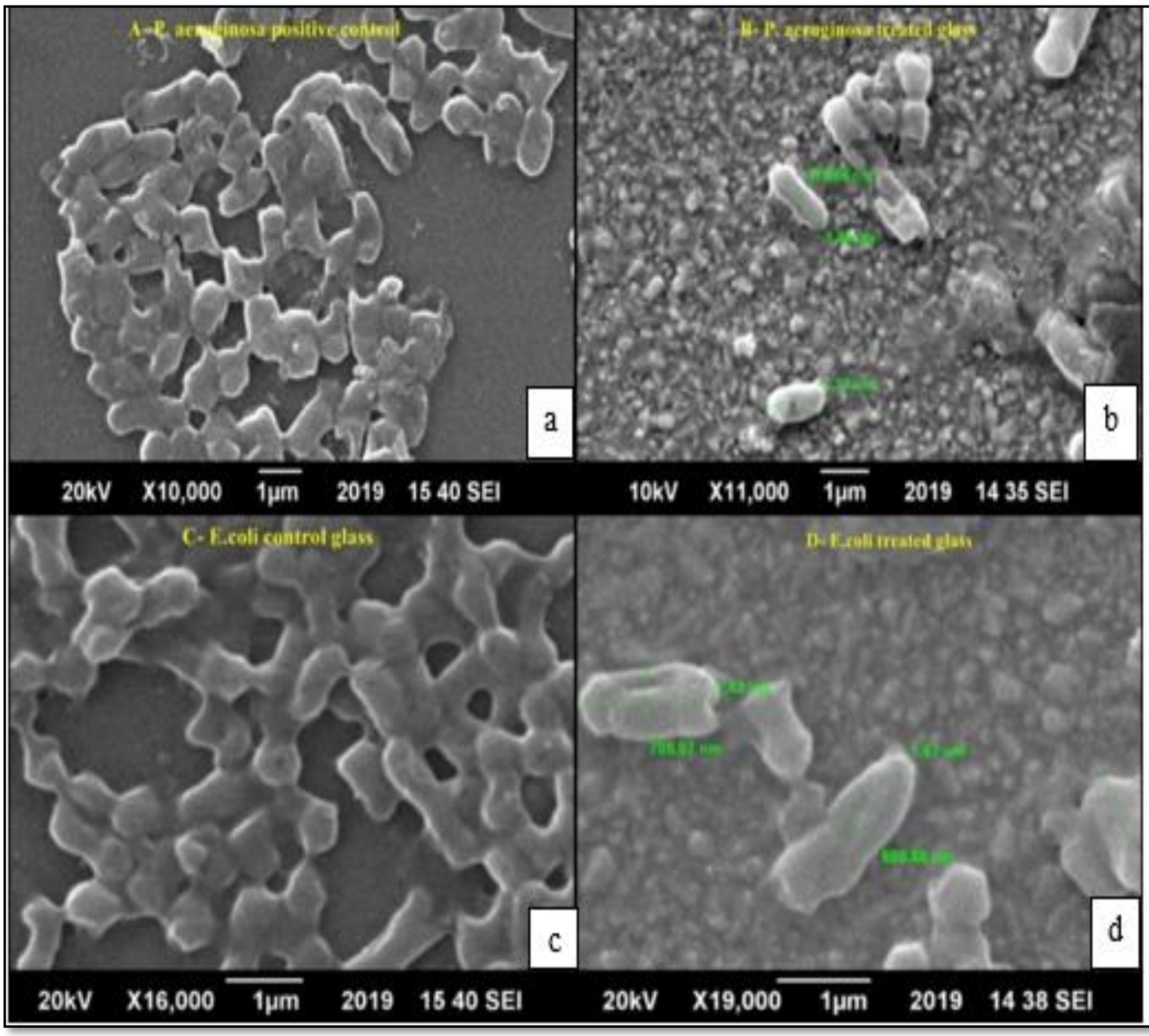

Figure 4.21: **SEM images for biofilm formation of *P. aerugionsa* and *E. coli* at 24 hr**

(a) *E. coli* positive control (b) *E. coli* treated sample (c) *P. aeruginosa* positive control

(d) *P. aeruginosa* treated sample

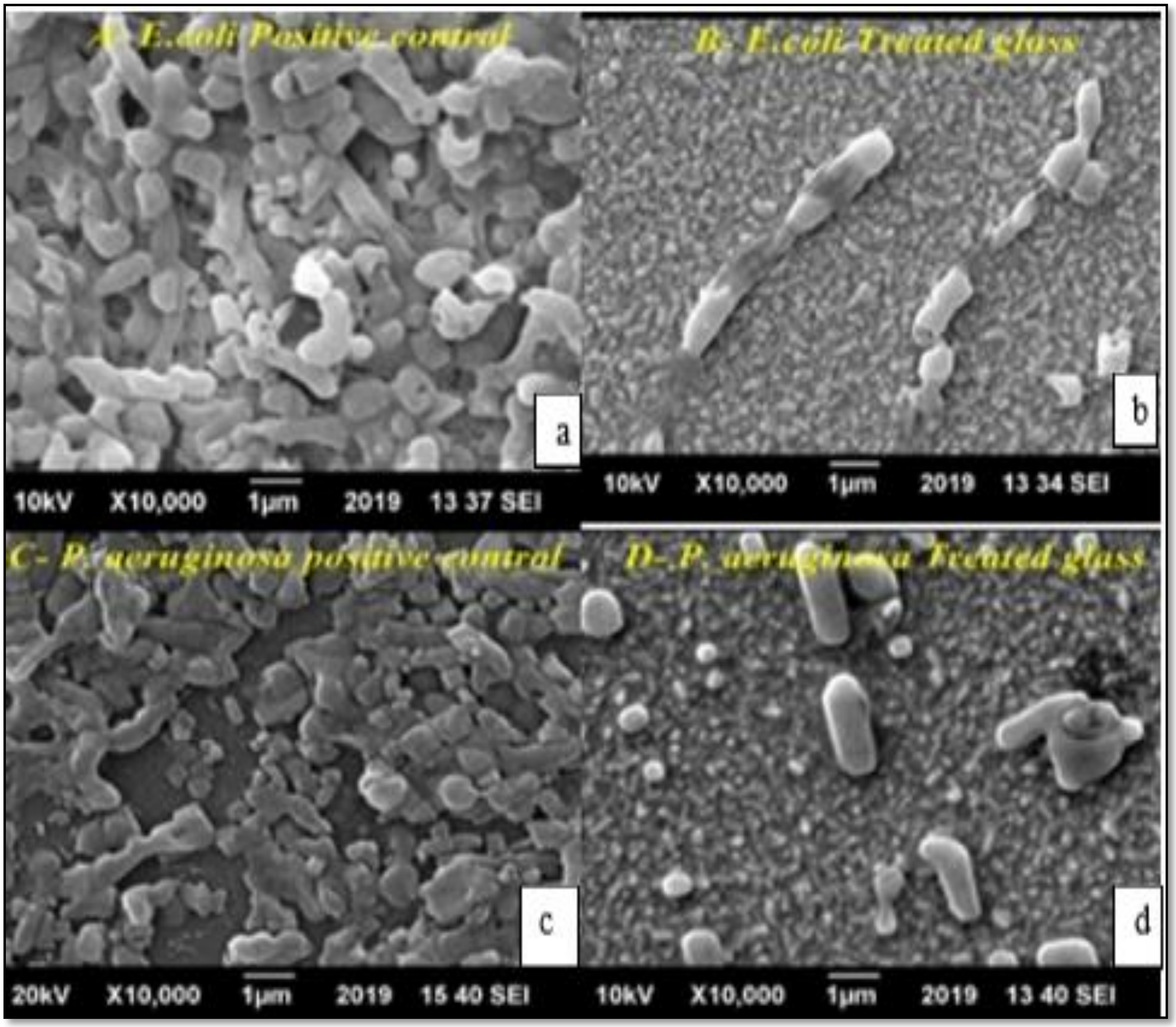

Figure 4.22:**SEM images for biofilm formation of P. aerugionsa and E. coli at 72 hr**

(a) *E. coli* positive control (b) *E. coli* treated sample (c) *P. aeruginosa* positive control

(d*)* *P. aeruginosa* treated sample

4.9.2.3 Confirmation of Biofilm Inhibition through OD

After fixing the samples for SEM analysis the liquid left in each well of both 6-well plates of 24 hours and 72 hours assays were taken in cuvettes for measuring their OD using spectrophotometer (UVD-2950). The results are stated in Table 4-1.

TSB media was used as negative control, TSB media with bacterial inoculum on bare glass was taken as positive control. TSB media containing inoculum on NTF coated glass was the test substrate. These results confirmed that the assay was free of any bacterial contamination and preventive anti- biofilm assay was effective after 24 hour and 72 hours.

Table 4-1: Table for measurement of confirmation biofilm prevention

Bacteria	**Biofilm 24 hours**			**Biofilm 72 hours**		
	OD (nm)					
	–ve control	**+ve control**	**NTF coated glass**	**–ve control**	**+ve control**	**NTF coated glass**
E. coli	0.000	1.510	0.002	0.001	3.200	0.007
P. aeruginosa	0.000	1.856	0.01	0.000	4.812	0.03

4.10 UV Illumination Test

UV illumination test was performed in order to measure the ability of coated glass to function under sunlight. Fig 4.23 shows that the bare glass had a contact angle of 36.7° which shifted to 10° after incorporation of surface modifying nickel oxide nanoparticles on its surface. In UV illumination assay, the hydrophilic glass with contact angle of 10° was kept under UV illumination for 6 days and there was only slight change in contact angle from 10° to 12° which is insignificant.

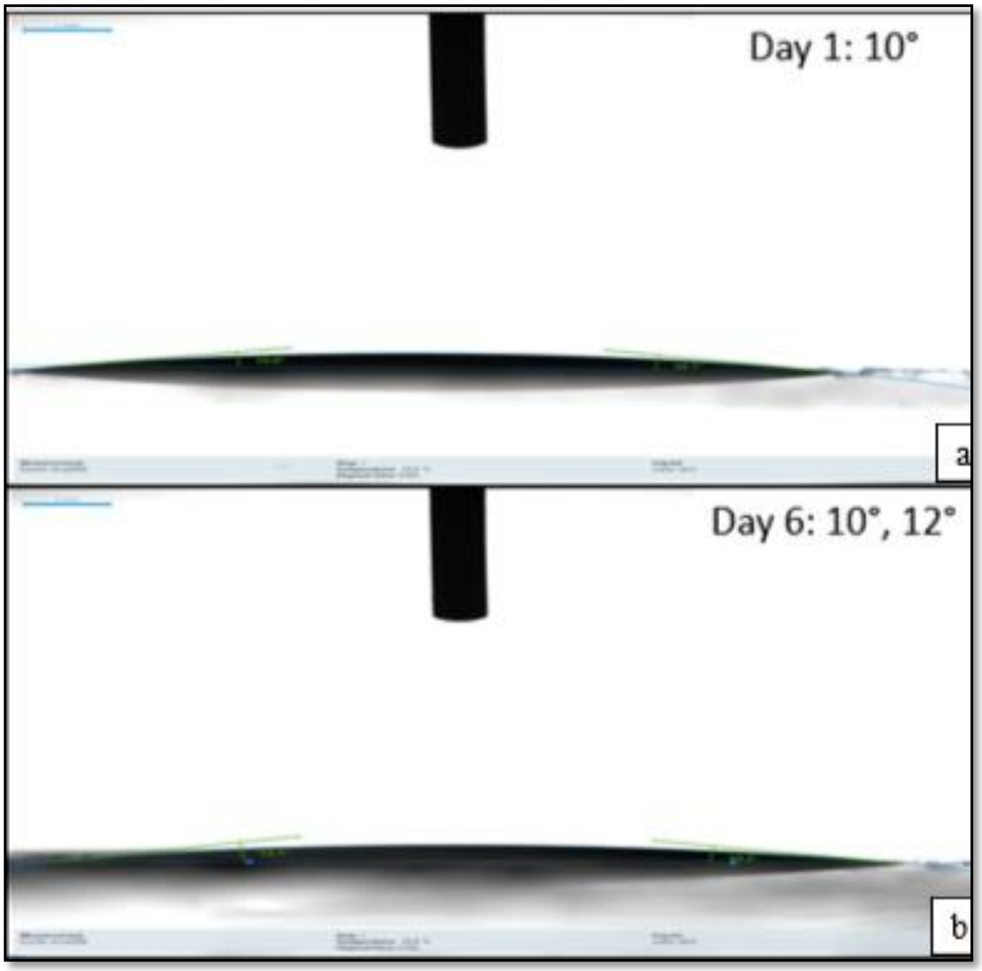

Figure 4.23: **UV illumination test** (a) water contact angle at day 1is 10◦ (b) water contact angle at day 6 is 12◦

4.11 Water Contact Angle Analysis in Dark

Water contact angle analysis was performed in dark in order to measure the functioning capacity under dark. Fig 4.24 shows that on day first the contact angle was measured at 10° which changed to 17.5° after 2 days of no light exposure. The contact angle further reduced to 19° over the next 4 days. This change in contact angle observed for 4 days signifies that the NiO thin film is stable under dark to a good extent, as the contact angle did not change significantly after day 4.

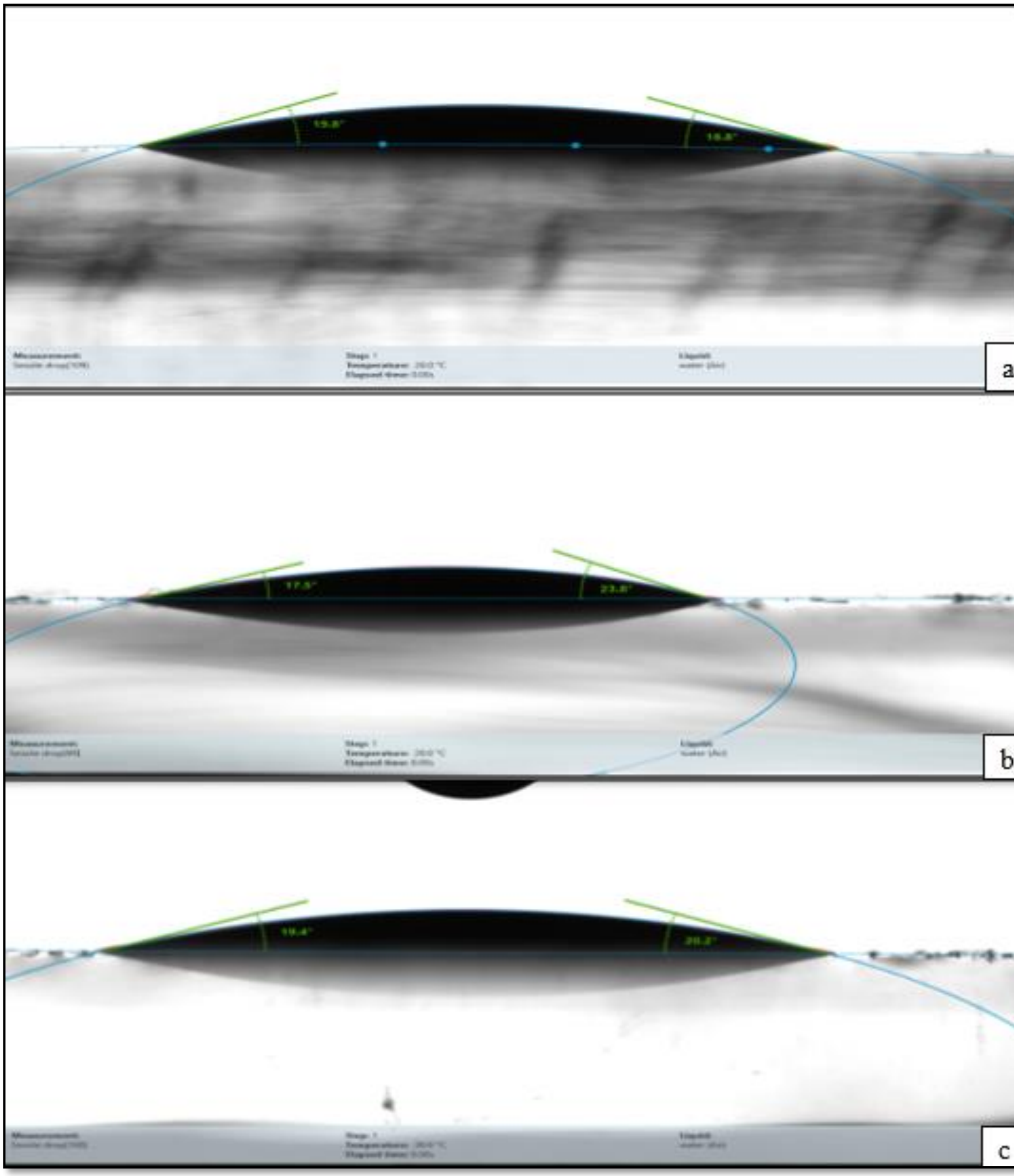

Figure 4.24: **Water Contact Angle of coated glass in dark** (a)at day 2 changed to 17.5◦ (b) at day 4 changed to 19◦(c) at day 6 remained at 19◦

4.12 Self-Cleaning Assay

In order to know the self-cleaning ability of the Nickel Oxide thin film coated glass, three assays were run using, dirt model, rain fall model and fogging model.

4.12.1 Self-Cleaning Assay using Dirt Model

When dirt solution was poured over coated and uncoated glass, dirt slipped off the coated glass because NiO thin film on the glass surface sweeps away the dirt physically by the spreading mechanism. Here watery content of the dirt solution made a sheet like appearance and it took dirt particles along with it. The coating satisfies self-cleaning through physical washing away of dirt. It can be noticed that NiO thin film coated glass has good water harvesting ability, it rapidly attracts moisture towards its surface and converts it into a film. Although a few particles of dirt would have left on the glass, so the maximum cleaning of the surface can be achieved by combining the use of water.

In case of bare glass, the dirt remained on the glass, producing smudges of dirt across the surface. Fig 4.25 presents coated and uncoated glass. The coated glass came out clean because, the contact angle of the coated surface is reduced to a lower value causing the water to form a thin layer which causes the dirt layer to get washed away. Lower contact angle reduces the adherence of inorganic dust on glass surface, such coating, although, cannot remove dirt elements such as paint.

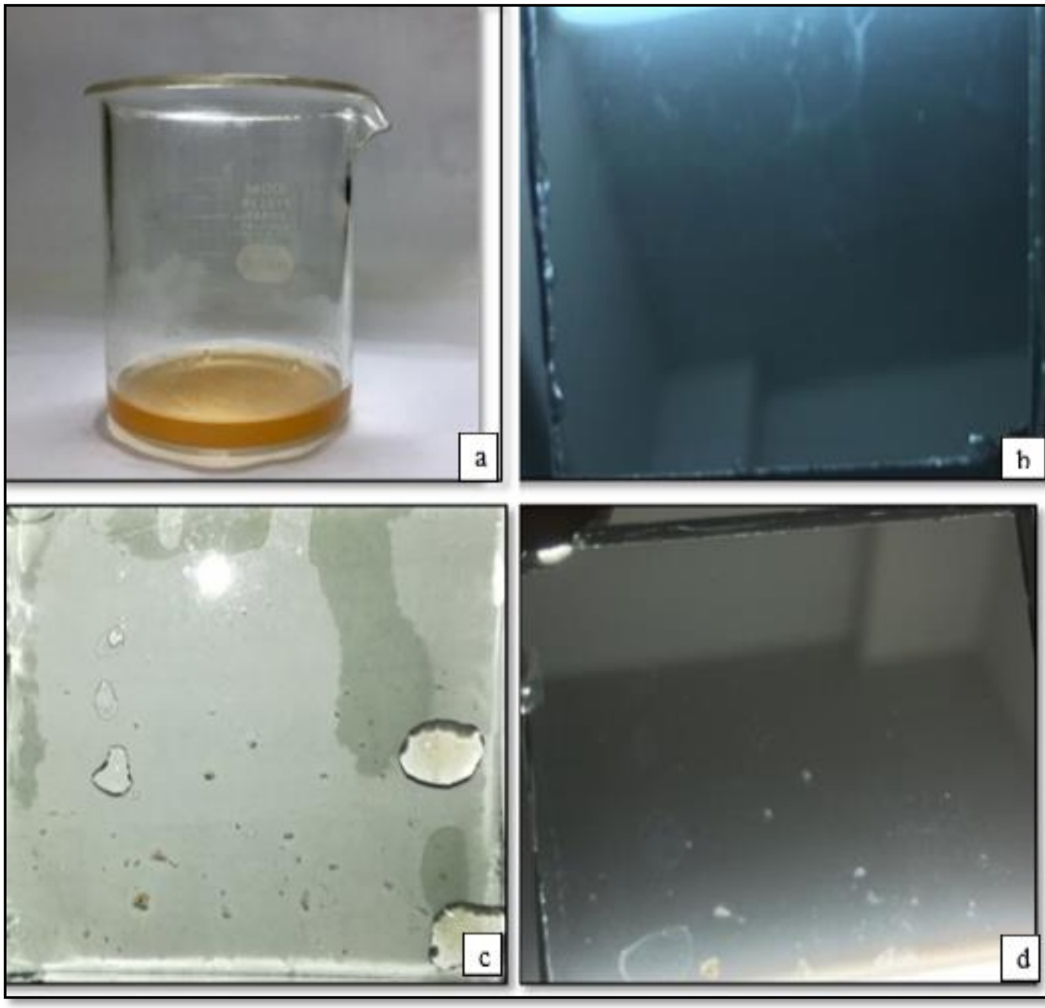

Figure 4.25**: Self-cleaning experiment images** (a) diluent ketchup dirt model (b) coated glass with clean surface due to spreading mechanism (c,d) uncoated glass with dirt droplets on its surface

4.12.2 Rainfall Spray Test

The nickel oxide thin film coated glass came out clean without any water droplets on its surface, the water spread throughout the coated glass like a thin film, which flowed through the glass and within a minute, the glass was dry.

In case of bare glass large water droplets were appeared on its surface and stayed there for several minutes. It took 25 minutes for the bare glass to get completely dried. The images of bare and coated glass are given in Fig 4.26. The water contact angle of the coated glass checked again after rain and it retained superhydrophilicity.

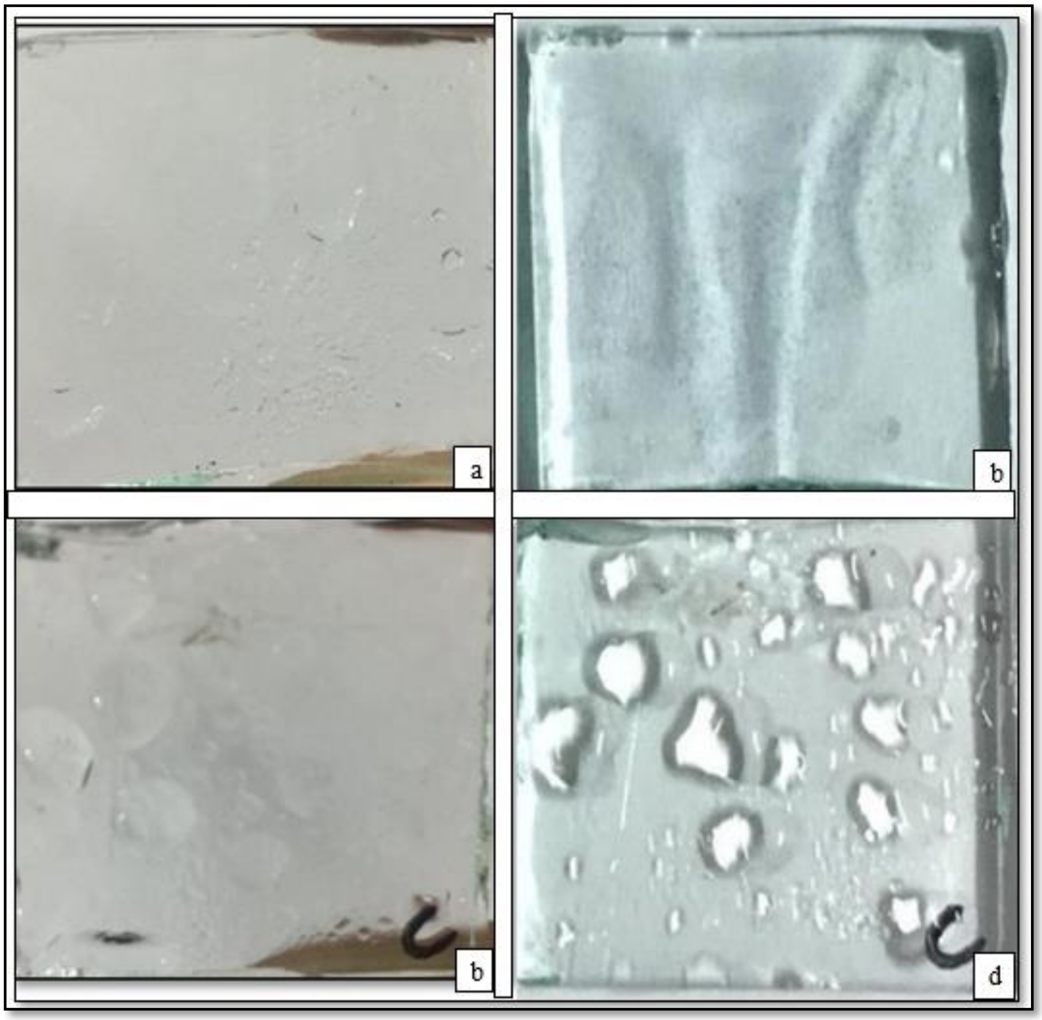

Figure 4.26: **Rain fall spray test images on coated glass where water forms thin layer** (a,b) and control glass where water forms larger droplets (c,d).

4.12.3 Anti-fog Analysis

In anti-fog test, conclusion is made on visual basis whether coating keeps the vision through the glass clean or it gets blurry. After 10 minutes of fog exposure, when the glass samples were placed on a white paper, it showed the presence of tiny water droplets on the surface of bare glass which hindered the vision across the glass. The control glass was completely dry after 20 minutes. Whereas in case of coated glass, the water made a thin layer and it surged through the rough surface of coated glass and it comes out clean and dry in a minute time with no water droplets or mist formation. This phenomenon is due to the hydrophilic nature of the coating which agrees well with Wenzel's model for hydrophilic surfaces. The images of coated and uncoated glass are presented in Fig 4. 27.

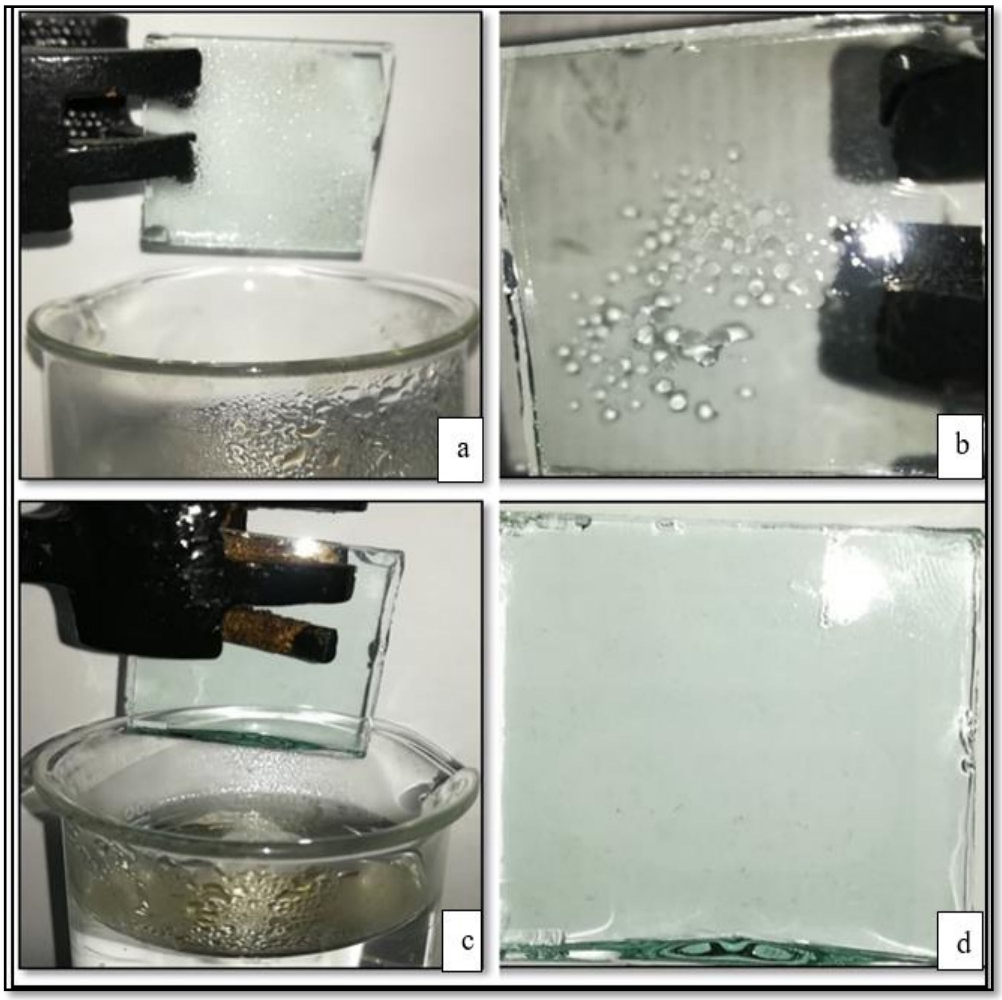

Figure 4.27: **Antifog experiment images** (a, b) uncoated glass with water droplets on its surface (c, d) nickel oxide thin film coated glass without water droplets on its surface

CHAPTER 5: DISCUSSION

There are two mechanisms of self-cleaning, one is through chemical breakdown of dirt, other is the physical washing away of dirt, the NiO fabricated glass falls under later category.

NiO coated thin film somehow behave like amphiphilic films, i.e. they act hydrophilic under sun and tend to gain hydrophobicity under dark. This is the reason why the contact angle kept on increasing in dark when analyzed through its analysis under dark. We can conclude from this experiment that our glass is photo-active and inert in dark.

The thin film used for coating glass surface in this study was fabricated from NiO nanoparticles which were synthesized prior, using algal extract. The shape, size and degree of agglomeration of the resulting nanoparticles is decided through the nature of the reducing agent. These SEM images prove the ability of algal extract of strain *Dictyospherium* sp. Strain DHM 2 (LC159306). The agreeable size of NiO nanoparticles also makes NiO thin film formation convenient. Few particles with aggregation were also seen which arise from the magnetic property of the synthesized NiO nanoparticles. Matching of the synthesized NiO nanoparticles with JCPDS carad no 01-089-7130 at 84% purity confirmed the quality was agreeable and the particle morphology also matched that of SEM results. face centered cubic. The AFM result is also in complete accordance with SEM images, proving the quality of NiO nanoparticles even further. The NiO nanoparticle selected for this thin film have energy band gap value of 3.47eV, which also indicates its aability of multi-dimensional functionality in face of its wide band gap. Zeta potential is the study of surface potential by determining the magnitude of electrical double layer repulsion. For this analysis, firstly refractive index between particles and solvent is measured which decides the value of Hamaker's constant. In case of NiO nanoparticle sample, the Hamaker's constant value is large because the zeta potential value is low i.e. 8.66 mV which indicates that there will be aggregation between particles in dispersion, although the report indicates that the quality of particles is good. The aggregation of NiO nanoparticles is basically attributed to the magnetic nature of NiO nanoparticles.

FTIR analysis depicts information about biomolecules responsible for reducing metal salts in more stable form, i.e. the metal oxide nanoparticles. These biomolecules act as capping, stabilizing and reducing agents for the synthesis of nanoparticles. FTIR peaks corresponding to biomolecules which are responsible for bio reduction should appear only in the FTIR of algal extract and not in the FTIR result of nanoparticles. This phenomenon aids us in understanding the elements responsible for reduction of nanoparticles (Chiba & Chen, 2014). In the obtained absorption spectrum of algal extract and NiO nanoparticles, plentiful information regarding the reducing agents from the algal extract can be deduced. The presence of flavonoids, phenols and proteins has also been confirmed from the phytochemical analysis of the extract as well.

The incorporation of these NiO nanoparticles in the form of thin film increases the surface energy of the glass surface which provides more area for surface reactions to take place. The hydrophilic nature of nickel oxide nanoparticles in the thin film makes the surface to turn super hydrophilic. The standard criteria for superhydrophilicity is at 10° or below. The super hydrophilic nature of the coated glass makes it a good candidate for smart self-cleaning glass. The superhydrophilicity of coated glass allows water or dirt to form a sheet or membrane of water which slides off of the glass due to spreading mechanism.

This study confirms that the contact angle decreases with increase in NiO nanoparticle concentration in coating emulsion within range of 0.5% to 4%. This decrease in CA may be attributed to high surface energy due to small size of nanoparticles and increased surface roughness of coated glass because of NiO nanoparticles incorporation on glass surface. Nickel oxide nanoparticles tend to agglomerate in emulsion due to their magnetic nature but the use of THF and water mixture as a solvent makes an unstable suspension in which the nanoparticles float on the surface, this unique feature reduces their aggregation. The use of THF as solvent has many edges, one of them being its low boiling point i.e. 66°C, the drying and annealing of coated SLG ensures complete evaporation of THF leaving behind only NiO nanoparticle (Cholewinski et al., 2014).

Sonication process also aided in maintaining the size of NiO nanoparticles at a smaller scale 20-60 nm through sheer force. As the concentration in the emulsion is increased beyond 4%, a change in CA trend is observed, the contact angle instead, increases to 14°. In coatings with NiO nanoparticles concentration less than 4%, the NiO nanoparticles are well dispersed and the coatings have microporous structure with NiO nanopillars which increase the surface roughness.

Whereas the coatings with higher concentration (5%-6%) of NiO nanoparticles in THF emulsion have aggregation of nanoparticles in them which in turn reduces the surface energy (Syafiq et al., 2018). The SEM analysis proves that the coating was very uniform and pin hole free. It had even distribution of NiO nanoparticles on overall surface with almost the same size range of 80-90 nm of NiO nanoparticles which is partly due to sonication and use of THF as appropriate solvent and partly owing to the annealing conditions provided to the NiO thin film. SEM clearly demonstrates the heterogeneity of NiO nanoparticles morphology on the surface of glass is due to nanoparticle size distribution and it contributes to increased surface roughness. The increased surface roughness is responsible of higher wettability. The pinhole free nature of coating is good for achieving self-cleaning applications.

The AFM image analysis proves the NiO thin film coating is uniform and has good surface roughness. Heating during annealing process increases the uniformity and efficiency of the NiO thin film in terms of self-cleaning since the increase in roughness increases the hydrophilicity of the NiO thin film as the contact angle between water and NiO thin film baseline decreases. The NiO thin film formed has a contact angle of 10° which agrees well with the Wenzel model of hydrophilic surface. The spin-coating procedure which was adopted for formation of NiO thin film coated glass in this study pertains higher surface roughness as compared to other coating methods such as spray-pyrolysis (Chtouki et al., 2017) because spin-coating is associated with smoother surface effect on the thin film topography (Chtouki et al., 2017).

The XRD peaks corresponding to 111, 220, 311 and 222 are present but their peak intensity is very small as compared to 200. As the concentration chosen for NiO thin film formation was 4%, at higher concentration the intensity of the peak increases which is the reason for film thickness. XRD of the NiO thin film demonstrates that annealing temperature has an important role in deciding the orientation of NiO and the XRD plot indicates that (200) is the most suitable direction for ion exchange (Chtouki et al., 2017). The Xpert analysis also proved that there are no other unwanted phases as all the peaks were matched perfectly to the allotted JCPDS card number.

Since the change of water contact angle is not significant after long exposure to UV light, we can conclude that the NiO thin film is photoactive under UV light very well and this slight change of contact angle form 10° to 12° can be attributed to the gas molecules, vapor and pollutants absorbed by the surface due to long exposure to open environment (Chtouki et al., 2017). The change in

NiO nanoparticle in first four days indicates the establishment of hydrophobicity by NiO nanoparticles in the absence of light. However, there is no further change in contact angle after fourth day which indicates that NiO thin film coated glass possesses good surface robustness due to incorporation of NiO nanoparticles. It’s also shows that the synthesized nanoparticles in general impart good surface roughness to the surface. The consistency in the surface roughness and hydrophilicity partly comes from the aspect of tetrahydrofuran. Since THF is not soluble in water but is miscible, THF and water tend to form hydrogen bonds with each other so does it with NiO making the surface hydrophilic in general owing to free Hydrogen atoms available on THF surface. This also explains the role of THF as binder in this coating procedure.

The application of such coated glass are vast, apart from being used in hospitals, this NiO coated glass can also be used in cars and high rise buildings, this way, it could lessen accident rates, lessen the time, money and excessive chemical exposure needed for optimum cleaning operations. Added, in case of hospitals and other clinical settings, the chances of infection are reduced through biofilm prevention.

Wenzel’s model of hydrophilic surface states that the surface wettability of naturally hydrophilic surfaces increases with increasing surface roughness. Wettability is the ability of water droplet to maintain contact with solid surfaces through interaction between adhesive and cohesive forces, these are the two types of forces exerted by the liquid on the glass. When these two forces create a balance, water contact angle is established which is a static phenomenon.

In addition to the self-cleaning property attributed to glass surface through nickel oxide thin film, it also imparts antibacterial property to the glass. To date the exact mechanism by which NiO nanoparticles kill microorganisms has not been established completely but the mechanism of action of NiO nanoparticle for killing of microorganisms can be one of the two, by direct contact of NiO nanoparticle with bacterial surface which leads to membrane damage as a result of change in physiological pH or by the generation of electron hole pairs upon activation of NiO through light or UV which leads to hydrolysis and redox reaction which in turn produce hydrogen peroxide, thid hydrogen peroxide can enter the cell membrane and kill bacteria (Sathyavathi et al., 2014). The nature of this antibacterial glass is preventive, it inhibits the formation of biofilm over its surface, and this property has been well elaborated through SEM imaging of inhibited biofilms of tested organisms which was counter-confirmed using optical density measurements. This glass has a potential to be used in environments where the indirect spread of nosocomial infection needs to be reduced such as hospitals and other clinical settings

5.1 Conclusions

The aim of the designed study was to create an antibacterial and self-cleaning glass in order to minimize the risk of nosocomial infections along with reduction of traditional cleaning efforts. Nano coatings are more cutting-edge strategy in achieving self-cleaning and antibacterial purpose as compared to most customary methods. The objectives of the planned project were successfully achieved. In the first phase, face centered cubic nickel oxide nanoparticles of bunsenite form had been synthesized and characterized using algal extract of *Dictyospherium* sp HM2, Strain DHM2.

In the second phase of the project, thin film coating with average roughness of 26.53 nm has been successfully prepared for achieving self-cleaning and antibacterial surface. In the final phase, the formed coating was then subjected to a range of characterization techniques and a variety of tests to confirm the efficacy as self-cleaning and antibacterial glass which is nearly super hydrophilic. We can conclude that our prepared thin film has efficient antibacterial capacity and it acts as optimum self-cleaning glass. Added benefit is the ease of synthesis and cost effectiveness.

5.2 Future Prospects

Nanobiotechnology has vast range of applications in the field of coating tehcnology. Coatings are being developed recently with an effort to cover various smart aspects in one, such as antibacterial, self-cleaning and low emissivity. In future there is a need to perform an elaborate study regarding annealing temperature and conditions such as subjecting the caoting to a vast range of annealing temperature under different environments which could further decrease the conatct angle of the surface by agreeing to the Wenzel model of hydrophilic surfaces. This would help in achieving more roboust self-cleaning functionality.

Real time application by coating a large area glass and testing sample in open environment for an extended time period to assess their result as a self-cleaning glass. This coated application is not just limited to glass, it can be applied and tested on other surfaces such as steel, leather, fabric etc to produce more antibacterial surfaces.

References

Aranda, A., et al. (2013). "Dichloro-dihydro-fluorescein diacetate (DCFH-DA) assay: a quantitative method for oxidative stress assessment of nanoparticle-treated cells." Toxicology in Vitro **27**(2): 954-963.

Berrington, A. and S. Pedler (1998). "Investigation of gaseous ozone for MRSA decontamination of hospital side-rooms." Journal of Hospital infection **40**(1): 61-65.

Bogusz, A., et al. (2013). "How quickly do hospital surfaces become contaminated after detergent cleaning?" Healthcare infection **18**(1): 3-9.

Boyce, J. M., et al. (2011). "Terminal decontamination of patient rooms using an automated mobile UV light unit." Infection Control & Hospital Epidemiology **32**(8): 737-742.

Chen, L.-K., et al. (2013). "Potential of bacteriophage ΦAB2 as an environmental biocontrol agent for the control of multidrug-resistant Acinetobacter baumannii." BMC microbiology **13**(1): 154.

Chinn, R. Y. and L. Sehulster (2003). "Guidelines for environmental infection control in health-care facilities; recommendations of CDC and Healthcare Infection Control Practices Advisory Committee (HICPAC)."

Davies, A., et al. (2011). "Gaseous and air decontamination technologies for Clostridium difficile in the healthcare environment." Journal of Hospital infection **77**(3): 199-203.

Hauert, R. (2003). "A review of modified DLC coatings for biological applications." Diamond and related materials **12**(3-7): 583-589.

Hirai, Y. (1991). "Survival of bacteria under dry conditions; from a viewpoint of nosocomial infection." Journal of Hospital infection **19**(3): 191-200.

Kingston, D. and W. Noble (1964). "Tests on self-disinfecting surfaces." Epidemiology & Infection **62**(4): 519-532.

Klibanov, A. M. (2007). "Permanently microbicidal materials coatings." Journal of Materials Chemistry **17**(24): 2479-2482.

Olson, B., et al. (1984). "Epidemiology of endemic Pseudomonas aeruginosa: why infection control efforts have failed." Journal of Infectious Diseases **150**(6): 808-816.

Page, K., et al. (2009). "Antimicrobial surfaces and their potential in reducing the role of the inanimate environment in the incidence of hospital-acquired infections." Journal of Materials Chemistry **19**(23): 3819-3831.

Sattar, S. A. and J.-Y. Maillard (2013). "The crucial role of wiping in decontamination of high-touch environmental surfaces: review of current status and directions for the future." American journal of infection control **41**(5): S97-S104.

Syed, A. K., et al. (2014). "Triclosan promotes Staphylococcus aureus nasal colonization." MBio **5**(2): e01015-01013.

Xi, Y. Y., et al. (2009). "Electrodeposition for antibacterial nickel-oxide-based coatings." Thin Solid Films **517**(24): 6527-6530.

Adekunle, A. S., et al. (2014). "Comparative catalytic properties of Ni (OH) 2 and NiO nanoparticles towards the degradation of nitrite (NO2-) and nitric oxide (NO)."

Ahoyo, T. A., et al. (2014). "Prevalence of nosocomial infections and anti-infective therapy in Benin: results of the first nationwide survey in 2012." Antimicrobial resistance and infection control **3**(1): 17.

Allegranzi, B., et al. (2011). "Burden of endemic health-care-associated infection in developing countries: systematic review and meta-analysis." The lancet **377**(9761): 228-241.

Baek, Y.-W. and Y.-J. An (2011). "Microbial toxicity of metal oxide nanoparticles (CuO, NiO, ZnO, and Sb2O3) to Escherichia coli, Bacillus subtilis, and Streptococcus aureus." Science of the total environment **409**(8): 1603-1608.

Basiron, N., et al. (2018). "Improved Adhesion of Nonfluorinated ZnO Nanotriangle Superhydrophobic Layer on Glass Surface by Spray-Coating Method." Journal of Nanomaterials **2018**.

Boyce, J. M., et al. (2011). "Terminal decontamination of patient rooms using an automated mobile UV light unit." Infection Control & Hospital Epidemiology **32**(8): 737-742.

Cheng, G., et al. (2007). "Inhibition of bacterial adhesion and biofilm formation on zwitterionic surfaces." Biomaterials **28**(29): 4192-4199.

Cholewinski, A., et al. (2014). "Bio-inspired polydimethylsiloxane-functionalized silica particles-epoxy bilayer as a robust superhydrophobic surface coating." Surface and Coatings Technology **254**: 230-237.

Chtouki, T., et al. (2017). "Comparison of structural, morphological, linear and nonlinear optical properties of NiO thin films elaborated by Spin-Coating and Spray Pyrolysis." Optik **128**: 8-13.

Dancer, S. J. (2014). "Controlling hospital-acquired infection: focus on the role of the environment and new technologies for decontamination." Clinical microbiology reviews **27**(4): 665-690.

Doll, M., et al. (2018). "Environmental cleaning and disinfection of patient areas." International Journal of Infectious Diseases **67**: 52-57.

Ezhilarasi, A. A., et al. (2018). "Green synthesis of NiO nanoparticles using Aegle marmelos leaf extract for the evaluation of in-vitro cytotoxicity, antibacterial and photocatalytic properties." Journal of Photochemistry and Photobiology B: Biology **180**: 39-50.

Haider, A. J., et al. (2019). "Enhance Preparation and Characterization of Nickel-Oxide as Self-Cleaning Surfaces." Energy Procedia **157**: 1328-1342.

Hauert, R. (2003). "A review of modified DLC coatings for biological applications." Diamond and related materials **12**(3-7): 583-589.

Hirai, Y. (1991). "Survival of bacteria under dry conditions; from a viewpoint of nosocomial infection." Journal of Hospital infection **19**(3): 191-200.

Imran Din, M. and A. Rani (2016). "Recent advances in the synthesis and stabilization of nickel and nickel oxide nanoparticles: a green adeptness." International journal of analytical chemistry **2016**.

Jlassi, M., et al. (2014). "Optical and electrical properties of nickel oxide thin films synthesized by sol–gel spin coating." Materials Science in Semiconductor Processing **21**: 7-13.

Khalil, A. T., et al. (2018). "Sageretia thea (Osbeck.) modulated biosynthesis of NiO nanoparticles and their in vitro pharmacognostic, antioxidant and cytotoxic potential." Artificial cells, nanomedicine, and biotechnology **46**(4): 838-852.

Klibanov, A. M. (2007). "Permanently microbicidal materials coatings." Journal of Materials Chemistry **17**(24): 2479-2482.

Lalithambika, K., et al. (2017). "Photocatalytic and antibacterial activities of eco-friendly green

synthesized ZnO and NiO nanoparticles." Journal of Materials Science: Materials in Electronics **28**(2): 2062-2068.
Lee, I. S., et al. (2006). "Ni/NiO core/shell nanoparticles for selective binding and magnetic separation of histidine-tagged proteins." Journal of the American Chemical Society **128**(33): 10658-10659.

Leng, C. W., et al. (2013). "Efficacy of titanium dioxide compounds in preventing environmental contamination by meticillin resistant Staphylococcus aureus (MRSA)." Int J Infect Control **9**(3).

Lozano, R., et al. (2012). "Global and regional mortality from 235 causes of death for 20 age groups in 1990 and 2010: a systematic analysis for the Global Burden of Disease Study 2010." The lancet **380**(9859): 2095-2128.

Matsunaga, T., et al. (1988). "Continuous-sterilization system that uses photosemiconductor powders." Appl. Environ. Microbiol. **54**(6): 1330-1333.

Medlin, J. (1997). "Germ warfare." Environmental health perspectives **105**(3): 290-292.

Mehta, Y., et al. (2014). "Guidelines for prevention of hospital acquired infections." Indian journal of critical care medicine: peer-reviewed, official publication of Indian Society of Critical Care Medicine **18**(3): 149.

Mittal, A. K., et al. (2013). "Synthesis of metallic nanoparticles using plant extracts." Biotechnology advances **31**(2): 346-356.

Naidu, K., et al. (2014). "A descriptive study of nosocomial infections in an adult intensive care unit in Fiji: 2011-12." Journal of tropical medicine **2014**.

Page, K., et al. (2009). "Antimicrobial surfaces and their potential in reducing the role of the inanimate environment in the incidence of hospital-acquired infections." Journal of Materials Chemistry **19**(23): 3819-3831.

Park, K. D., et al. (1998). "Bacterial adhesion on PEG modified polyurethane surfaces." Biomaterials **19**(7-9): 851-859.

Rakshit, S., et al. (2013). "Controlled synthesis of spin glass nickel oxide nanoparticles and evaluation of their potential antimicrobial activity: A cost effective and eco friendly approach." RSC Advances **3**(42): 19348-19356.

Rutala, W. A. and D. J. Weber (2008). "Guideline for disinfection and sterilization in healthcare facilities, 2008."

Saloojee, H. and A. Steenhoff (2001). "The health professional's role in preventing nosocomial infections." Postgraduate medical journal **77**(903): 16-19.

Salvadori, M. R., et al. (2014). "Nickel oxide nanoparticles film produced by dead biomass of filamentous fungus." Scientific reports **4**: 6404.

Sathyavathi, S., et al. (2014). "Extracellular synthesis and characterization of nickel oxide nanoparticles from Microbacterium sp. MRS-1 towards bioremediation of nickel electroplating industrial effluent." Bioresource technology **165**: 270-273.

Stobie, N., et al. (2010). "Dual-action hygienic coatings: benefits of hydrophobicity and silver ion release for protection of environmental and clinical surfaces." Journal of colloid and interface science **345**(2): 286-292.

Sütterlin, S., et al. (2014). "Relatively high prevalence of genetic and phenotypic silver resistance among Enterobacter cloacae isolates, poster P1016." ECCMID, Barcelona, Spain: http://eccmid. meetingxpert. net/ECCMID_699/poster_109206/program. aspx/anchor109206 Accessed June.

Syed, A. K., et al. (2014). "Triclosan promotes Staphylococcus aureus nasal colonization." MBio **5**(2): e01015-01013.

Taylor, L., et al. (2009). "Reduction of bacterial contamination in a healthcare environment by silver antimicrobial technology." Journal of infection prevention **10**(1): 6-12.

Weinstein, R. A. and B. Hota (2004). "Contamination, Disinfection, and Cross-Colonization: Are Hospital Surfaces Reservoirs for Nosocomial Infection?" Clinical Infectious Diseases **39**(8): 1182-1189.

Wilson, M. (2003). "Light-activated antimicrobial coating for the continuous disinfection of surfaces." Infection Control & Hospital Epidemiology **24**(10): 782-784.

Wong, K. K. and X. Liu (2010). "Silver nanoparticles—the real “silver bullet” in clinical medicine?" MedChemComm **1**(2): 125-131.

Xi, Y. Y., et al. (2009). "Electrodeposition for antibacterial nickel-oxide-based coatings." Thin Solid Films **517**(24): 6527-6530.

Yuvakkumar, R., et al. (2014). "Rambutan (Nephelium lappaceum L.) peel extract assisted biomimetic synthesis of nickel oxide nanocrystals." Materials Letters **128**: 170-174.

Adekunle, A. S., Oyekunle, J. A., Oluwafem, O., Joshua, A. O., Makinde, A. O., Ogunfowokan, A. O., . . . Ebenso, E. E. (2014). Comparative catalytic properties of Ni (OH) 2 and NiO nanoparticles towards the degradation of nitrite (NO2-) and nitric oxide (NO).

Bi, Z., & He, B. B. (2013). Characterization of microalgae for the purpose of biofuel production. Transactions of the ASABE, 56(4), 1529-1539.

Chiba, S., & Chen, H. (2014). sp 3 C–H oxidation by remote H-radical shift with oxygen-and nitrogen-radicals: a recent update. Organic & biomolecular chemistry, 12(24), 4051-4060.

Cholewinski, A., Trinidad, J., McDonald, B., & Zhao, B. (2014). Bio-inspired polydimethylsiloxane-functionalized silica particles-epoxy bilayer as a robust superhydrophobic surface coating. Surface and Coatings Technology, 254, 230-237.

Chougule, M. A., Pawar, S. G., Godse, P. R., Mulik, R. N., Sen, S., & Patil, V. B. (2011). Synthesis and characterization of polypyrrole (PPy) thin films. Soft Nanoscience Letters, 1(01), 6.

Chtouki, T., Soumahoro, L., Kulyk, B., Bougharraf, H., Kabouchi, B., Erguig, H., & Sahraoui, B. (2017). Comparison of structural, morphological, linear and nonlinear optical properties of NiO thin films elaborated by Spin-Coating and Spray Pyrolysis. Optik, 128, 8-13.

Coenye, T., Peeters, E., & Nelis, H. J. (2007). Biofilm formation by Propionibacterium acnes is associated with increased resistance to antimicrobial agents and increased production of putative virulence factors. Research in microbiology, 158(4), 386-392.

Couchman, P., & Karasz, F. (1978). A classical thermodynamic discussion of the effect of composition on glass-transition temperatures. Macromolecules, 11(1), 117-119.

Di Domenico, E. G., Toma, L., Provot, C., Ascenzioni, F., Sperduti, I., Prignano, G., . . . Bernardi, T. (2016). Development of an in vitro assay, based on the biofilm ring test®, for rapid profiling of biofilm-growing bacteria. Frontiers in microbiology, 7, 1429.

Haider, A. J., Al-Anbari, R., Sami, H. M., & Haider, M. J. (2019). Enhance Preparation and Characterization of Nickel-Oxide as Self-Cleaning Surfaces. Energy Procedia, 157, 1328-1342.

Heatley, N. (1944). A method for the assay of penicillin. Biochemical Journal, 38(1), 61.

Irwin, M. D., Buchholz, D. B., Hains, A. W., Chang, R. P., & Marks, T. J. (2008). p-Type semiconducting nickel oxide as an efficiency-enhancing anode interfacial layer in polymer bulk-heterojunction solar cells. Proceedings of the National Academy of Sciences, 105(8), 2783-2787.

Karunanidhi, A., Ghaznavi-Rad, E., Jeevajothi Nathan, J., Abba, Y., Belkum, A. v., & Neela, V. (2017). Allium stipitatum extract exhibits in vivo antibacterial activity against methicillin-resistant Staphylococcus aureus and accelerates burn wound healing in a full-thickness murine burn model. Evidence-Based Complementary and Alternative Medicine, 2017.

Khalid, M., Khalid, N., Ahmed, I., Hanif, R., Ismail, M., & Janjua, H. A. (2017). Comparative studies of three novel freshwater microalgae strains for synthesis of silver nanoparticles: insights of characterization, antibacterial, cytotoxicity and antiviral activities. Journal of applied phycology, 29(4), 1851-1863.

Khalil, A. T., Ovais, M., Ullah, I., Ali, M., Shinwari, Z. K., Hassan, D., & Maaza, M. (2018). Sageretia thea (Osbeck.) modulated biosynthesis of NiO nanoparticles and their in vitro pharmacognostic, antioxidant and cytotoxic potential. Artificial cells, nanomedicine, and biotechnology, 46(4), 838-852.

Lalithambika, K., Thayumanavan, A., Ravichandran, K., & Sriram, S. (2017). Photocatalytic and antibacterial activities of eco-friendly green synthesized ZnO and NiO nanoparticles. Journal of Materials Science: Materials in Electronics, 28(2), 2062-2068.

Marques, M. E., Mansur, A. A., & Mansur, H. S. (2013). Chemical functionalization of surfaces for building three-dimensional engineered biosensors. Applied Surface Science, 275, 347-360.

McFarland, J. (1907). The nephelometer: an instrument for estimating the number of bacteria in suspensions used for calculating the opsonic index and for vaccines. Journal of the American Medical Association, 49(14), 1176-1178.

Rakshit, S., Ghosh, S., Chall, S., Mati, S. S., Moulik, S., & Bhattacharya, S. C. (2013). Controlled synthesis of spin glass nickel oxide nanoparticles and evaluation of their potential antimicrobial activity: A cost effective and eco friendly approach. RSC Advances, 3(42), 19348-19356.

Sathyavathi, S., Manjula, A., Rajendhran, J., & Gunasekaran, P. (2014). Extracellular synthesis and characterization of nickel oxide nanoparticles from Microbacterium sp. MRS-1 towards bioremediation of nickel electroplating industrial effluent. Bioresource technology, 165, 270-273.

Sierra, L. S., Dixon, C. K., & Wilken, L. R. (2017). Enzymatic cell disruption of the microalgae Chlamydomonas reinhardtii for lipid and protein extraction. Algal research, 25, 149-159.

Syafiq, A., Vengadaesvaran, B., Pandey, A., & Rahim, N. A. (2018). Superhydrophilic Smart Coating for Self-Cleaning Application on Glass Substrate. Journal of Nanomaterials, 2018.

Tayade, U., Borse, A., & Meshram, J. (2018). First report on butea monosperma flower extract-based nickel nanoparticles green synthesis and characterization. Int. J. Sci. Res. Sci. Eng. Technol, 4(3), 43-49.

Vuong, C., Voyich, J. M., Fischer, E. R., Braughton, K. R., Whitney, A. R., DeLeo, F. R., & Otto, M. (2004). Polysaccharide intercellular adhesin (PIA) protects Staphylococcus epidermidis against major components of the human innate immune system. Cellular microbiology, 6(3), 269-275.